ISSN 2221-6413 (Print), ISSN 2223-2559 (Online)
Coden: PJSIB5 57(2) 59-124 (2014)

Pakistan Journal of Scientific and Industrial Research

Series A: Physical Sciences

Vol. 57, No.2, May-June, 2014

(for on-line access please visit web-site http://www.pjsir.org)

Published by
Scientific Information Centre
Pakistan Council of Scientific and Industrial Research
Karachi, Pakistan

Pakistan Journal of Scientific and Industrial Research
Series A: Physical Sciences

Pakistan Journal of Scientific and Industrial Research started in 1958, has been bifurcated in 2011 into:

Series A: Physical Sciences [**ISSN 2221-6413 (Print); ISSN 2223-2559 (online)]** (appearing as issues of January-February, May-June and September-October) and
Series B: Biological Sciences [**ISSN 2221-6421 (Print); ISSN 2223-2567 (online)]** (appearing as issues of March-April, July-August and November-December).
Each Series will appear three times in a year.

This Journal is indexed/abstracted in Biological Abstracts and Biological Abstracts Reports, Chemical Abstracts, Geo Abstracts, CAB International, BioSciences Information Service, Zoological Record, BIOSIS, NISC, NSDP, Current Contents, CCAB, Rapra Polymer Database, Reviews and Meetings and their CD-ROM counterparts etc.
Subscription rates (including handling and Air Mail postage): ***Local:*** Rs. 2000 per volume, single issue Rs. 350; ***Foreign:*** US$ 400 per volume, single issue US$ 70.
Electronic format of this journal is available with: Bell & Howell Information and Learning, 300, North Zeeb Road, P.O. 1346, Ann Arbor, Michigan 48106, U.S.A; Fax.No.313-677-0108; http://www.proquest.com
Photocopies of back issues can be obtained through submission of complete reference to the Executive Editor against the payment of Rs. 25 per page per copy (by Registered Mail) and Rs. 115 per copy (by Courier Service), within Pakistan; US$ 10 per page per copy (by Registered Mail) and US$25 per page per copy (by Courier Service), for all other countries.

Printed and Published by: PCSIR Scientific Information Centre, PCSIR Laboratories Campus, Shahrah-e-Dr. Salimuzzaman Siddiqui, Karachi-75280, Pakistan.

Editorial Address

Executive Editor
Pakistan Journal of Scientific and Industrial Research, PCSIR Scientific Information Centre
PCSIR Laboratories Campus, Shahrah-e-Dr. Salimuzzaman Siddiqui, Karachi-75280, Pakistan
Tel: 92-21-34651739-40, 34651741-43; Fax: 92-21-34651738; Web: http://www.pjsir.org, E-mail: info@pjsir.org

Pakistan Journal of Scientific and Industrial Research
Series A: Physical Sciences
Vol. 57, No. 2, May-June, 2014

Contents

Review

Pak. j. sci. ind. res. Ser. A: phys. sci. 2014 **57**(2) 59-62

Percentage Discrepancies Assessment Between Measured and Calculated Behaviour of Percent Depth Dose in External Beam Radiotherapy

Muhammad Isa[ab]*, Khalid Iqbal[ab], Muhammad Jahanzeb Ashraf[a], Muhammad Afzal[a] and Saeed Ahmad Buzdar[a]

[a]Department of Physics, The Islamia University, Bahawalpur, Pakistan
[b]Department of Radiation Oncology, Shaukat Khanum Cancer Hospital and Research Center, Lahore, Pakistan

(received October 24, 2012; revised February 25, 2013; accepted April 19, 2013)

Abstract. The aim of this study was to calculate percentage discrepancies (PD) of the measured and calculated percentage depth doses (PDDs) values. The 6 MV photon beam produced by the Varian linear accelerator 2100 C/D was used in this study. PDDs, tissue maximum ratios (TMR) and phantom scatter factor (S_P) were measured using the PTW 31006 ionisation chamber in water phantom. PD between PDD values of the measured and calculated was ranging between 0.30% and 2.38%. Percentage discrepancies were also found higher against 20 cm depth in water for (20×20) cm^2 field size. These discrepancies should be taken into account, while delivering any medical dose in radiation therapy centers.

Keywords: percentage depth dose, percentage discrepancies, ionisation chamber

Introduction

Medical linear accelerators are playing important role in radiation centres all over the world. Specific radiation dose is applied to cancer patients for curative as well as palliative treatment. However, for each case the prescribed dose ought to be delivered accurately both in quantity and quality. Over or under-dosage could be harshly destructive to the patient or may lead to unwanted outcomes. For accuracy concerns supercomputers have been introduced in radiation therapy centres. These computers exploit commercial programmes and algorithms for the management of model dose distributions within the irradiated part of the patient. In order to attain precised output from these modern facilities, they have to be fed with exact beam data measured from the modern treatment machines. Hence, medical physicists are more concerned about quality assurance of accelerators and consistency of the radiation measurements. These measurements are based on daily, monthly and yearly procedures to assure accurate delivery of dose to patient. International Associations and Agencies of Physicists in Medicine (such as AAPM and IAEA) produce updated publications of acceptable tolerance for mechanical actions and radiation field output. These publications are found to promise accomplishment of immense accuracy of dose delivery to the right body volume (IAEA, 2000; Peter *et al*., 1999).

*Author for correspondence; E-mail: isaiub@yahoo.com

Though, measurements of percentage depth dose (PDD) could be exaggerated by factors, which are not commonly taken into account. These contains movement of water during PDD or beam profile measurements, predominantly when measuring surface dose and physical dimensions of the measuring apparatus such as the ionisation chamber or TLD. Direct formulas can also be sometime used to determine vital radiation quantities. These formulas can be used when the other variable quantities are known. Monte Carlo simulations could be practical in calculating the amount of certain quantities such as PDD, beam profiles; flux and dose delivery to definite position in the treatment room or within the patient (Rogers, 2002; Ahnesjo and Aspradakis, 1999; Bloch and Altschuler, 1995).

Percentage discrepancies may exist due to some properties of measuring devices or attributed to some issues such as movement of water during measurements. It is not understandable why such discrepancies subsist. Exactness in manufacturing may also affects on accuracy (Sameer, 2007). Percentage discrepancies (PD) have been calculated between measured and calculated PDDs at different field sizes and depths. The calculated PDDs were worked out by using formula, with constant SSD. Phantom scatter factor and tissue maximum ratios (TMR) were measured and used in the formula to evaluate the calculated PDDs values. The PD and PD gradient values were computed between the calculated

and measured PDDs for 6 MV energy. This work provides an alternative approach to radiation oncology physicists about the necessity of quality assurance and this ultimately improves the quality of the treatments.

Materials and Methods

Since the water behaviour is quite similar with human body, therefore, beam profile and PDDs are usually measured in water phantoms to resemble a patient after introducing correction factors for temperature and pressure. This study was carried out on a PTW scanning water phantom (40×40) cm^2 with ionisation chamber of active volume of 0.5 cm^3. The ionisation chamber was installed on the moveable sampling holder of the phantom. Another chamber was fixed on the phantom as a reference chamber. The Varian medical accelerator 2100 C/D having energy of 6 MV was used. The field chamber was moved when the radiation was "ON" and reference chamber was fixed. The output was read out on the electrometer and then the ratio of both chambers' reading was used to make the PDD or dose profile data. The peak absorbed dose on the central axis occurs at the end of build up region. By definition (Birgani and Karbalaee, 2009) the PDD is:

$$PDD = \frac{D_d}{D_{max}} \quad \text{.....(1)}$$

where:

D_d = dose at depth; D_{max} = depth of maximum dose.

Dosimetry studies show that the PDD initially increases rapidly until the depth of the maximum dose is achieved. Beyond this the dose decreases slowly with depth. This study was confirmed by calculating the PDD using the formula of Khan (2010).

$$P(d,r,f) = TMR(d,r_d)\left(\frac{f+t_o}{f+d}\right)^2 \left(\frac{S_p(r_d)}{S_p(r_{to})}\right).100 \quad \text{.....(2)}$$

where:

$TMR(d, r_d)$ = measured tissue maximum ratio;

f = SSD; $r_d = r.\left(\frac{f+d}{f}\right)$; $r_{to} = r.\left(\frac{f+t_o}{f}\right)$; d = depth; r_d = field size at reference depth; t_o = reference depth at maximum dose; $S_p(r_d)$ = phantom scatter factor at reference depth d; $S_p(r_{t0})$ = phantom scatter factor at reference depth at maximum dose.

TMR is used for high energy photon beams. PDDs, TMR and S_p values were measured by fixing the reference depth at 1.5 cm of ionisation chamber in water phantom. S_p was found by small diameter chamber using measured PDD data. Then these measured values of TMR, S_p and PDDs were used in formula containing equation (2) to calculate PDDs.

Results and Discussion

Table 1 reveals the S_p, TMR, PDDs values, which were measured using the arrangement as show in Fig. 1. These TMR, S_p, PDDs values were used in formula (2) and new PDDs were calculated. Table 2 shows the measured values and Table 3 shows the calculated values at some selected depths in water. PD was found between the measured and calculated PDDs.

Percentage discrepancies (PD) between PDD values for measured and calculated values are shown in Table 2 at same depth and field size. Taking PDD measured values as a reference; PD values were calculated using the following formula (Sameer, 2007).

$$PD = \frac{PDD_{Calculated} - PDD_{Measured}}{PDD_{Measured}} \times 100\%$$

The uppermost PD value was found in Fig. 2 and by Table 2 at (15×15) cm^2 field size, while the minute value was observed at 1.5 cm depth for both the (20×20) cm^2 and (25×25) cm^2 field sizes. Table 3 illustrates the maximum PD value in this study at 6MV was 2.38% at depth 20 cm with (15×15) cm^2 field size, while minimum value (0.30%) with the same field size was found at 1.5 cm near the water surface.

Figure 2 demonstrates the relationship between PD values in Table 2 and field size at each selected depth in water at 6 MV.

Figure 2 confirms the values of Table 2 i.e., the PD values improve with depth in water and depreciate with field size. PD gradient shows an increment or decrement in values at each step during delivery of doses. A medical physicist must know the change in dose at every step, while delivering the accurate doses to patients. The maximum PD gradient between these values can be found as:

$$= \frac{2.38 - 0.3}{15} = 0.1386 \text{ cm}^{-1}$$

This shows a 0.1386% increment in PD occurring from every 1 cm from D_{max} to depth of 20 cm that correspond to maximum PD gradient. Similarly, the minimum PD gradient was found at field size of 20×20 cm^2 as calculated by:

$$= \frac{0.22 - 0.1}{20} = 0.006 \text{ cm}^{-1}$$

Table 1. Measured values of TMR, Phantom scatter factor and others at certain depths and field sizes for 6 MV photon beam

Field size (r)	Depth (d)	TMR	r_d	$S_p(r_d)$	r_{to}	$S_p(r_{to})$	Calculated PDD	Measured PDD
5×5	1.5	0.992	5.075	0.968	5.075	0.968	99.2	99.6
	5	0.913	5.25	0.968	5.075	0.968	85.3	85.7
	10	0.754	5.5	0.968	5.075	0.968	64.1	64.6
	15	0.611	5.75	0.968	5.075	0.968	47.5	48
	20	0.499	6	0.974	5.075	0.968	35.4	36
10×10	1.5	0.993	10.15	1	10.15	1	99.3	99.7
	5	0.929	10.5	1	10.15	1	86.8	87.3
	10	0.797	11	1.005	10.15	1	67.5	68
	15	0.658	11.5	1.005	10.15	1	51.0	51.8
	20	0.545	12	1.01	10.15	1	38.6	39.5
15×15	1.5	0.995	15.225	1.022	15.225	1.022	99.5	99.8
	5	0.938	15.75	1.022	15.225	1.022	87.6	88.1
	10	0.816	16.5	1.022	15.225	1.022	69.4	70
	15	0.692	17.25	1.022	15.225	1.022	53.9	54.4
	20	0.581	18	1.035	15.225	1.022	41.0	42
20×20	1.5	0.998	20.3	1.035	20.3	1.035	99.8	99.9
	5	0.944	21	1.035	20.3	1.035	88.2	88.4
	10	0.83	22	1.035	20.3	1.035	70.6	70.9
	15	0.713	23	1.035	20.3	1.035	55.5	55.8
	20	0.611	24	1.041	20.3	1.035	43.4	43.9
25×25	1.5	0.996	25.375	1.041	25.375	1.041	99.6	99.7
	5	0.947	26.25	1.041	25.375	1.041	88.4	88.7
	10	0.84	27.5	1.041	25.375	1.041	71.5	71.7
	15	0.731	28.75	1.043	25.375	1.041	56.8	57.1
	20	0.629	30	1.043	25.375	1.041	44.9	45.1

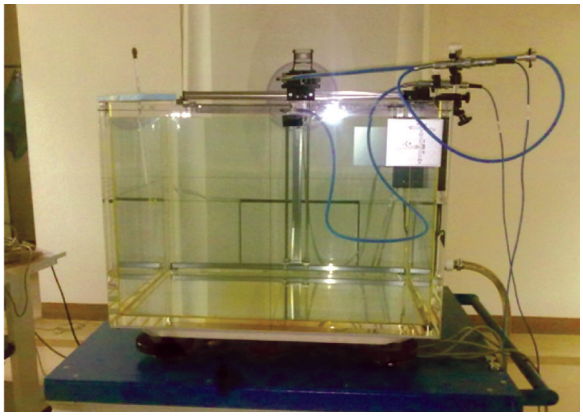

Fig. 1. Set-up of water phantom and ionisation chamber.

Table 2. Calculated PD values between measured and calculated values for 6MV photon beam

Depth in water (cm)	Field size (cm×cm)				
	5×5	10×10	15×15	20×20	25×25
1.5	0.40	0.40	0.30	0.10	0.10
5	0.11	0.57	0.56	0.22	0.27
10	0.77	0.73	0.85	0.42	0.27
15	1.04	1.5	0.91	0.53	0.52
20	1.66	2.2	2.38	1.13	0.44

Table 3 summarizes the conspicuous statistical values for PD and PD gradient.

Error range between maximum and minimum PD was 2.28 and between PD gradient was 0.1326 by origion Pro-7 software.

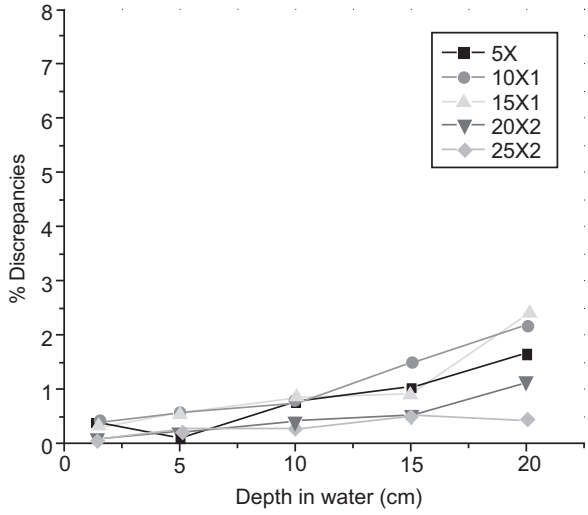

Fig. 2. Variation of PD with depth in water at 6 MV.

Table 3. Statistical summary of PD and PD gradient values

	PD	PD gradient (cm^{-1})
Maximum	2.38	0.1386
Minimum	0.10	0.006
Mean	1.24	0.0723

Previously, Sameer (2007) reported for comparative study of measurements. The PDD measurements were done between two different medical linear accelerators and the PD values were calculated. It was concluded that these discrepancies should be considered, while, delivering dose to the cancer patient.

Conclusion

Percentage discrepancies (PD) were found out between measured and calculated values. PD describes how much calculated values resemble to measured values. For the same depth and field sizes, PDDs were found minute different for both the measured and calculated values at 6 MV. PD ranged between a maximum of 2.38 and minimum of 0.010 with mean value of 1.24 for 6 MV. It may depend on some factors such as properties of measuring devices and movement of water during measurements. PD gradients were also calculated and found ranging between a maximum of 0.1386 cm^{-1} and a minimum of 0.006 cm^{-1} with a mean value of 0.0723 cm^{-1} for 6 MV.

Acknowledgement

Authors are thankful to Higher Education Commission of Pakistan and Radiation Oncology Department, Shaukat Khanum Cancer Hospital and Research Centre, Lahore, providing facilitations to complete this project.

References

Ahnesjo, A., Aspradakis, M.M. 1999. Dose calculations for external photon beams in radiotherapy. *Physics in Medicine and Biology*, **44:** R99-R155.

Birgani, M.J.T., Karbalaee, S.M. 2009. Calculation of anylitical expressions for measured percentage depth dose data in megavoltage photon therapy. *Iranian Red Crescent Medical Journal*, **11:** 140-144.

Bloch, P., Altschuler, M.D. 1995. Three-dimensional photon beam calculations. In: *Radiation Therapy Physics, Medical Radiology*, A. R. Smith (ed.), pp. 33-42, Springer Berlin Heidelberg, Germany.

IAEA, 2000. *Absorbed Dose Determination in External Beam Radiotherapy*: *An International Code of Practice for Dosimetry Based on Standard of Absorbed Dose to Water*, Technical Report Series No. 398, International Atomic Energy Agency (IAEA), Vienna, Austria.

Khan, F.M. 2010. *The Physics of Radiation Therapy*: *M-Medicine Series*, 531 pp., 4th edition, Lippincott Williams & Wilkins Ltd., Baltimore, USA.

Peter, R.A., Peter, J.B., Coursey, B.M., Hanson, W.F., Huq, M.S., Nath, R., Rogers, D.W.O. 1999. AAPM's TG-51 protocol for clinical reference dosimetery of high-energy photon and electron beams. *Medical Physics*, **26:** 1847-1870.

Rogers, D.W. 2002. Monte Carlo techniques in radiotherapy. *Medical Physics*, **58:** 63-70.

Sameer, S.A.N. 2007. A comparative study of measured percentage depth doses for two medical linear accelerators. *Umm Al-Qura University Journal of Science Medicine and Engineering*, **19:** 145-151.

Pak. j. sci. ind. res. Ser. A: phys. sci. 2014 **57** (2) 63-69

Dynamics of Electron Concentration for Ionospheric Region of Pakistan

Syed Nazeer Alam[a]* and Muhammad Ayub Khan Yousufzai[b]

[a]Department of Electronics & Power Engineering, Navy Engineering College, National University of Sciences & Technology Karachi, Pakistan

[b]Department of Applied Physics, Solar-Terrestrial & Atmospheric Research Wing and Institute of Space & Planetary Astrophysics, University of Karachi, Karachi-75270, Pakistan

(received February 13, 2013; revised June 2, 2013; accepted June 19, 2013)

Abstract. The fluctuating dynamics of electron density is highly dependent on altitude from center of the earth. The long distance communication *via* F_2 layer is the best suited through refraction of radio wave in the range of 3-30 MHz. In present study, the F_2 layer hourly data for 2006, recorded at SUPARCO Islamabad Ionosphere Station (SIIS), located at latitude 33.75°N and longitude 72.87°E have been considered. The recorded ordinary wave frequency has been utilised to compute relationship with variation in electron concentration. The estimation of variability is determined for forecast and modeling purposes. The standard techniques have been performed such as regression, stochastic analysis and parameter estimation using data obtained from source. Predicting sky wave propagation at Pakistan ionospheric region has been presented.

Keywords: ionosphere, ordinary wave frequency, total electron count, electron density, temporal variations

Introduction

Our atmosphere is divided into several regions: the troposphere, the stratosphere and the ionosphere above the sea-level. The ionosphere resembles an optical device that reflects and refracts the radio waves. This process depends on the degree of ionisation of the ionosphere. This region is comprised of ionised structure with varying electron-ion concentration highly dependent upon solar radiation. It lies between altitudes of 70 to 600 km and participate in radio propagation. The ionosphere tends to be stratified, rather than regular, in its distribution. The existence of ionosphere as an electronically conducting region had been postulated in 1883 to explain the daily and seasonal variations in the geomagnetic field in 1902, appropriately that ionosphere contains free electrons and ions produced by solar ionising radiation (Robert and Andrew, 2004). The two reflecting layers in the ionosphere 90 to 110 Km called Heaviside layer (E region) and Appleton layer is 240 Km (Harrison, 1958). The ionosphere structure (C, D, E and F layers) characterised by level of ionisation depends upon strength of ultraviolet (UV), alpha and gama radiations from the sun and cosmic rays. The ionisation is the greatest in summer and day time, least in the winter and night. The sunspot, a standard index of solar activity has influence on the radio flux density of ionosphere (Barclay, 2003). The Appleton layer is about four times as strong a reflector as the Heaviside layer owing to the stronger concentration of electrons and ions (Harrison, 1958). It is this layer, which makes possible propagation of short waves round the world. In case of oblique-incidence ionospheric soundings the signal can be propagated *via* single hop, as is in present case or through successive reflections of the waves from the earth-ionosphere waveguide walls (Afanasiev *et al.,* 2001).

The layer. All ionosphere layers vary in altitude and density according to the solar cycles but these variations do not always have the sense in the different layers. The F layer extends 100 Km to 300 Km in night above the earth‘s surface. The bifurcation of F layer into F_1 and F_2 is observed by low noon value, evening concentration of ionisation and slow electron disappearance after sunset (Nazeer and Yousufzai, 2013). The F_1 layer is located at an altitude 150 Km to 210 Km and is called Chapman layer. This presents a regular stratification at moderate latitudes. Its maximum electron density (N_e) is given by equation (1), where R_o is sunspot number (Armal, 1974).

*Author for correspondence; E-mail: nazeer@pnec.nust.edu.pk

$$N_e = 2.5 * 10^{11} (1+ 0.0062 R_o) \text{ ..... (1)}$$

The altitude of the F_2 layer is at about 300 Km, its behaviour is different, since it exhibits seasonal anomaly from other layers and well supported for long distance ionosphere communication. The electron concentration varies between $20 * 10^{11}$ e/m^3 during the day and $5 * 10^{11}$ e/m^3 during the night. In fact the total electron concentration (TEC) in F_2 layer is > F_1 layer due to (i) smaller electron loss and (ii) variation in solar radiation (Dolukhanov, 1971).

Materials and Methods

Long distance propagation of electromagnetic waves for frequencies less than 30 MHz is controlled by the ionosphere. Martyn's theory suggests its principal characteristics (Armal, 1974). The ionosphere study has been carried out using radio methods by ground stations located at Islamabad, Pakistan. The mathematical model strategy has been implemented to compute electron concentration (N_e) as a result of temporal and seasonal variation in refractive index (μ) for recorded hourly ordinary wave frequencies of F_2 layer for 2006 using Digisond DG-256 equipment at Islamabad station. To evaluate relationship between ionosphere parameters statistical technique has been implemented to study parametric variability using Statistica and Minitab tools.

Ordinary wave frequency. The critical frequency is the limiting frequency at or below which a radio wave is reflected by an ionosphere layer using oblique incidence. The highest frequency returned to earth, when radiated upward in the vertical direction. Its varying value is dependent on electron-ion measurement round the clock. For F_2 layer the ordinary wave frequency (f_o) is related to peak value of electron concentration (Henry and Owen, 1969) given in equation (2).

$$f_o = \sqrt{80.8 N_e} \cong 9 \sqrt{N_{e(max)}} \text{ .....(2)}$$

For the 244 samples recorded hourly for year 2006, the maximum and minimum ordinary wave frequency are 9.49 MHz and 3.16 MHz, respectively. The reflection and refraction from the F_2 layer is the major factor in HF communications.

Electron density. The uv, α and γ emission have a greater ionising power, when the radiation frequency is higher. The density of electrons in the ionosphere varies as a function of geomagnetic latitude, diurnal cycle, annual cycle, and sunspot cycle. The peak value of electron density of F_2 layer is calculated with respect to measured ordinary critical frequency as given in the expression, equation (3) postulated by Anderson and Matsushita in 1974 (Robert and Andrew, 2004; Barclay, 2003).

$$N_{e(max)} = 1.24*10^4 f_o^2 \text{ (MHz) e/cm}^3 \text{ ..... (3)}$$

The calculated electron density maximum value is $1.1167 * 10^{12}$ and minimum value is $1.2382* 10^{11}$ e/m^3, respectively, with mean of $3.4274 * 10^{11}$ having standard deviation of 1.2871 e/m^3. King *et al*. (1964) calculated refractive index and absorption coefficient of weakly ionised air and showed that with the increase of ion density, the refractive index decreases. The gradual decrease in refractive index from layer to layer causes the upward obliquely incident ray to gradually bend away from the normal and ultimately return to the earth after total refraction (Ghosh, 1998). The ionosphere is weak plasma. Larmor (1924) suggested that plasma possesses dielectric constant > unity. The established relationship to compute value of refractive index of ionosphere layers ignoring influence of magnetic field is mentioned in equation (4) and (5).

$$\mu^2 = 1 - \left[\frac{\omega_p}{\omega} \right]^2 \text{ ..... (4)}$$

$$f_p = \sqrt{\frac{N_e^2}{\pi m \varepsilon_o}} \text{ ..... (5)}$$

where;

ω_p and ω are plasma frequency and frequency of the wave, mass of electron (m), with ε_o, medium characteristic constants (Ghosh, 1998). The total refraction occurs when the collision frequency of the ionosphere is less than the radio frequency and if the electron density in the ionosphere is great enough.

In present study, the variation in the computed values of refractive index is 0.94823 to 0.95226 with mean 0.95007 and a least standard deviation of 0.00059 offering bending of EM wave from F_2 layer at day and night finally providing skip distance mean value of 4099.5 Km with standard deviation of 357.4 Km and refraction of waves from layers of varying altitude.

Exploratory data analytic approach. The exploratory data analytic approach (EDAA) plays an important role

in statistical analysis. EDA approach relies heavily on graphical methods i.e., scheming of histogram for representation of distribution with single quantitative variable. The continuous envelope provides the hypothetical limit of samples. In this particular study, the sampling distribution of critical frequency and electron concentration are presented in histogram plots shown in Fig. 1-2. The distribution shows slight right

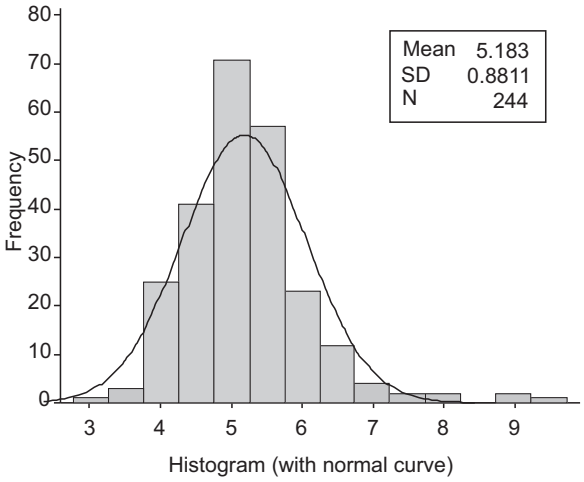

Fig. 1. Distribution of observed ordinary wave frequency.

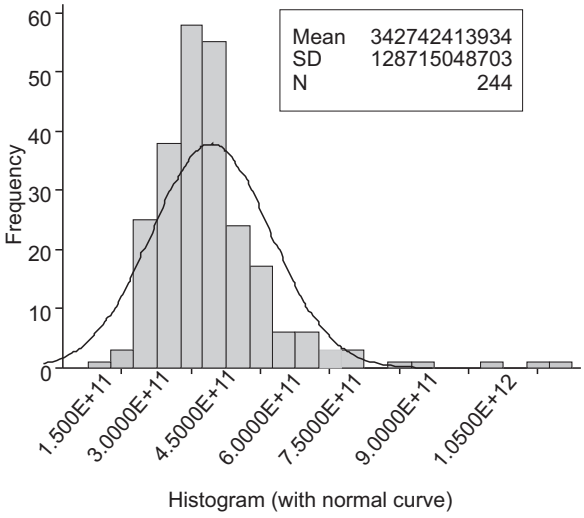

Fig. 2. Distribution of computed electron concentration.

scenes with few outliers those can be minimised in the later studies using robustness. The coefficient of variation (C_v), a normalised measure of dispersion of probability distribution is defined as ratio of standard deviation to the mean. From computed statistical data, C_v = 0.17 and 0.37 for ordinary wave frequency and electron concentration, respectively, show distribution with low variance i.e., C_v<1. The corresponding signal-to-noise ratio, inverse of C_v determined as 5.88 and 2.66. The other important statistical values are presented in Table 1.

Regression analytic strategy. According to Sir Francis Galton worked quantifying the strength of relationship to estimate or predict the known values of one variable with other variable is given by Walpole *et al*. (2012). The bivariate analysis presented in scatter plot in Fig. 3(a-b) displays positive correlation between ordinary wave critical frequency and electron concentration for linear and quadratic fit models of F^2 layer. The linear regression depicts line having an intercept equal - 4.05 * 10^{11} with slope of 1.44 * 10^{11} shows fairly fits through our sample data consisting of 244 observations. The Pearson's statistic, coefficient of determination, R^2 = 0.9750, R^2 (adj) = 97.5 %, R^2 (pred) = 97.26 % and Durbin-Watson statistic of 1.27183. The

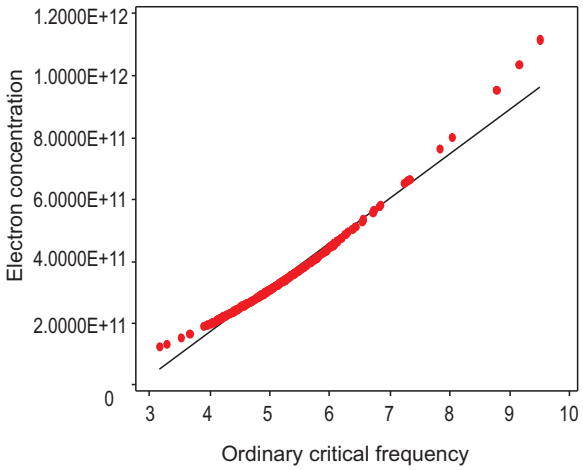

Fig. 3(a). Scatter plot for ordinary wave frequency and electron concentration.

Table 1. Computed parameter values

Parameter	Trim mean	Median	Variance	IQR	Skewness	Kurtosis	P value
f_o	5.12	5.07	0.7763	0.9290	1.45	4.60	0.000
N_e	3.29*10^{11}	3.19*10^{11}	1.65*10^{22}	1.17*10^{11}	2.52	10.52	0.000

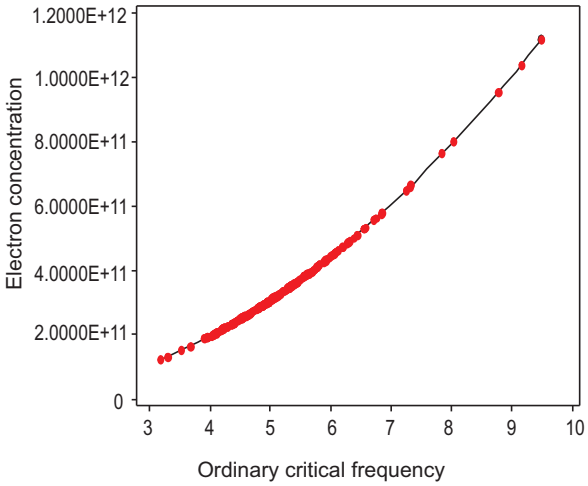

Fig. 3(b). Scatter plot for ordinary wave frequency and electron concentration.

linear fit regression model equation is mentioned in equation (6).

$$N_e = -4.05 * 10^{11} + 1.44 * 10^{11} f_o \quad \text{.....(6)}$$

The quadratic model incorporating all the values suggest the best fit with = 97.55 %. The quadratic fit regression model equation is mentioned in equation (7).

$$N_e = 2.1847*10^6 - 8.763*10^5 f_o + 1.24*10^{10} f_o^2 \text{ .....(7)}$$

These results show strong relationship i.e., changes in ordinary wave critical frequency are in accordance and relevant to real time astrophysics variations in ionosphere (Allan and Richard, 1985).

Stochastic approach. The stochastic approach suggesting correlation between adjacent points in time is the best investigation in terms of dependence of the present and the past values (Diebold, 1998). In this study seasonal pattern with periodic behaviour of variation in ordinary wave frequency and electron concentration against time with the best data fit in case of both linear and quadratic are shown in Fig. 4(a-b) and 5(a-b), respectively. The time plots show variations reflecting increase and decrease of data in the ionosphere of F^2 layer in day and F layer during night at Islamabad ionosphere region.

The simplest exponential characterisation method is single exponential smoothing (SES). This method, when properly applied, reveals more clearly the underlying trend, seasonal, cyclic components and non-stationarity

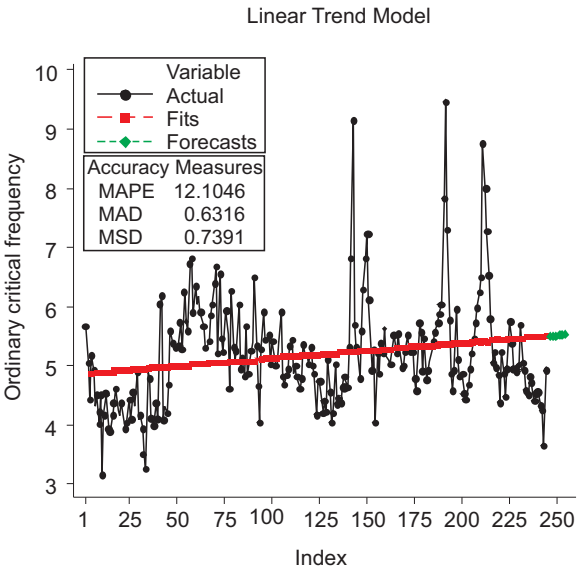

Fig. 4(a). Time plot of ordinary wave frequency.

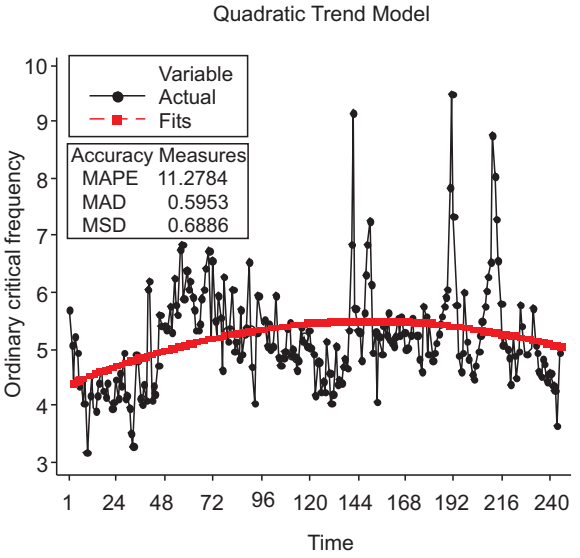

Fig. 4(b). Time plot of ordinary wave frequency.

present in time series plots are removed by differencing the data or by fitting some type of trend curve. The stochastic plots indicated in Fig. 4-5 exhibit rising trend for electron concentration and ordinary wave frequency under investigation. These plots witness a linear fit is sufficient to remove the trend but the variance (amplitude) is still varying with time. The single smoothing forecasting expression is mentioned in Equation (8). The forecast plots along with actual time series and single exponential smoothed series for fitting with linear trend curve for both parameters are shown

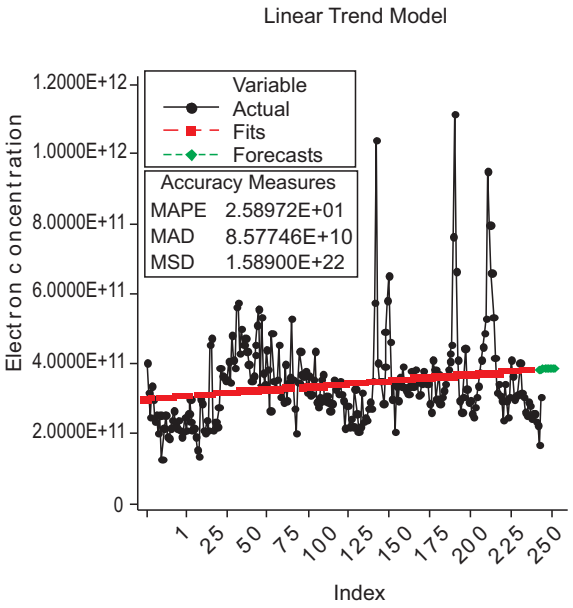

Fig. 5(a). Time plot of electron frequency.

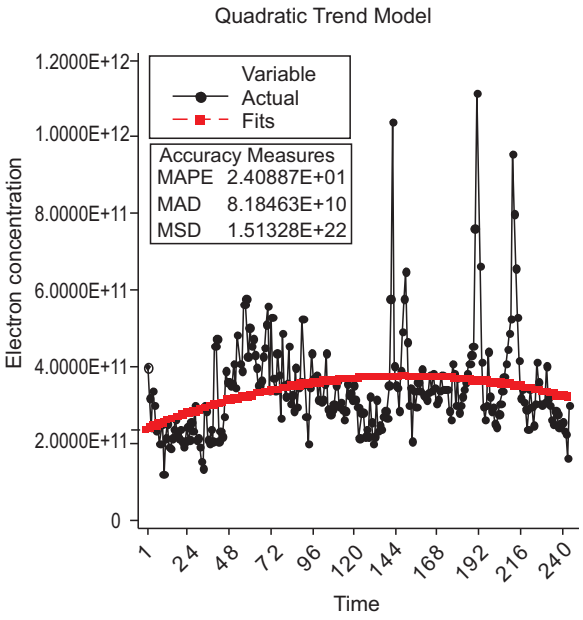

Fig. 5(b). Time plot of electron concentration.

separately (Walpole *et al*., 2012) in Fig. 6-7. In our case a 95% confidence interval will contain the true value of the population parameter with probability 95%.

$$F_{t+1} = \alpha Y_t + (1 - \alpha) F_t \quad \text{..... (8)}$$

$$0 < \alpha \leq 1 \text{ for } t > 0$$

The single smoothing coefficient, $\alpha = 0.718347$ and 0.824733 explain level of smoothing for mean percentage

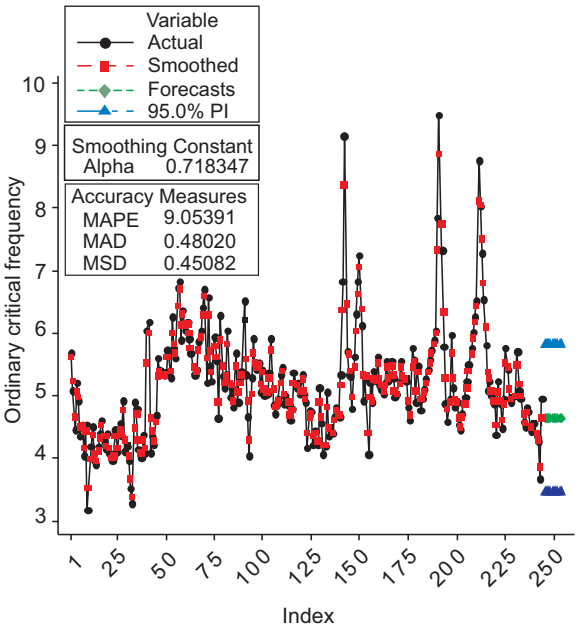

Fig. 6. Ordinary wave frequency-actual and exponential smoothing values.

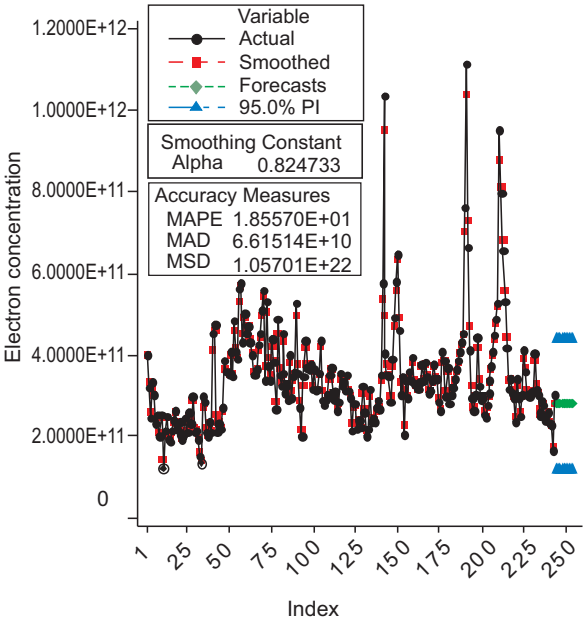

Fig. 7. Electron concentration-actual and exponential smoothing values.

error (MPE), mean absolute percentage error (MAPE) witness degree of accuracy in quantitative forecast with least residual with 95% prediction interval and how responsive the model is to show fluctuation in the data. This could be illustrated using ordinary wave critical frequency and electron concentration (Makridakis *et al.*, 1983). The summary of errors for both parameters is

mentioned in the expressions inside the illustration.

$$F_{t+1} = F_t + \propto (X_t - F_t) = F_t + \alpha\ (e_t) \quad \text{..... (9)}$$

The forecast values for ordinary wave frequency and electron concentration are computed using Bootstrapping technique, which estimates the distribution of an estimate by generating a large number of samples with replacement from the sample and re-computing the estimate for each of them (Ricardo *et al.*, 2006) mentioned in model equation (10).

$$F_{t+1} = \alpha\ Y_{origin} + (1 - \alpha)\ F_t \quad \text{..... (10)}$$

$$F_{245} = (0.718347)\ (4.94) + (1 - 0.718347)(4.63078) = 4.853 \text{ MHz}$$

$$F_{245} = (0.824733)\ (3.022605 * 10^{11}) + (1- 0.824733)\ (2.80586 * 10^{11}) = 2.987 * 10^{11} \text{ e/m}^3$$

Table 2. Forecast values obtained from bootstrap technique

Sample no	f_o MHz	N_e e/m^3
245	4.853	$2.987 * 10^{11}$
246	4.915	$3.018 * 10^{11}$
247	4.933	$3.024 * 10^{11}$
248	4.933	$3.025 * 10^{11}$
249	4.938	$3.025 * 10^{11}$

Results and Discussion

In this study physical mechanism of electron-ion production in the ionosphere have been discussed and quantified. The changeability observed in electron concentration is due to solar radiations received by the ionosphere. The presence of vertically distributed layered ionosphere structure, its temporal behaviour cause deviation in wave path and effect on radio wave communication have been analysed and values are predicted using boot strap smoothing approach. The data demonstrate evidence of parameter's fluctuating dynamic over period of time and season at low latitude ionosphere medium. To obtain results Digisound-256 hourly recorded data of ordinary wave frequency provided to compute the other parameters. The techniques implemented have been performed and the values of parameters are determined. The data distribution and trends have been found appropriate leading to the physical interpretation of the process occurred in the ionosphere. The forecast values have been obtained from the models developed for ionosphere region of Pakistan. These parametric values are useful for public, government and private sector organisations.

Acknowledgement

The authors are grateful to the officials of Pakistan Space & Upper Atmosphere Research Commission (SUPARCO) for providing ionosphere data. These data helped us in carrying out this research work.

References

Afanasiev, N.T., Grozov, V.P., Nosov, V.E., Tinin, M.V. 2001. On the chirp-signal structure along the oblique-incidence ionospherric sounding path. *Journal of Atmosphere and Solar-Terrestrial Physics,* **63:** 11-16.

Allan, H.M., Richard, W.K. 1985. *Probability, Statistics, and Decision Making in the Atmospheric Sciences,* pp. 301-304, Westview Press, Michigan, USA.

Armal, P. 1974. *Radio Wave Propagation,* pp. 122-123, Macmillan Press, Ltd., UK.

Barclay, L.W. 2003. *Propagation of Radio Waves,* pp. 160-168, 2nd edition, Institution of Electrical Engineers, London, UK.

Diebold, F.X. 1998. *Elements of Forecasting,* pp. 4-77, South-Western College Publication, USA.

Dolukhanov, M. 1971. *Propagation of Radio Waves,* pp. 214-215, translated by B.V., Kuznetsov, Mir Publisher, Moscow, Russia.

Durbin, J., Watson, G.S. 1951. Testing of serial correlation in least square regression, II. *Biometrika,* **38:** 159-179.

Ghosh, S.N. 1998. *Electromagnetic Theory and Wave Propagation,* pp. 118-119, Narosa Publishing House, New Delhi, India.

Harrison, J.A. 1958. *The Story of the Ionosphere; or, Exploring with Wireless Waves,* pp. 62-65, Hulton Educational Publications, London, UK.

Henry, R., Owen, K. 1969. *Introduction to Ionospheric Physics,* Academic Press, Inc, Library of Congress No. 69-12280 111 Fifth Avenue, New York, 10003, USA.

King, J.W., Smith, P.A., Eccles, D., Fooks, G.F., Helm, H. 1964. Preliminary investigation of the structure of the upper atmosphere as observed by the topside sounder satellite, alouette. *Proceeding of the Royal Society London, Series A*, **281:** 464-487.

Larmor, J. 1924. Why wireless electric rays can bend round the earth. *Nature*, **114:** 650-651.

Makridakis, S., Wheelwright, S.C., Victor, E.M. 1983. *Forecasting: Methods and Applications,* pp. 84-93; 355-356, 2nd edition, John Wiley & Sons, New York, USA.

Nazeer, A., Yousuzai, A. 2013. Study the stochastic perception of refractive index variability of ionosphere, *International Journal of Scientific & Engineering Research,* **4:** 217-221.

Ricardo, A. M., Martin, R.D., Victor, J. Y. 2006. *Robust Statistics: Theory and Methods*, pp. 140-141, John Wiley & Son Ltd., England, UK.

Robert, W.S., Andrew, F.N. 2004. *Ionospheres Physics, Plasma Physics, and Chemistry*, (Cambridge Atmospheric and Space Science Series), 570 pp., Cambridge University Press, Cambridge, UK.

Walpole, R.E., Myers, R.H., Myers, S.L., Ye, K.E. 2012. *Probability & Statistics for Engineers & Scientists*, 816 pp., 9th edition, Pearson Education International, Boston, USA.

Pak. j. sci. ind. res. Ser. A: phys. sci. 2014 **57** (2) 70-73

Extraction, Purification and Characterisation of Nutraceutical Grade Fulvic Acid from Lignite Coal of Lakhra-Jamshoro, Pakistan

Mahboob Ali Kalhoro[a]*, Amanat Ali[a], Abdul Hafeez Laghari[b] and Aftab Ahmed Kandhro[b]

[a]Fuel Research Centre (FRC- PCSIR), Off University Road, Karachi-75280, Pakistan

[b]PCSIR Laboratories Complex, Shahrah-e-Dr. Salimuzzaman Siddiqui, Karachi-75280, Pakistan

(received June 3, 2013; revised July 13, 2013; accepted July 26, 2013)

Abstract. Fulvic acid, a water-soluble substance was extracted from Pakistani coal. Pure fulvic acid fraction was recovered before the start of its decomposition. The mechanism forming the precipitates was based on re-crystallisation of fulvic acid in water (2.45% yields). Fourier transform infra red (FT-IR) as well uv-vis spectroscopic techniques were successfully employed to characterise and confirm the obtained crystals as fulvic acid. It was observed that the spectral features obtained from FT-IR and uv-vis spectroscopy were similar to those reported for fulvic acid fractions from other sources. Recovered pure fraction of fulvic acid was characterised by the suggested simple techniques.

Keywords: lignite coal, extraction, purification, fulvic acid, characterisation

Introduction

Humic deposits are unusual remains in earth's soil and deposits (e.g., coal). They also came from that ancient lush vegetation. These humic deposits never did turn into oil or coal. They are quite rare and can be found in various areas of the world. Some of these deposits are exceedingly rich in a little known substance called fulvic acid.

Fulvic acid is one of the nature's most powerful organic electrolytes that can balance and energise biological properties it comes into contact with (Baker, 1973). Like all common electrolytes, which are soluble in water and capable of conducting electricity (Gamble and Schnitzer, 1974), fulvic acid has also been proven to be powerful organic electrolyte, serving to balance cell life. If the individual cell is restored to its normal chemical balance and thereby in turn its electrical potential, could make possible to give life, where death and disintegration would normally occur within plant and animal cells (Laghari *et al.,* 2011). In test experiments on animal cells, it has been observed that upon withdrawing electrolyte potential cell got ruptured and disintegrated into the surrounding fluid causing death. However, reintroducing electrical potential resulted in cell reconstructing and the cell became active and healthy (Crile, 1926). Similarly, in human also, decrease in electric potential causes progressive weakness due to unchecked haemorrhage, overwhelming emotional stress, uncontrolled infections, unbalanced diet, prolonged loss of sleep and surgical shock. Whereas, balancing electric potential by an electrolyte like fulvic acid may lead to overcome these problems and hence it is convincingly proved that the physical well being of plants, animals and human beings is determined by proper electric potential that reduces to zero at death (Senesi *et al.,* 1989). Of all the electrolytes, fulvic acid has the outstanding ability to accomplish the objective of balancing electric potential in numerous ways and appeals to be explored by cheaper available sources with minimum efforts to extract. Keeping that in view, present study was focused on the extraction, purification and characterisation of neutraceutical grade fulvic acid from lignite coal of Lakhra-Jamshoro, Pakistan.

*Author for correspondence;
E-mail: kalhoro786pk@yahoo.com

Materials and Methods

All aqueous solutions were prepared with deionised water that was passed through a Millipore Milli-Q Plus water purification system. Sodium hydroxide, hydrochloric acid and phosphoric acid were purchased from Merck Schuchardt OHG 85662 Hohenbrunn, Germany.

Extraction of fulvic acid. Coal was collected from Lakhra coal reserves located near Jamshoro district of Sindh province of Pakistan. Coal sample was ground into powder and passed through sieves of 60 mesh size. The fine powder of ideally identical size was added

into a 250 mL vessel already containing 0.1 M sodium hydroxide. The whole stuff was thoroughly mixed and was kept for overnight. The mixture was filtered and 0.1 mL/M HCl was added to the filtrate and was kept for overnight. Resulting solution was filtered again and filtrate was neutralised with sodium hydroxide and concentrated by gentle heating. The concentrated mixture was kept at -4 °C and crystals formation started which were either white or yellow in colour (2.45% yields). Fine crystals were then subjected to characterise by using spectroscopic analytical techniques.

Characterisation of fulvic acid. ***FTIR spectral measurements.*** All infrared spectra were obtained using a Thermo Nicolet Avatar 320 FTIR spectrometer equipped with a removable diamond cell smart accessory, retreated triglycine sulphate (DTGS) detector and KBr optics, controlled by OMNIC software (Thermo Nicolet Analytical Instruments, Madison, WI). All spectra were collected by co-addition of 32 scans at a resolution of 4 cm^{-1} in the range of 4000-650 cm^{-1}. Remaining settings were kept as sample gain, mirror velocity and aperture 8.0, 0.6329 and 100.0.

The spectrum of each standard or sample was in ratio against a fresh background spectrum recorded from the bare ATR crystal; prior to collection of each background spectrum, the ATR crystal was carefully cleaned with propanol to remove any residual contribution of the previous sample, and remaining solvent was then evaporated using a stream of nitrogen gas (Sherazi *et al.,* 2009ab).

Results and Discussion

Humic acid was extracted from humus by first mixing the humus with a dilute alkali and then precipitating the humic acid out of solution by acidifying the mixture to a pH of 1 to 2. Fulvic acid, which is soluble at all pH levels, remains in the acid solution. It is yellow to brownish black in colour. Extraction of fulvic acid from other sources like from soil is not feasible as the presence of inorganic impurities decrease the net yield. Aquatic humus, predominantly has high percentage of fulvic acid and so is the preferred source for fulvic acid extraction.

Considerably, higher quantity of fulvic acid from lignite coal was extracted by the simple method therefore, it may be used to optimise this source for fulvic acid. Moreover, the purity of fulvic acid by suggested extraction method is one stepped simple and cheaper than other methods to recover the neutraceutical grade which can easily be brought to pharmaceutical grade. Fig. 1.

A representative ATR-FTIR spectrum of fulvic acid sample is shown in Fig. 2, which clearly shows the characteristic bands of the expected functional groups (Table 1). The exhibited broad band at 3393.7 cm^{-1}, which can be attributed to stretch of hydrogen bonded O-H group. The ester and acid carbonyl (C=O) functional groups show characteristic stretching bands at 1677.0 cm^{-1}, the bands were also observed in the region of 1620.6 cm^{-1} (aromatic C=C double bond, H-bonded C=O of conjugated ketones). The bending vibrations of C-O, C-N groups are observed at 1103.9 cm^{-1} due to presence of polysaccharide or polysaccharide like compounds (Mahesar *et al.,* 2010; Khanna *et al.,* 2008).

Fig. 1. Crystals of fulvic acid purified from coal.

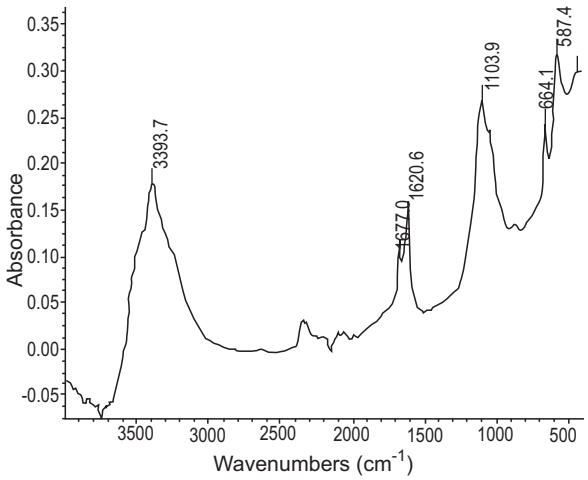

Fig. 2. ATR-FTIR spectrum of fulvic acid.

Table 1. ATR-FTIR, frequencies, intensity and functional group of fulvic acid sample

Frequency (cm^{-1})	Intensity	Assignment	Notes
3393.7	0.177	O-H	Alcohols and phenols
1677.0	0.0998	C=O	carboxylic acids
1620.6	0.142	C=C	often weak
1103.9	0.266	C-O, C-N	Polysaccharide or polysaccharide like compounds
664.1	0.242	R-C-H	Unsaturated alkenes and aromatics
441.4	0.297	C-Br, C-I	Often out of range of instrumentation
587.4	0.317	-	

The bands at 664.1 cm^{-1} is due to bending vibrations of R-C-H groups of unsaturated alkenes and aromatics. The bands at 587.4 and 441.4 belong to bending vibrations of C-Br, C-1 and often out of range of instrumentation. The FTIR spectra of fulvic acid extracted from coal showed bands of hydrogen bonded OH groups and conjugated C=C double bonds as well as C-O stretching of polysaccharide or sugar like substances (Mahesar *et al.,* 2011; Duarte *et al.,* 2003). Though, it is a matter of fact that due to complex structure, uv measurements of fulvic acid is not a considerable data to obtain an idea about structure. However, in some studies few measures have been taken to make it useful. Same were followed in this study and results complied with reported results. The strong absorbance at short wavelength s below 250 nm was attributed to the benzonoid bands of the carboxyphenols (Baes and Bloom, 1990), was most important evident to support characterisation of fulvic acid obtained by the Lakhra lignite coal. A similar nature of work was carried out by Saqib *et al.* (2011) and structural elucidation of humic acids was extracted from Pakistani lignite using spectroscopic and thermal degradative techniques

Conclusion

A simple approach for the extraction of fulvic acid from coal has been suggested. It is an easy extraction technique to obtain fulvic acid crystals from coal in pure form as neutraceutical grade. Its characterisation through analytical techniques mostly available in laboratories is also an additional feature of method simplicity. It is expected that the extraction method could be very helpful to industries of functional foods searching for neutraceuticals through cheaper sources and easy methods.

References

Aziz, S., Suhail, A., Soomro, A.H., Tunio, I.N., Qureshi, K.M., Begum, R. 2010. Environmental and health hazards of fly ash and SOx from FBC power plant at Khanote. *Pakistan Jouranl of Analytical & Environmental Chemistry,* **11:** 56-62.

Baes, A.U., Bloom, P.R. 1990. Fulvic acid ultraviolet-visible spectra: Influence of solvent and pH. *Soil Science Society of America Journal,* **54:** 1248-1254.

Baker, W.E. 1973. The role of humic acids from Tasmanian podzolic soils in mineral degradation and metal mobilization. *Geochimica et Cosmochimica Acta,* **37:** 269-281.

Crile, G. 1926. Decrease in electrical Potential. In: *A Bipolar Theory of Living Processes,* G. Crile (ed.), McMillan, New York, USA.

Duarte, R.M.B.O., Santos, E.B.H., Duarte, A.C. 2003. Spectroscopic characteristics of ultrafiltration fractions of fulvic and humic acids isolated from an eucalyptus bleached Kraft pulp mill effluent. *Water Research,* **37:** 4073-4080.

Gamble, D.S., Schnitzer, M. 1974. The chemistry of fulvic acid and its reaction with metal ions. In: *Trace Metals and Metals-Organic Interactions in Natural Waters,*P.C. Singer (ed.), 380 pp., Ann Arbor Science Publishers Inc., Ann Arbor, Michigan, USA.

Janos, P., Kozler, J. 1995. Thermal stability of humic acids and some of their derivatives. *Fuel,* **74:** 708-713.

Khanna, R., Witt, M., Anwer, M.A., Agarwal, S.P., Koch, B. 2008. Spectroscopic characterization of fulvic acids extracted from the rock exudate Shilajit. *Organic Geochemistry,* **39:** 1719-1724.

Laghari, A.H., Memon, S., Nelofar, A., Khan, K.M. 2011. *Alhagi maurorum*: A convenient source of lupeol. *Industrial Crops and Products,* **34:** 1141-1145.

Saqib, N., Sarfaraz, T.B., Verheyen, T.V., Chaffee, A.L. 2011. Structural elucidation of humic acids extracted from Pakistani lignite using spectroscopic and thermal degradative techniques. *Fuel Processing Technology*, **92:** 983-991.

Mahesar, S.A., Sherazi, S.T.H., Kandhro A.A., Bhanger, M.I.. Khaskheli, A.R., Talpur M.Y. 2011. Evaluation of important fatty acid ratios in poultry feed lipids by

ATR FTIR spectroscopy. *Vibrational Spectroscopy,* **57:** 177-181.

Mahesar, S.A., Kandhro, A.A., Cerretani, L., Bendini, A., Sherazi, S.T.H., Bhanger, M.I. 2010. Determination of total trans fat content in Pakistani cereal-based foods by SB-HATR FT-IR spectroscopy coupled with partial least square regression. *Food Chemistry,* **123:** 1289-1293.

Senesi, N., Miano, T.M., Provenzano, M.R., Brunetti, G. 1989. Spectroscopic and compositional comparative characterization of i.h.s.s. reference and standard fulvic and humic acids of various origins. *Science of the Total Environment,* **81-82:** 143-156.

Sherazi, S.T.H., Talpur, M.Y., Mahesar, S.A., Kandhro, A.A., Arain, S. 2009a. Main fatty acid classes in vegetable oils by SB-ATR-Fouriertransform infrared (FTIR) spectroscopy. *Talanta,* **80:** 600-606.

Sherazi, S.T.H., Kandhro, A., Mahesar, S.A., Bhanger, M.I., Talpur, M.Y., Arain, S. 2009b. Application of transmission FT-IR spectroscopy for the trans fat determination in the industrially processed edible oils. *Food Chemistry,* **114:** 323-327.

Pak. j. sci. ind. res. Ser. A: phys. sci. 2014 **57** (2) 74-85

Evaluation of Free Radical Scavenging Activity of Tea Infusion of Commercial Tea Products Available in UAE

Fazilatun Nessa* and Saeed Ahmed Khan
Department of Pharmaceutical Chemistry and Natural Products, Dubai Pharmacy College,
P.O. Box 19099, Dubai, United Arab Emirates

(received September 25, 2012; revised November 19, 2012; accepted December 5, 2012)

Abstract. In the present study, twenty four commercial tea samples were assayed to determine their free radical scavenging activity and polyphenolic contents based on the brewing/infusing period. Tea samples were infused/brewed in 200 mL boiled water at 120 °C for 1, 2 and 5 min, respectively. The radical scavenging activities of tea infusion/brewing were measured using 1,1-diphenyl-2-picrylhydrazyl radical (DPPH) assay method. The results were ranged from 67.81-90.51% for black tea bags, 90.37-94.51% for green tea bags, 24.66-92.25% for black tea powder, 16.08-93.06% for green tea powder and 32.90-45.54% for Camomile herbal infusion. The results showed that 1 or 2 min black tea bags infusion exhibited highest radical scavenging activity than 5 min infusion. Antioxidant activities of tea powders were variable with the amount of tea powder. It was observed that antioxidant activity increased with increasing boiling time for smaller amount of sample. In contrary, shorter boiling time was better for larger amount of sample. The polyphenol contents of tea infusion were determined and the results were expressed as milligram quercetin equivalent/200 mL of tea infusion. The polyphenol content was increased with increased brewing period. In contrary, brewing for longer time rendered extract less antiradical activity. This study suggests that infusing tea bag for 1 or 2 min is sufficient for getting infusion with maximum radical scavenging activity and in case of tea powder, shorter boiling time is better for larger amount of powder or small amount of powder should be boiled for minimum 5 min for rendering extract with maximum radical scavenging activity.

Keywords: tea bag, tea powder, antioxidants, polyphenols, 1,1-diphenyl-2-picrylhydrazyl radical

Introduction

Tea is an infusion of the leaves of the *Camellia sinensis* (Theaceae) plant. It is one of the most popular beverages in the world and currently revealed that it can promote health and helps to prevent a number of diseases (Arab *et al.*, 2009; Peters *et al.*, 2001). Tea is rich in flavonoids and other polyphenols known as catechins. The type of flavonoids found in different types of tea will depend on the level of processing the tea leaves. Depending on the manufacturing process, teas are classified into three major types, green tea non-fermented, oolong tea semi-fermented and black tea-fermented (Gupta *et al.*, 2008; Zuo *et al.*, 2002). During the oxidation process, enzymatic activity allows for the catechins to be polymerised and thus alter their structure. Typically, green tea leaves undergo minimal oxidation hence, retaining the majority of catechins. Black tea receives significant oxidation under controlled temperatures and humidity and results in the polymerisation of catechins into theaflavins and thearubigins. Theaflavins possess benzotropolone rings with dihydroxy or trihydroxy substitution systems which give the characteristics colour and taste of the black tea (Menet *et al.*, 2004). These catechins and their polymer can protect against heart disease and cancer (Higdon and Frei, 2003; Lambert and Yang, 2003; Vita, 2003; Yang and Landau, 2000; Lin *et al.*, 1999; Buschman, 1998). Black tea extracts containing thearubigins, also effectively protect against the paralytic actions of botulinum neurotoxins (Satoh *et al.*, 2001). Recently, reported green tea polyphenols exhibited beneficial effect on pathological states related to oxidative stress of the kidney (Yokozawa *et al.*, 2012) and in oral health (Narotzki *et al.*, 2012). The beneficial effects of tea are many, be ascribed to tea's antioxidant activity for their polyphenol contents. A number of studies reported that tea contained a number of polysaccharides which also exhibited good antioxidant activity (Wang *et al.*, 2012; Xiao *et al.*, 2011). However, the structural criteria of flavonoids for the potent free-radical scavengers are the presence of *ortho*-hydroxylation on the B-ring, a C_2-C_3 double bond in C-ring and the presence of 3-hydroxyl groups (Nessa *et al.*, 2004; Bors *et al.*, 1997; 1990; Rice-Evans *et al.*, 1996). Levels of flavonoids in a tea brew will depend on many factors that include

*Author for correspondence; E-mail: nessa1995@yahoo.com

type of tea used or present in the tea bag as well as how long the tea is left to infuse in the water etc., (Peterson *et al.*, 2004). Though, extensive work already done on the antioxidant potential of tea products (Nkubana and He, 2008; Su *et al.*, 2007; Gramza *et al.*, 2005; Cao *et al.*, 1996), but very little information is available to study the free radical scavenging activity of tea infusion based on the brewing period. Therefore, the main aim of this research was to qualify the effectiveness of black, green and herbal tea infusion as the free radical scavengers based on the brewing period.

Materials and Methods

Samples. A set of 24 processed commercial tea products that includes: 8 black tea bag samples, 9 black tea powder samples, 5 green tea bag samples, 1 green tea powder sample and 1 herbal tea sample were purchased from the supermarket of Dubai, UAE during the September-October, 2011. The samples had been manufactured in different commercial factories using standard manufacturing conditions. The descriptions of samples are shown in the Table 1.

Table 1. Description of tea products

Product	Manufacturer	Origin/country
Black tea bags		
Ahmed Tea London (English Tea No.1)	Packed in Sirlanka Ahmed Tea Limited	England (Sirlanka, India)
Red Label (Brooke Bond)	Packed in UAE by Unilever Gulf FZE	India
Lipton (Yellow Label Tea)	Packed in UAE by Unilever Gulf FZE	-
Lulu (Blender's special)	Packed in UAE by Unilever Gulf FZE	India , Sirlanka, Africa
Alokozay (Premium Tea)	Packed in UAE by Alokozay Tea International	Sirlanka
Tetley London	Packed in India for Tetley GB Ltd	England
(Drawstring Pure Black Tea)	TATA Tea Enterprise	
Kanan devan (TATA Tea)	Packed & Exported by TATA Tea Limited	India
Premium (TATA Tea)	Packed & Exported by TATA Tea Limited	India
Black tea powder		
Ahmed Tea London (English Tea No.1)	Packed in Sirlanka Ahmed Tea Limited	India
Red Label (Brooke Bond)	Packed in UAE by Unilever Gulf FZE	-
Lipton (Yellow Label Tea)	Packed in UAE by Unilever Gulf FZE	India , Sirlanka, Africa
Lulu (Blender's special)	Packed in UAE by Unilever Gulf FZE	Srilanka
Alokozay (Premium Tea)	Packed in UAE by Alokozay	Tea International Ltd., India
Kanan Devan (TATA Tea)	Packed & Exported by TATA Tea Limited	India
Premium (TATA Tea)	Packed & Exported by TATA Tea Limited	India
Leone (Finest Indian Tea)	Crown Oriental Food Ltd Wembley Mildx HAO U.K	India
Society Tea (From the house of Hasmukhxai & Co)	Packed by Amerty privet Ltd	-
Green tea bags		
Twinings of London (Green Tea & mint)	Packed R.Twining & Company Limited	-
Lipton (Clear Green)	Packed in UAE by Unilever Gulf FZE	England
Tetley (Drawsting Pure Green Tea)	Packed in India for Tetley GB Ltd	Sirlanka
Alokozay (Premium Tea) Green Tea	Packed in UAE by Alokozay	Sirlanka -
Tea International Ltd.,		
Dilma (Special Green Tea with natural Jasmine Petals)	Packed in Sirlanka Dilmah Australia Pty Ltd	UAE
Green tea powder		
Packed R.Twining & Company Limited	Twining of London (Green Tea & mint)	-
Herbal tea product		
Camomile Herbal Infusion (Safa)	Hassani Tea & Herbs Factory,	UAE

Chemicals. 1,1-Diphenyl-2-picrylhydrazyl (DPPH) radical, quercetin, anhydrous sodium carbonate, Folin-Ciocalteu reagent, L-ascorbic acid, 1,1-diphenyl-2-picrylhydrazyl, and methanol (spectroscopic grade) were purchased from Sigma Chemical Co. (USA).

Sample preparation. Tea infusions were prepared by infusing and steeping without stirring. For tea infusion, different tea bags were infused in 200 mL boiled distilled water at 120 °C for 1, 2 and 5 min, respectively. The tea brew were prepared for tea powder, where different amounts of tea powder were boiled in 200 mL at 120 °C in a thermostatic hot plate for 1 and 5 min, respectively. The tea infusion and brew was filtered through Whatman No. 1 filter paper, and brought at room temperature (25 °C). The aqueous tea filtrates were then immediately used for the determination of solid contents (yield), total polyphenolic contents and antioxidant activities.

Measurement of antioxidant activity. ***DPPH free radical scavenging method.*** The antioxidant activity of different aqueous tea extracts were evaluated using a stable radical, 1,1-diphenyl-2-picrylhydrazyl in a methanol solution according to the method of Nessa *et al.* (2004). Briefly, 100 µL tea infusion solution was placed in a cuvette and 3.9 mL of 0.1 mM methanolic solution of DPPH radical was added. The solution was incubated for 30 min at 25 °C in dark and the absorbance was measured at λ517 nm with a Shimadzu-1700 uv-vis spectrophotometer. A blank sample (without tea infusion) containing methanolic DPPH radical was measured with the sample. All determinations were performed in three replicates. The percent inhibition of DPPH radical by the samples was calculated according to the formula, as follows:

$$\% \text{ inhibition} = [(A_{C(0)} - A_{A(t)})/A_{C(0)}] \times 100$$

where:

$A_{C(0)}$ is the absorbance of the control at t = 0 min and $A_{A(t)}$ is the absorbance of the antioxidant at t = 30 min.

A dose response curve was plotted for few selected tea products for studying hydrogen donating abilities of tea extracts. In this study, absorbance measurement commenced immediately. The decrease in absorbance at λ517 nm was determined continuously with data capturing at 2 min intervals until absorbance stabilised (± 30 min). L-ascorbic acid was used as positive control.

Determination of total polyphenol content. Total polyphenolic contents were determined by the Folin-Ciocalteau method described by Scalbert *et al.* (1989). Folin Ciocalteu reagent was diluted (1:10) with distilled water. Briefly, the 100 µL tea infusion/brewing solution (three replicates) were mixed with 2 mL diluted Folin Ciocalteu reagent and then 2 mL aqueous Na_2CO_3 (7.5%). The mixture was allowed to stand for 1.5 h and the absorbance was measured at λ765 nm with a Shimadzu-1700 uv-vis spectrophotometer. The standard curve was prepared from 1-300 g/mL solutions of quercetin in methanol: water (80:20, v/v). The regression equation was y = 0.004x + 0.0166 with regression coefficient (r) 0.999. Total polyphenol values were expressed as milligram of quercetin equivalents per 200 mL of tea infusion.

Results and Discussion

Antioxidant activity of tea product infusion. Antioxidant activities of tea leaves infusion were determined according to the DPPH radical scavenging method. The DPPH radical has been widely used to test the free radical scavenging ability of various natural products (Sanchez-Moreno, 2002; Chen *et al.*, 1999; Yamaguchi *et al.*, 1998). According to this method, a compound with high antioxidant activity effectively binds with the radical hence, prevent its propagation and the resultant chain reaction. The results were expressed as mean ± standard deviation (SD). The data of 1, 2 and 5 min infusion of tea bags were compared for each product and were subjected to a one-way analysis of variance (ANOVA). Tukey's test ($P<0.05$) was performed to determine the significance of the difference between means.

Black tea bag products. Eight black tea bags and one herbal sample were infused for 1, 2 and 5 min, respectively. For 1 min infusion, Tetley and Kanan Devan showed the highest free radical scavenging activity as decreased in the order of: Tetley ≥ Kanan Devan > Lulu > Alkozay > Red Label > Lipton > Ahmed > Camomile. In case of 2 min infusion, Lipton, Red Label and Kanan Devan exhibited highest free radical scavenging activity as decreased in the order of, Kanan Devan ≥ Lipton ≥ Red Label ≥ Lulu > Tetley > Ahmed > Alkozay > Tata > Camomile. For 5 min infusion, Lipton, Red Label, Kanan Devan and Ahmed showed equal and highest free radical scavenging activity than other black tea bag products as decreased in the following order: Lipton ≥ Red Label ≥ Ahmed Kanan Devan ≥ Alkozoay ≥

Tetley > Lulu > Tata > Camomile. Overall, Lipton, Red Label, Kanan Devan and Tetley showed the highest free radical scavenging activity and Camomile was the least free radical scavengers (Table 2). In comparison between 1, 2 and 5 min tea infusion for each product, overall 2 min tea infusion gave higher antioxidant activity than 1 min. Tea infusion for 5 min gave lowest antioxidant activity except Ahmed tea bag, which gave higher antioxidant activity with increasing infusion time (5 min > 2 min > 1 min) (Fig. 1). Amongst the studied black tea bag products Tata tea bag showed comparatively lower antioxidant activity than other tea products and showed highest antioxidant activity at 2 min infusion. But the mean differences were not significantly different ($P<0.05$) for Lulu (1, 2 min), Lipton (2, 5 min), Red Label (2, 5 min), Tetly (1, 2 min), Kanan (1, 2, 5 min), Ahmed (2, 5 min) and Alkozay (1, 5 min). Camomile, a herbal infusion showed lowest antioxidant activity and was significantly, lower than the other tea bag samples (Fig. 1). The antioxidant activity of tea infusion depends on many factors, one of these factor is the amount of leaves present in a tea bag (Peterson *et al.*, 2004). All the studied black tea bags contained tea leaves in the ranges of 2.03 to 2.68 g except Camomile herbal tea which contained about 0.95 g leaves in a bag. It seems the lowest antioxidant activity of Camomile was due to the lower amount of leaves present in the tea bag. From the results it was concluded that brewing the black tea bags for 1 to 2 min was sufficient to obtain higher antioxidant activity.

Green tea bag products. Five tea bag samples were infused for 1 and 5 min for determination of their free

Table 2. Free radical scavenging activity and total polyphenol concentration of tea infusion of different black tea bag samples. Results are mean ± SD ($n = 3$)

Products	Av. wt. of tea leaves/bag (g)	Brewing period (min)	Solid contents (mg/mL)	Scavenging of DPPH$^{\bullet}$ (% ± SD)	Polyphenol /200 mL products tea infusion (mg ± SD)
Lulu	2.04	1	2.01	88.64 ± 0.50	35.13 ± 1.95
		2	2.98	88.50 ± 0.77	73.14 ± 1.35
		5	3.98	86.49 ± 0.33	124.25 ± 2.55
Lipton	2.07	1	2.21	82.18 ± 0.66	30.51 ± 1.47
		2	3.13	90 ± 0.55	49.82 ± 1.65
		5	4.29	88.9 ± 0.43	156.2 ± 2.41
Tata	2.03	1	1.76	78.44 ± 0.11	59.84 ± 1.28
		2	2.44	82.90 ± 0.88	82.14 ± 2.72
		5	4.01	80.17 ± 0.67	122.25 ± 1.25
Red Label	2.07	1	2.4	84.77 ± 0.50	24.64 ± 1.99
		2	3.78	89.94 ± 0.66	66.49 ± 0.91
		5	4.35	88.64 ± 0.88	103.34 ± 1.25
Tetley	2.68	1	2.36	89.79 ± 0.99	75.22 ± 0.95
		2	3.69	88.79 ± 0.32	106.75 ± 1.14
		5	4.43	87.06 ± 0.58	209.47 ± 0.75
Kanan Devan	2.07	1	1.72	89.94 ± 0.34	46.37 ± 1.16
		2	2.39	90.51 ± 0.88	78.4 ± 1.23
		5	3.87	88.21 ± 0.95	121.25 ± 1.35
Ahmed	2.06	1	1.74	67.81 ± 0.54	21.43 ± 1.15
		2	2.01	87.5 ± 0.56	77.68 ± 1.12
		5	3.66	88.6 ± 0.37	133.52 ± 1.50
Alkozay	2.06	1	1.50	86.06 ± 0.66	29.69 ± 1.77
		2	2.41	85.63 ± 0.44	74.5 ± 1.11
		5	3.33	87.35 ± 0.79	139.68 ± 0.94

radical scavenging capacity (Table 3). All products exhibited in the ranges of 90.37-94.51% free radical scavenging activity as long as it brewed. In comparison between 1 min infusion of green tea bag samples, Tetley tea bag showed highest antioxidant activity than other studied samples as decreased in the order of: Tetley > Dilma ≥ Lipton > Alkozay > Twinings. For 5 min infusion, the antioxidant activity decreased in the order of: Lipton > Dilma > Alkozay > Tetley > Twinings (Fig. 1). But the mean differences between 1, 2 and 5 min infusion were not statistically significant (P > 0.05). It seemed 1 min infusion was enough to get maximum antioxidant activity and infusion for longer time did not significantly increase or decrease the antioxidant activity. The detailed analytical value for all studied tea bag herbal products are tabulated in Table 2-3.

Black and green tea powder products. In this study, 9 black tea powders and one green tea powder samples were analysed. Four different amounts (0.1 g, 0.5 g, 1.0 g and 2.0 g) of tea leaves powder for each product were boiled for 1 min and 5 min separately (Fig. 2). For 1 min infusion of all samples, the free radical scavenging activity significantly (P > 0.05), increased

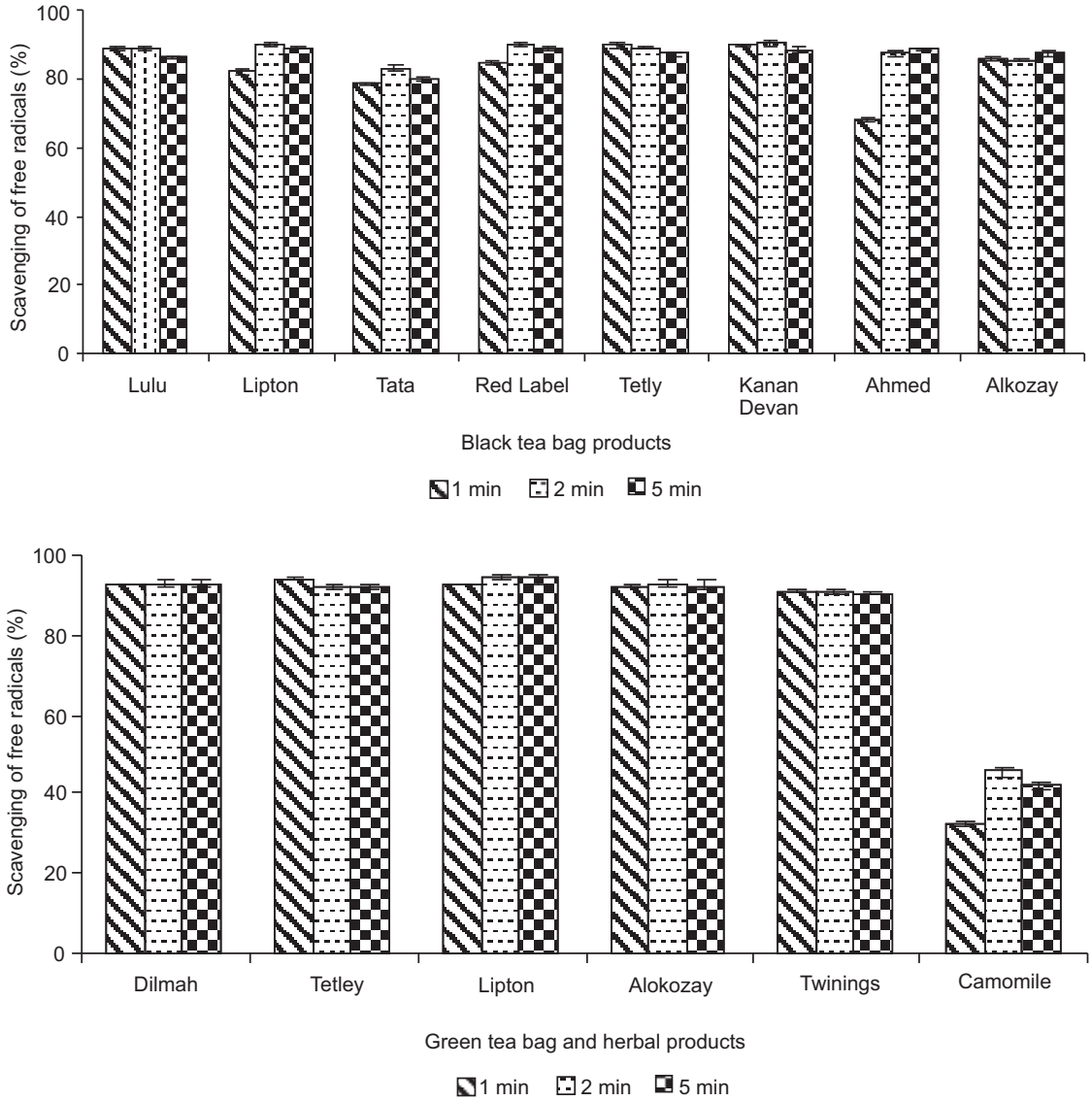

Fig. 1. Free radical scavenging activity of different manufacturer's tea bags (black, green and herbal) samples measured using the DPPH assay. Results are mean ± SD (n = 3).

with increasing the amount of samples. For 5 min infusion, free radical scavenging activity only increased for 0.1 and 0.5 g samples but in contrary, decreased for 1.0 and 2.0 g samples with increasing boiling period from 1 min to 5 min (Table 4-5). It seems shorter brewing period was better for larger amount of powder, in contrary, longer brewing period was necessary for brewing smaller amount of tea powder for getting higher antioxidant activity.

For a few selected tea samples the rate of reaction with the free radicals was also evaluated. In dose response studies it was found that tea infusion scavenged the free radicals very fast as it can be seen in Fig. 3-4 and reached a steady state within 5 min. Camomile, a herbal sample very slowly scavenged free radicals as compared to Lipton tea samples (Fig. 3B). In comparison of green tea with black tea bag samples, black tea scavenged free radicals comparatively slowly than green tea bag

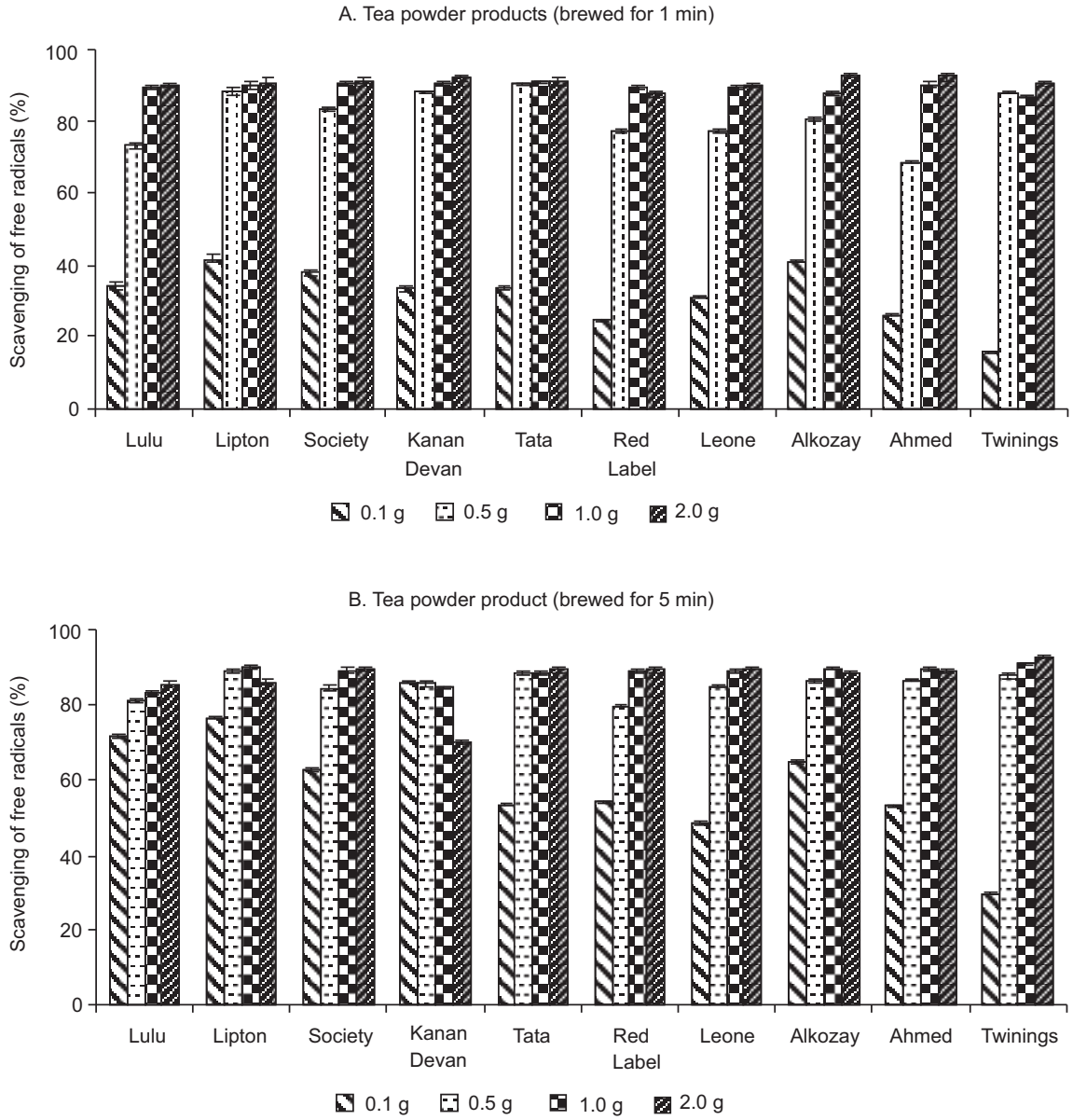

Fig. 2. Free radical scavenging activities of tea infusion prepared from different amount of tea powder leaves *vs*. the scavenging of free radicals, measured using the DPPH assay. Results are mean ± SD (n = 3). Samples were brewed for 1 min (A) and 5 min (B).

Table 3. Free radical scavenging activity and total polyphenol concentration of tea infusion of different green tea bag/herbal samples. Results are mean SD (n = 3)

Products	Av. wt. of tea leaves/bag (g)	Brewing contents (min)	Solid period (mg/mL)	Scavenging of DPPH$^{\bullet}$ (% ± SD)	Polyphenol /200 mL products tea infusion (mg ± SD)
Dilma	2.11	1	1.82	93.11 ± 0.32	41.49 ± 1.05
		2	2.99	93.32 ± 0.73	86.45 ± 0.9 5
		5	3.53	93.32 ± 0.92	137.55 ± 1.11
Tetley	2.16	1	1.43	94.07 ± 0.34	63.17 ± 0.96
		2	3.11	92.46 ± 0.73	95.23 ± 1.26
		5	3.92	92.46 ± 0.63	165.50 ± 1.84
Lipton	1.54	1	1.52	93.11 ± 0.25	64.65 ± 0.60
		2	3.04	94.51 ± 0.62	72.67 ± 0.60
		5	3.68	94.51 ± 0.83	92.23 ± 1.63
Alkozay	1.95	1	1.90	92.68 ± 0.25	68.33 ± 2.45
		2	3.16	92.89 ± 0.62	89.34 ± 1.60
		5	4.01	92.89 ± 0.15	164.57 ± 0.73
Twinings	2.04	1	1.31	91.09 ± 0.45	140.85 ± 2.62
		2	2.97	90.94 ± 0.74	158.65 ± 2.62
		5	3.65	90.37 ± 0.31	171.85 ± 1.21
Camomile	0.95	1	0.99	32.90 ± 0.73	62.17 ± 1.89
		2	1.34	45.54 ± 0.92	61.46 ± 1.39
		5	2.44	42.09 ± 0.87	63.2 ± 1.27

infusion, but after 5 min there were no significant differences in their scavenging activities (Fig. 3A). In dose-response studies of tea power (2.0 g) and tea bag (2.04 g), infusion of tea bag scavenged free radicals comparatively little faster than the powder leaves infusion as it can be depicted from the Fig. 4. In dose-response studies, L-ascorbic acid was used as a reference standard and reacted with DPPH immediately and reached a steady state within a minute (Nessa *et al.*, 2004). Its scavenging capability was rapid and dependent on concentration/dose (Fig. 3B). In this study, all the studied tea infusions also reacted rapidly with DPPH radical and reached a steady state within 2 to 5 min. It seemed tea infusion also acted as fast free radical scavenger as ascorbic acid.

The total polyphenols content of tea bag and tea powder products. Free radical scavenging activity of tea extracts depends mainly on its polyphenolic content (Gupta *et al.*, 2008; Higdon and Frei, 2003; Yang and Landau, 2000). Therefore, the polyphenolic contents of all studied tea products were determined and the results were expressed as milligram quercetin equivalent/ 200 mL of tea infusion. The results are presented in Table 2-5. In case of black and green tea bags, the polyphenolic content increased with increasing brewing time from 1 min to 5 min. In comparison amongst 1 min infusion of black tea bag samples, lowest concentration was recorded in Ahmed tea bag (21.43 ± 1.15) and highest amount recorded in Tetly tea bag (75.22 - 0.95). The overall results were decreased in the order of: Tetly > Tata > Kanan Devan > Lulu > Lipton ≥ Alkozay > Red Label > Ahmed. In case of 2 min infusion, highest concentration was recorded in Tetly tea bag (106.75 ± 1.14) and the results decreased in the order of: Tetly > Tata > Ahmed ≥ Kanan Devan > Alkozay > Lulu > Red Label > Lipton. For 5 min infusion, the lowest amount recorded in Red Label (103.34 ± 1.25) and the results decreased in the order of: Tetly > Lipton > Alkozay > Ahmed > Lulu > Tata > Kanan Devan > Red Label. However, Tetley exhibited highest polyphenolic content amongst the studied tea bag samples, in contrary, the polyphenolic content of Camomile (a herbal infusion) was not increased with increasing infusion time and the values were in the ranges of 61.24 mg to 63.2 mg. The polyphenolic content of all studied black tea bag samples are tabulated in Table 2.

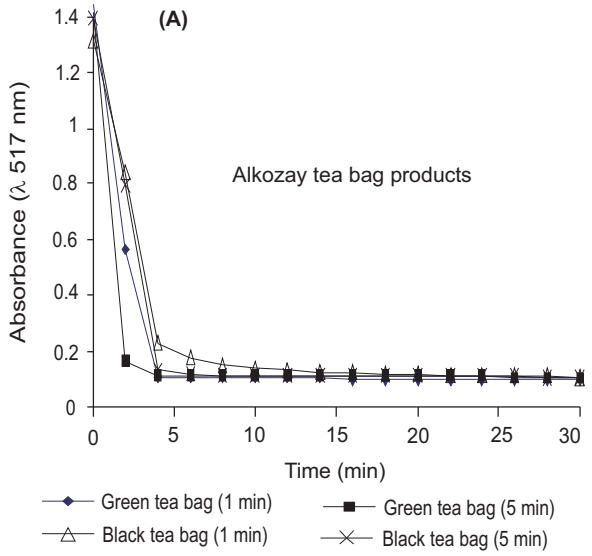

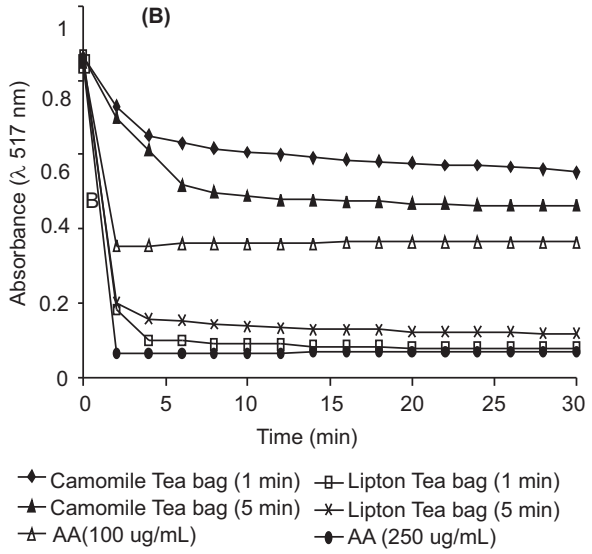

Fig. 3. Hydrogen donating abilities of Alkozay tea bag products (A) Camomile, Lipton tea bag products and Ascorbic acid (AA, 100 and 250 μg/mL) (B) on 1,1-diphenyl-2-picrylhydrazyl (DPPH) radical.

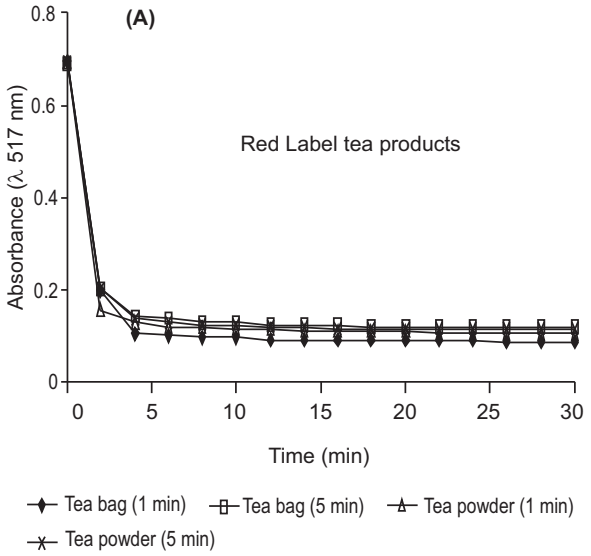

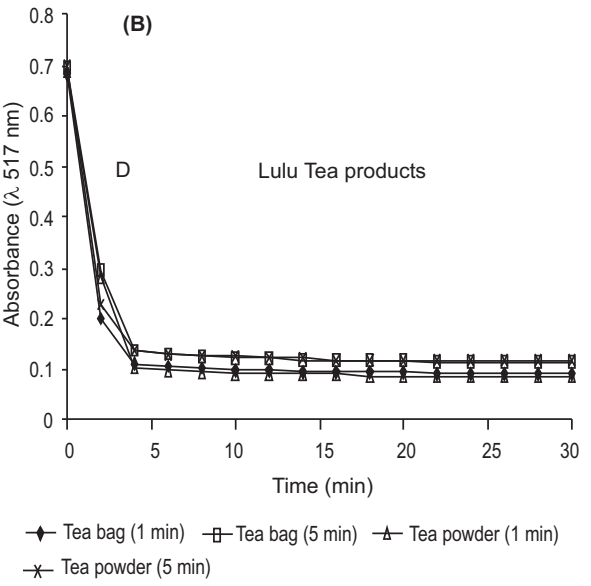

Fig. 4. Hydrogen donating abilities of Red Label tea products (A) and Lulu tea products (B) on 1,1-diphenyl-2-picrylhydrazyl (DPPH) radical.

For green tea bag samples, 5 min infusion exhibited higher concentration of polyphenols than 1 min infusion. Dilma tea bag showed lowest polyphenol content (41.49 mg) for 1 min infusion and Twinings exhibited highest content about 140.85 mg. For 5 min infusion, again Twinings showed highest polyphenol content (171.85 mg) and lowest amount recorded in Tetley (63.17 mg). Though, polyphenol content of all tea bag samples increased with increasing infusion time but in contrary, DPPH radical scavenging activity was not increased with increasing polyphenol content. Though polyphenol content of Dilma was lower for 1 min infusion than 5 min, but both infusions scavenged free radicals effectively. Other studied green tea bag samples also exhibited similar results, as it can be depicted from Table 3. It seems that some other chemical compounds such as tannin extracted at longer boiling time, which might interfered the free radical scavenging

Table 4. Free radical scavenging activity and total polyphenol concentration of infusion of tea leaves powder samples (Lulu, Lipton, Society, Kanan Devan, Tata and Red Label). Results are mean SD (n = 3)

Tea product (powder)	Wt. of tea powder (g)	Brewing period			
		(1 min)		(5 min)	
		Scavenging of DPPH$^{\bullet}$ (% ± SD)	Polyphenol mg/200 mL tea infusion	Scavenging of DPPH$^{\bullet}$ (% ± SD)	Polyphenol mg/200 mL tea infusion
Lulu	0.1032	34.19 ± 0.97	2.94 ± 0.52	71.79 ± 0.33	7.94 ± 1.05
	0.5012	73.24 ± 0.87	26.26 ± 2.09	81.05 ± 0.51	34.57 ± 1.06
	1.023	89.47 ± 0.56	58.06 ± 1.59	83.33 ± 0.45	83.03 ± 1.50
	2.012	90.32 ± 0.57	86.2 ± 1.42	85.75 ± 0.73	155.83 ± 1.71
Lipton	0.1002	41.83 ± 0.89	0.29 ± 0.16	76.43 ± 0.38	4.06 ± 0.49
	0.5015	88.33 ± 1.22	23.34 ± 2.00	89.04 ± 0.57	39.62 ± 1.11
	1.011	90.06 ± 0.99	58.16 ± 1.03	89.90 ± 0.59	104.90 ± 1.41
	2.015	90.86 ± 0.89	175.36 ± 1.87	86.35 ± 0.91	116.99 ± 1.56
Society	0.1012	37.87 ± 0.78	5.15 ± 0.06	63.08 ± 0.51	8.68 ± 0.89
	0.5011	83.49 ± 0.56	30.47 ± 0.99	84.77 ± 0.69	48.43 ± 1.00
	1.014	90.61 ± 0.45	77.79 ± 0.63	89.06 ± 0.81	103.73 ± 1.62
	2.005	91.21 ± 0.55	107.03 ± 0.93	89.47 ± 0.57	166.99 ± 1.56
Kanan Devan	0.1000	33.24 ± 0.64	8.73 ± 0.76	86.36 ± 0.44	9.48 ± 0.83
	0.5024	88.31 ± 0.16	20.79 ± 1.67	85.97 ± 0.65	41.94 ± 1.27
	1.024	90.61 ± 0.65	46.51 ± 1.04	84.90 ± 0.38	104.51 ± 1.03
	2.055	91.71± 0.54	89.53 ± 1.12	70.21 ± 0.49	145.43 ± 1.02
Tata	0.1004	33.51 ± 0.39	11.55 ± 1.08	53.13 ± 0.33	8.92 ± 0.96
	0.5025	90.61 ± 0.19	29.36 ± 1.64	88.47 ± 0.41	41.24 ± 1.50
	1.014	91.18 ± 0.43	62.51 ± 2.02	88.33 ± 0.49	105.85 ± 1.13
	2.013	91.09 ± 0.81	185.36 ± 1.87	89.36 ± 0.71	93.72 ± 1.61
Red Label	0.1011	24.66 ± 0.22	2.38 ± 1.30	53.95 ± 0.36	14.5 ± 0.93
	0.5021	77.38 ± 0.43	19.29 ± 1.84	79.8 ± 0.48	43.81 ± 1.69
	1.004	89.61 ± 0.35	40.52 ± 1.78	89.04 ± 0.39	93.29 ± 0.87
	2.015	87.63 ± 0.73	170.75 ± 2.56	89.36 ± 0.71	101.58 ± 2.46

activity as it can be observed from the appearance of tea infusion. The appearance of 1 min infused tea was clear in colour and 5 min infused tea was cloudy and turbidity appeared upon standing as it contained more solids. The solid contents of tea infusion were higher in 5 min infused/brewed tea than 1 min and the values are tabulated in Table 2-3.

For black and green tea powder brew, when lower amount of tea leaves powder (0.1 g) boiled for 1 min produced infusion with lower polyphenol content, on the other hand when same quantity (0.1 g) boiled for 5 min produced infusion having higher polyphenol contents. Similarly, tea brew prepared with increasing the quantity of tea leaves powder from 1.0 g to 2.0 g, 2.0 g of tea leaves powder produced infusion with higher polyphenol contents than 1.0 g powder. From this study, it was clear that the polyphenol contents of tea leaves powder products increased with increasing infusion/ steeping time as well as with increasing the amount of tea leaves powder (Fig. 5). Table 4-5 represents the total polyphenol contents of all studied tea powder samples.

Correlation between DPPH radical scavenging activity of black tea leaves powder and their polyphenol content by linear regression analysis was also evaluated and correlation coefficients values were decreased for 1 min infusion in the order of: Lulu (0.7883) > Ahmed (0.7755) > Alkozay (0.7152) > Society (0.6543) > Leone (0.4599) > Kanan Devan (0.4164) > Twinings (0.3365) > Lipton (0.3365) > Red Label (0.3049) > Tata (0.2705); and for 5 min infusion in the order of: Red Label (0.8499) > Lulu (0.7201) > Alkozay (0.6697) > Kanan Devan

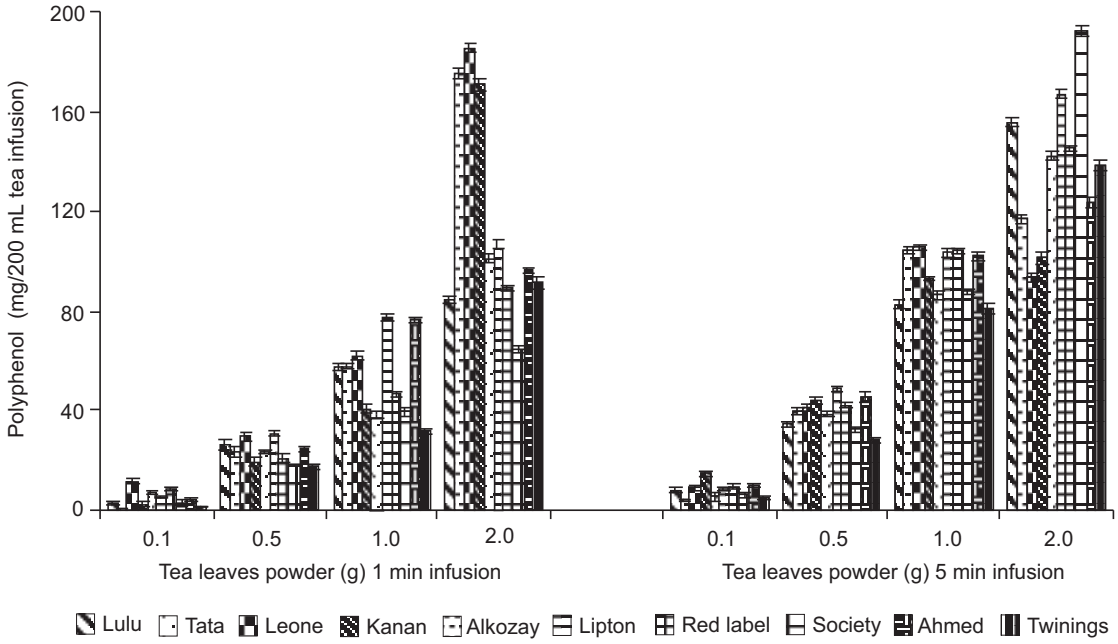

Fig. 5. Total polyphenol concentration of black tea and green tea leaves powder products boiled in 200 mL distilled water for 1 and 5 min. Results are mean ± SD (n = 3).

Table 5. Free radical scavenging activity and total polyphenol concentration of infusion of tea leaves powder samples (Leone, Alkozay, Ahmed and Twinings). Results are mean SD (n = 3)

Tea product (powder)	Wt. of tea powder (g)	Brewing period			
		(1 min)		(5 min)	
		Scavenging of DPPH$^{\bullet}$ (% ± SD)	Polyphenol mg/200 mL tea infusion	Scavenging of DPPH$^{\bullet}$ (% ± SD)	Polyphenol mg/200 mL tea infusion
Leone	0.1001	30.65 ± 0.28	7.37 ± 0.06	48.50 ± 0.63	5.47 ± 0.89
	0.5001	77.52 ± 0.39	23.34 ± 0.99	85.34 ± 0.43	38.51 ± 1.85
	1.008	89.61 ± 0.51	38.11 ± 1.63	89.04 ± 0.55	86.73 ± 1.72
	2.005	90.40 ± 0.53	101.75 ± 1.93	89.59 ± 0.32	142.35 ± 1.88
Alkozay	0.1018	41.28 ± 0.38	4.01 ± 0.59	64.58 ± 0.63	9.94 ± 0..86
	0.5004	80.22 ± 0.45	24.42 ± 1.02	86.91 ± 0.54	45.35 ± 1.90
	1.014	87.91 ± 0.44	76.79 ± 1.26	89.75 ± 0.44	102.4 ± 1.80
	2.059	92.25 ± 0.61	96.53 ± 1.01	88.67 ± 0.43	123.68 ± 2.12
Ahmed	0.1011	26.15 ± 0.19	2.37 ± 1.30	52.99 ± 0.29	6.19 ± 1.07
	0.5010	68.27 ± 0.28	18.02 ± 0.51	86.91 ± 0.22	32.44 ± 1.10
	1.002	90.46 ± 0.99	39.30 ± 1.66	89.61 ± 0.45	88.04 ± 1.11
	2.051	92.25 ± 0.77	64.81 ± 1.53	89.0 ± 0.42	192.03 ± 2.12
Twinings (Green tea leaves powder)	0.1014	16.08 ± 0.27	1.45 ± 0.29	29.43 ± 0.39	4.89 ± 0.91
	0.5004	88.05 ± 0.31	15.85 ± 1.51	87.9 ± 0.49	28.14 ± 1.18
	1.011	86.91 ± 0.19	31.5 ± 1.07	91.03 ± 0.39	81.25 ± 1.89
	2.014	90.98 ± 0.20	91.7 ± 2.35	93.06 ± 0.33	138.36 ± 2.01

(0.6605) > Society (0.649) > Tata (0.6232) > Leone (0.578) > Twinings (0.4951) > Ahmed (0.3916). The analytical data clearly showed that their relationship were not linear (Table 6). However, in the present study, it was observed that, free radical scavenging activity of tea infusion determined by DPPH radical scavenging method were not increased with increasing of their polyohenol contents. Moreover, antioxidant activity decreased with increasing brewing period for larger amount of tea leaves powder inspite of their higher concentration of polyphenolic content.

Table 6. Correlation coefficients between free radical scavenging activity and polyphenol content of black tea leaves powder samples

Tea leaves powder products	Correlation coefficients (r)* brewing period	
	1 (min)	5 (min)
Leone	0.4599	0.578
Alkozay	0.7152	0.6697
Ahmed	0.7755	0.3916
Lulu	0.7883	0.7201
Lipton	0.3365	0.4698
Society	0.6543	0.6490
Kanan Devan	0.4164	0.6605
Tata	0.2705	0.6232
Red Label	0.3049	0.8499
Twinning	0.3601	0.4951

*In the linear regression analysis, polyphenolic content was regarded as X and % DPPH radical scavenging activity as Y.

Conclusion

Free radical scavenging activity depends on the amount of tea leaves used and the brewing period. From this study, it is clear that infusion of black or green tea bag for 1 or 2 min is enough to get higher antioxidant activity. Boiling of black tea powder products for longer time loses its antioxidant properties as well as decrease its health beneficial effect. Therefore, shorter boiling time is better for large amount of powder or small amount of powder should brew for minimum 5 min for getting higher antioxidant activity. However, several methods need to employ to study the antioxidant activity of tea infusion to find out the reason behind decreased free radical scavenging activity with increasing infusion time inspite of increasing polyphenol content.

Acknowledgement

The authors are grateful to Sana E. Taher, Shaima A. Jenebi, Asma Y. Rashid, Nehad M. Nafad and Hunain N. Salman, B. Pharm students of Dubai Pharmacy College for their valuable help in the preparation of tea infusion during carrying out this study.

References

Arab, L., Liu, W., Elashoff, D. 2009. Green and black tea consumption and risk of stroke: a meta-analysis. *Stroke*, **40:** 1786-1792.

Bors, W., Michel, C., Stettmaier, K. 1997. Antioxidant effects of flavonoids. *Bio-factors*, **6:** 399-402.

Bors, W., Heller, W., Michel, C., Saran, M. 1990. Flavonoids as antioxidants: determination of radical scavenging efficiencies. *Methods in Enzymology*, **186:** 343-355.

Buschman, J.L. 1998. Green tea and cancer in humans: a review of the literature. *Nutrition and Cancer*, **31:** 151-159.

Cao, G.H., Sofic, E., Prior, R.L. 1996. Antioxidant capacity of tea and common vegetables. *Journal of Agricultural and Food Chemistry*, **44:** 3426-3431.

Chen, Y., Wang, M., Rosen R.T., Ho, C.T. 1999. 2,2-Diphenyl-1-picrylhydrazil radical scavenging active components from *Polygonum multiflorum* Thunb. *Journal of Agricultural and Food Chemistry*, **47:** 2226-2228.

Gramza, A., Pawlak-Lemañska, K., Korczak, J., Wsowicz, E., Rudzinska, M. 2005. Tea extracts as free radical scavengers. *Polish Journal of Environmental Studies*, **14:** 861-867.

Gupta, J., Siddique, Y.H., Beg, T., Ara, G., Afzal, M. 2008. A review on the beneficial effects of tea polyphenols on human health. *International Journal of Pharmacology*, **4:** 314-338.

Higdon, J.V., Frei, B. 2003. Tea catechins and polyphenols: health effects, metabolism, and antioxidant functions. *Critical Review in Food Science and Nutrition*, **43:** 89-143.

Lambert, J.D., Yang, C.S. 2003. Cancer chemopreventive activity and bioavailability of tea and tea polyphenols. *Mutation Research*, **523-524:** 201-208.

Lin, Y.L., Tsai, S.H., Lin-Shiau, S.Y., Ho, C.T., Lin, J.K. 1999. Theaflavin-3,3-digallate from black tea blocks the nitric oxide synthase by down-regulating the activation of NF-B in macrophages. *European Journal of Pharmacology*, **367:** 379-388.

Menet, M.C., Sang, S., Yang, C.S., Ho, C.T., Rosen, R.T. 2004. Analysis of Theaflavins and Thearubigins from black tea extract by MALDI-TOF mass spectrometry. *Journal of Agricultural and Food Chemistry*, **52:** 2455-2461.

Narotzki, B., Reznick, A.Z., Aizenbud, D., Levy, Y. 2012. Green tea: a promising natural product in oral health. *Archives of Oral Biology*, **57:** 429-435.

Nessa, F., Ismail, Z., Mohamed, N., Mas Haris, M.R.H. 2004. Free radical scavenging activity of organic extracts and of pure flavonoids of *Blumea balsamifera* DC. leaves. *Food Chemistry*, **88:** 243-252.

Nkubana, A., He, Q. 2008. A comparative study of antioxidant activity between black tea from Rwandan highlands with green and oolong teas from China. *International Journal of Food Safety, Nutrition and Public Health*, **1:** 159-166.

Peterson, J., Dwyer, J., Jacque, P., Rand, W., Prior, W., Chui, K. 2004. Tea variety and brewing techniques influence flavonoid content of black tea. *Journal of Food Composition and Analysis*, **17:** 397-405.

Peters, U., Poole, C., Arab, L. 2001. Does tea affect cardiovascular disease? A meta-analysis. *American Journal of Epidemiology*, **154:** 495-503.

Rice-Evans, C.A., Miller, N.J., Paganga, G. 1996. Structure antioxidant activity relationship of flavonoids and phenolic acids. *Free Radical Biology and Medicine*, **20:** 933-956.

Sanchez-Moreno, C. 2002. Review: Methods used to evaluate the free radical scavenging activity in foods and biological systems. *Food Science and Technology International*, **8:** 121-137.

Satoh, E., Ishii, T., Shimizu, Y., Sawamura, S.I., Nishimura, M. 2001. Black tea extract, thearubigin fraction, counteract the effects of botulinum neurotoxins in mice. *British Journal of Pharmacology*, **132:** 797-798.

Scalbert, A., Monties, B., Janin, G. 1989. Tannins in wood: comparison of different estimation models. *Journal of Agricultural and Food Chemistry*, **37:** 1324-1329.

Su, X., Duan, J., Jiang, Y., Duan, X., Chen, F. 2007. Polyphenolic profile and antioxidant activities of oolong tea infusion under various steeping conditions. *International Journal of Molecular Sciences*, **8:** 1196-1205.

Vita, J.A. 2003. Tea consumption and cardiovascular disease: Effects on endothelial function. *The Journal of Nutrition*, **133:** 3293S-3297S.

Wang, Y., Yang, Z., Wei, X. 2012. Antioxidant activities potential of tea polysaccharide fractions obtained by ultra filtration. *International Journal of Biological Macromolecules*, **50:** 558-564.

Xiao, J., Huo J, Jiang, H., Yang, F. 2011. Chemical compositions and bioactivities of crude polysaccharides from tea leaves beyond their useful date. *International Journal of Biological Macromolecules*, **49:** 1143-1151.

Yang, C.S., Landau, J.M. 2000. Effects of tea consumption on nutrition and health. *The Journal of Nutrition*, **130:** 2409-2412.

Yamaguchi, T., Takamura, H., Matoba T., Terao, J. 1998. HPLC method for evaluation of the free-radical scavenging activity of foods by using DPPH. *Bioscience, Biotechnology and Biochemistry*, **62:** 1201-1204.

Yokozawa, T., Noh, J.S., Park, C.H. 2012. Green tea polyphenols for the protection against renal damage caused by oxidative stress. *Evidence-based Complementary and Alternative Medicine*: *ecm*, **2012:** 845917. 10. doi:10.1155/ 2012/845917. Epub 2012 July.

Zuo, Y., Chen, H., Deng, Y. 2002. Simultaneous determination of catechins, caffeine and gallic acids in green, Oolong, black and pu-erh teas using HPLC with a photodiode array detector. *Talanta*, **57:** 307-316.

Pak. j. sci. ind. res. Ser. A: phys. sci. 2014 **57** (2) 86-94

Quality of Wastewater Used for Conventional Irrigation in the Vicinity of Lahore and its Impact on Receiving Soils and Vegetables

Farzana Bashir*, Muhammad Tariq, Rauf Ahmad Khan and Tahira Shafiq
CEPS, PCSIR Labs Complex, Lahore-54600, Pakistan

(received March 30, 2012; revised July 16, 2013; accepted August 5, 2013)

Abstract. The quality of wastewater was evaluated from Rohi Nullah, Lahore, Pakistan, for one year (2008-2009) from those points where it is used for irrigation of crops on both sides of Nullah. The quality of wastewater was evaluated for pollution load including pH, sulphide, phenol, methylene blue active substances, chemical oxygen demand (COD), biochemical oxygen demand (BOD), irrigation quality (electric conductivity, total dissolved solids, total suspended solids, sodium adsorption ratio, residual sodium carbonate and chlorides) nutritional value (total nitrogen, total phosphorus and total potassium) and for metal concentration. The metals analysed were cadmium, nickel, chromium, zinc, manganese, cobalt and copper. With respect to pollution load BOD, COD and sulphide concentration was above the National Environmental Quality Standard (NEQS) limit. Nitrogen and phosphorus were contained at levels of concern in wastewater but the level of potassium was below crop requirements. The concentration of nickel, chromium, manganese and copper was above the FAO standards, while the concentration of cadmium, zinc and cobalt fell within FAO standards. Considering NEQS standards, the metals concentration was within limits. Temporal variations were prominent in some parameters and mostly higher values were observed in summer and lower in winter season. There was accumulation of heavy metals in soils receiving wastewater for irrigation. The metal contents in soils follow the order Mn> Co> Zn> Cr > Ni > Cu > Cd. It was observed that the concentration of all studied toxic metals in edible part of the vegetables was above the critical level. Finally, it was concluded that the practice of using wastewater in irrigation for growing vegetables and other crops is non-sustainable.

Keywords: wastewater, irrigation quality, COD, BOD, SAR, metal ions

Introduction

Wastewater consists of the effluent discharged from household, industries, institutions and commercial buildings. It contains organic matter, some food nutrients and heavy metals. Growing crops with such water for longer periods may lead to accumulation of these toxic metals in soils and plants. The safe disposal of wastewater is a severe problem faced by large metropolitan areas like Karachi, Lahore etc., with limited space for land based treatment and disposal. Wastewater is also a resource and may increase the agricultural productivity due to its nutrient contents and irrigation with wastewater can lower the fertiliser requirements and also increase crop yields (Quinn, 1979).

Under arid and semiarid conditions the use of wastewater for irrigation is considered by far the best option because this practice not only minimizes the environmental pollution but also aids in expansion of irrigated agriculture. In our conditions the two most important factors limiting soil productivity are water and organic matter, both substances as well as plant nutrients are supplied if wastewater is used on agricultural land. There are many studies indicating the beneficial effects of wastewater nutrients on plant growth (Kipnis *et al.,* 1979; Overman, 1978; Day and Tucker, 1977; Day *et al.,* 1975). However, there are some hazards associated with the use of wastewater in irrigation. These are trace heavy metals, soluble salts and other organic and inorganic constituents that may be dangerous for plants causing phytotoxicity. Repeated application of wastewater can accumulate metals in soil and then ultimately be taken up by plants (Antonious *et al.,* 2011; Magdaleno *et al.,* 2011; Bigdeli and Seilsepor, 2008; Bashir *et al.,* 2007; Abdel-Saheb *et al.,* 1994; Wallace and Wallace, 1994). Salinity however, is presumably the most important single water quality factor which affects both soil and crop production.

Quality of wastewater when used for broad irrigation is of particular importance in our climatic conditions where, extremes of temperature and low relative humidity result in high rates of evaporation. It results

*Author for correspondence; E-mail: beefarzana@yahoo.com

in salt deposition from applied water which tends to accumulate in the soil profile. Physical and mechanical properties of the soil such as pH, cation exchange capacity, dispersion of particles and soil structure are very sensitive. Thus, when wastewater reuse is planned, its composition and impact on receiving soils must be taken into consideration. The present study was therefore, designed to determine temporal variations on the pollution load, irrigation quality, nutrient value and metal concentration of wastewater. The other objective was to study the impact of untreated wastewater irrigation on soil and to evaluate the uptake of heavy metals by vegetables and fodder under the effect of application of wastewater.

Materials and Methods

Study area. Rohi Nullah, is the storm water drain in the vicinity of Lahore. Industrial and domestic wastewater dumping has turned it into a perennial drain. There are approximately 120 industries of different nature situated along this Nullah. The major are textile, food, electroplating, paper, tanneries, and polymer production etc. Almost all industries discharge their untreated effluent into it. In addition domestic sewage of some parts of the city and of other villages also enters into it.

There are agricultural lands on both sides of the Nullah and the farmers of that area are pumping out the wastewater and using it for irrigating their field for growing vegetables and fodders.

Sampling procedures and analysis. The wastewater samples from Rohi Nullah were periodically collected on monthly bases for one year (2008-2009) from a site, where, it is used directly for surface irrigation. The grab method was used for sample collection. Each sample consisted of four sub-samples, preserved accordingly (APHA, 2005) and placed in 1 litre polyethylene containers. Temperature, pH and electric conductivity (EC) were measured in the field, while, other chemical properties of wastewater were measured by using standard methods (APHA, 2005). The concentration of metals (Cd, Co, Cr, Cu, Mn, Ni and Zn) was determined by AAS (Model Varian Spectr AA – 40).

Composite surface soil samples (0-15 cm) were collected from two sites which were irrigated partially or completely with wastewater of Rohi Nullah. At site I, 6 agricultural fields were selected that had previously been irrigated with tube-well water but currently are under partial wastewater irrigation and considered as control soil (CS) because in that area there is no agricultural field that is not irrigated by wastewater. From site II, 24 agricultural fields were randomly selected that had been irrigated with Rohi Nullah wastewater from 35 years or longer (WWS). From CS, fodder (*Zea mays*) sample was collected, while, from WWS vegetable samples (spinach, bitter gourd, chili and gourd) were collected. The samples were placed in labeled poly-ethylene bags and transported to the laboratory. Soil samples were air-dried under shade, ground and sieved through 2 mm sieve and stored in plastic jar, for further analysis. Samples were analysed for pH, EC, SAR and cation exchange capacity (CEC) following methods described by US Salinity Staff (Richards, 1954), texture by hydrometric method and organic matter by Walky-Blake method of US Salinity Lab Staff, (Richards, 1954). The soil was digested by using method described by Tessier *et al.* (1979) and concentration of total metals were determined by AAS (Model Varian, Spectr AA-40).

Vegetables *viz*. spinach (*Spinacia oleracea*), bitter gourd (*Momordica charantia*), chili (*Capsicum annum*) and gourd (*Lagenaria vulgarius*) from site WWS and maize (*Zea mays*) were collected from site CS. The plant materials was digested according to AOAC (2005) methods and analysed for metals (Cd, Ni, Cr, Zn, Mn, Co and Cu) by AAS (Model Varian Spectr AA–40).

Results and Discussion

Quality of wastewater. The quality of wastewater was evaluated for pollution load, irrigation quality, nutritional value and metal ion concentration and is described in Table 1.

Pollution load of waster water. *Temperature, pH, sulphide, phenol, MBAS, COD, BOD*. During the study period, the temperature varied for different sampling dates at sampling points. The average value of temperature was 26.86±7.44 ºC (Table 1) ranging from lower values during winter and higher in the summer (Fig. 1). The average value of pH was 7.81±0.29. According to National Environmental Quality Standards (NEQS) as described by Pakistan Environmental Protection Act (PEPA, 1997), the permissible limits for temperature and pH are 40 ºC and 6-10, respectively. The analysed wastewater has pH and temperature within NEQS limits.

The average concentration of sulphide was 8.12±2.33 mg/L. Sulphide is produced in wastewater naturally

Table 1. Pollution load, irrigation quality, nutrient value and metal ion concentration of wastewater of Rohi Nullah used for irrigation during 2008-2009

Parameter	Temperature (ºC)	pH	Sulphide (mg/L)	Phenol (mg/L)	Methylene blue active substances (mg/L)	Chemical oxygen demand (mg/L)	Biochemical oxygen demand (mg/L)
Average ± SD	26.86 ± 7.44	7.81±0.29	8.12±2.33	0.09±0.03	3.23±1.30	476.4±99.2	179.0±44.9
National Environmental Quality Standard	40 ºC	6-10	1.0	0.1	10	150	80

Parameter		pH	Electric conductivity (dS/m)	Total dissolved solids (mg/L)	Total suspended solids (mg/L)	Sodium adsorption ratio	Residual sodium carbonate	Chlorides (mg/L)
Average ± SD		7.81± 0.29	1.147 ± 0.258	917±198	92.8±20.6	5.44±0.76	2.19±0.58	4.08±0.95
FAO	None		<0.7	<450		<3	<1.25	<4
(degree of	slight to		0.7-3.0	450-2000		3-9	1.25-2.5	4-10
restriction	moderate	6.5-8.4						
on use)	severe	-	>3.0	>2000		>9	>2.5	>10

Parameter	Cadmium (mg/L)	Nickel (mg/L)	Chromium (mg/L)	Zinc (mg/L)	Manganese (mg/L)	Cobalt (mg/L)	Copper (mg/L)
Average ± SD	0.01±0.003	0.42±0.36	0.21±0.05	0.78±0.21	0.17±0.03	0.02±0.003	0.37±0.12
FAO standard (mg/L)	0.01	0.2	0.1	2.0	0.2	0.05	0.2

Parameter	Total nitrogen	Total phosphorus	Total potassium	–	–	–	–
Average ± SD	38.97±9.6	8.96±2.83	27.25±9.81	–	–	–	–

and also as a result of human activities and causes offensive odours. Natural sources include non-specific and anaerobic bacterial reduction of sulphates and sulphur containing organic compounds. The permissible limit is 1.0 mg/L and all samples had sulphide concentration above the limit. Offensive odours can be harmful in many ways such as (i) reduction in appetite for food (ii) lowering in water consumption (iii) impaired respiration, nausea and vomiting and (iv) cause for mental perturbation.

Phenol is a by product in the biosynthesis of carbohydrates. It is also present in wastewater of iron and steel industry, organic chemical industry, photochemical and plastic industry. The average concentration of phenol in wastewater samples was 0.09±.03 mg/L and was within NEQS limit of 0.1 mg/L.

Detergents are used in many industries and in everyday life. They affect aquatic environments by causing foaming, limiting oxygen production and causing eutrophication. Anionic detergents are also called MBAS (methylene blue active substances) due to their method of detection in wastewater. In this study, the average value was 3.23±1.30 mg/L. The NEQS limit for detergent is 10 mg/L and all the samples fell within permissible limits. This is due to the fact that the anionic detergents used are biodegradable in the environment.

The concentration of organic matter could be measured by BOD_5, while COD is the measure of the total quantity of oxygen required to oxidise all organic matter into CO_2 and H_2O. The average results of BOD_5 and COD are presented in Table 1. Low BOD_5 is an indicator of less polluted water, while high BOD_5 indicates polluted water. When sewage is applied to the soil it tends to affect status of oxygen in the soil in two ways, first directly by which the oxygen in the soil pores is consumed by microorganisms for the decomposition of organic matter added through wastewater. Secondly indirectly, the fine organic matter in sewage adversely affects soil porosity. This gradually reduces the capacity of the soil to exchange air and as a consequence of which the oxygen status of the soil is lowered as described by Mohan (1989). According to NEQS the permissible limit for BOD_5 is 80 mg/L and for COD is 150 mg/L. In the studied samples the average concentration of BOD_5 and COD was 179.0±44.9 and 476.4±99.2 mg/L, respectively. The reason for high COD and BOD_5 may be due to the presence of a large number of industries that discharge their untreated effluents into

the drain. The high values of COD and BOD_5 are in agreement with other studies as described by literature (Kamel and Nada, 2008; Rahmani, 2007).

Temporal variations in wastewater temperature, pH, sulphide, phenol, MBAS, COD and BOD_5 are shown in Fig.1. As expected lower values of temperature observed in winter and high in summer. No temporal variations were observed with respect to effluent pH and MBAS. Sulphide concentration remained high during winter and declined in summer which may be due to high temperature and heavy rains during this period. The dilution factor of monsoon rain was also observed in case of COD and BOD because lower values of COD and BOD were observed during summer and higher in winter. The presence of phenol shows an inconsistent patron during the whole year and did not show any particular trend about its presence or absence.

Irrigation quality. ***pH, EC, TDS, TSS, SAR, RSC, Chlorides.*** Traditionally, irrigation water is grouped into various quality classes that provide a rough indication of potential adverse affects on crop growth. According to FAO guidelines as described by Pescod (1992), the validity of irrigation water has three degrees of severity (i) none (ii) slight to moderate and (iii) severe as described in Table 1. Values shown are applicable under normal field conditions prevailing in most irrigated areas in the arid and semiarid regions of the world.

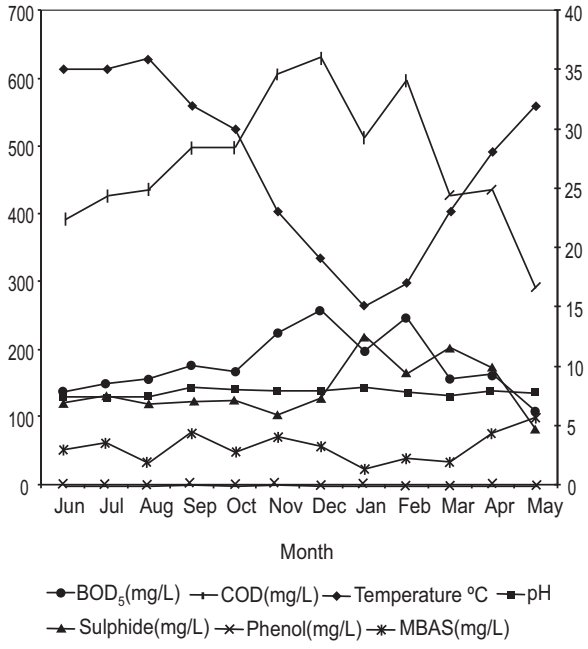

Fig. 1. Temporal variations in pollution load of wastewater at Rohi Nullah during 2008-2009.

As described by Richard (1954), the characteristics of irrigation water that appear to be most important in determining its quality are (1) total concentration of soluble salts; (2) relative proportion of sodium to other cations and (3) concentration of other elements that may be toxic like heavy metals.

The average pH in studied wastewater samples was 7.81 that lies within normal range. Concentration of total dissolved solids (TDS) and electric conductivity (EC) are important characteristics of water that determines its quality. The average values of EC and TDS was 1.147 dS/m and 917.93 mg/L, respectively. According to FAO guidelines these results fall in the category, where degree of restriction on use is slight to moderate.

At low concentrations chloride content of water for surface irrigation should be in the range of 4-10 mg/L and high concentration creates problem and is harmful for crops. In wastewater of Rohi Nullah the average concentration of chlorides was 4.06 mg/L that falls within normal range of FAO standard .

The sodium adsorption ratio (SAR) is a useful index for designing the sodium hazard of water used for irrigation. The critical value for SAR is > 9.0. Above this range there is danger of sodium hazard. The average value of SAR was 5.44 that lies in the second category of FAO i.e., restriction on use was slight to moderate. With respect to residual sodium carbonate (RSC) the values also lies within normal range.

Temporal variations in irrigation quality of wastewater are presented in Fig. 2 and 3. With respect to EC, TDS and TSS higher values were observed in winter and less in summer, which may be due to heavy monsoon in summer. The trend for SAR, RSC and chlorides is more or less similar to EC over this period.

Nutrient values. ***Total nitrogen, Total phosphorus, potassium.*** Wastewater contains nutrients in a variety of chemical forms with seasonal variation in concentration. The average concentrations of total nitrogen, total phosphorus and potassium were 38.97, 8.96 and 27.25, respectively, as described in Table 1. Total nitrogen in water is formed by combination of ammonia nitrogen, organic nitrogen, nitrate nitrogen and nitrite nitrogen. Nitrogen and phosphorus were contained at levels of concern in wastewater but the level of potassium was

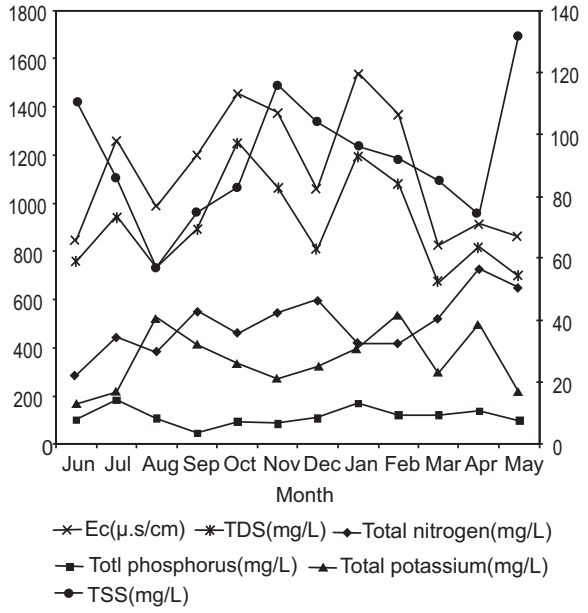

Fig. 2. Temporal variations in irrigation quality and nutrient value of wastewater at Rohi Nullah during 2008-2009.

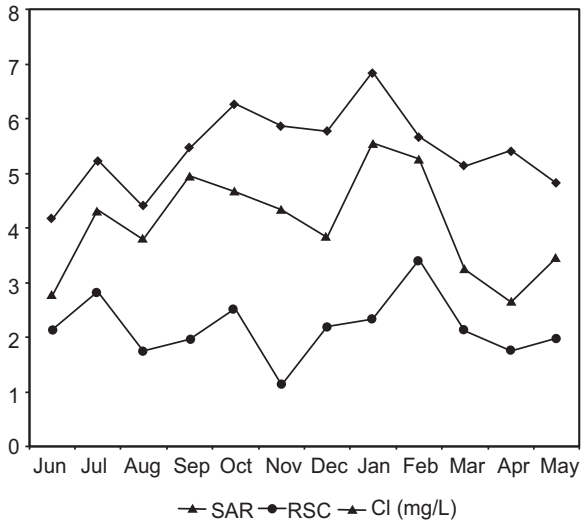

Fig. 3. Temporal variations in irrigation quality of wastewater at Rohi Nullah during 2008-2009.

below crop requirement. Such findings are also available in literature as reported by Feigin *et al.* (1991). Temporal changes in wastewater nutrient values are shown in Fig.3. The prominent variations were observed with respect to total nitrogen and potassium i.e., higher values in winter and lower in summer, while total phosphorus showed not prominent variations.

Metal ions. The concentration of metal ions is presented in Table 1. The concentrations of nickel, chromium, manganese and copper were above the FAO standards, while the concentration of cadmium, zinc and cobalt fell within FAO standards. Considering NEQS standards, the metals concentration was within limits. The high concentration of nickel, chromium, manganese and copper may be due to the effluents of leather industry, and other cottage industry, but especially the electroplating industry that discharges their untreated wastewater into drain.

The comparison of heavy metal concentration in untreated wastewater from the data of Pakistan and other countries suggested that the values were higher than the level observed by van der Hoek *et al.* (2002) but in comparison with Rai and Tripathi (2007) investigated in industrial wastewater in Lotha village.

Gupta *et al.* (1986) has indicated that the concentration of heavy metals in wastewater varied depending upon the type of industry these effluents come from. They reported that effluents from industries manufacturing sewing machines, bicycles and their spare parts contained higher concentration of pollutant elements compared to those from textile, woolen, and dairy industries.

Temporal variations in metal ion concentration showed (Fig.4) inconsistent information about the presence of heavy metals in wastewater.

Impacts of wastewater irrigation on soil and crops. The texture of the soils studied was silt loam and loam. The average values of pH of WWS were slightly lower as compared to soil of CS (Table 2). Production of organic

Table 2. Some physicochemical properties of sewage irrigated soils collected from WWS and CS site

Parameter	Wastewater irrigated soils				Control soil
	Spinach	Bittergourd	Chilli	Gourd	Maize
pH	7.75±0.22	7.86±0.33	7.86±0.22	7.92±0.09	8.30±0.33
Sodium adsorption ratio	10.53±1.06	10.67±1.14	10.58±1.38	11.81±1.32	8.38±0.73
Cation exchange capacity (cmol/kg)	8.60±0.62	7.79±0.70	7.43±0.58	7.65±0.90	5.38±0.48
Organic matter (%)	1.10±0.21	1.06±0.21	1.06±0.13	1.13±0.45	0.82±0.13
Electric conductivity(dS/m)	2.30±0.30	2.27±0.43	2.55±0.31	2.15±0.64	1.73±0.38

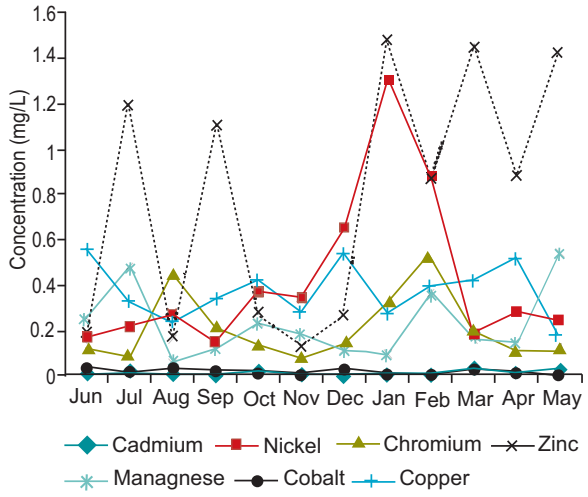

Fig. 4. Temporal variations in metal ion concentration of wastewater at Rohi Nullah during 2008-2009.

acids due to decomposition of organic matter may be the cause of lowering the pH of the soils irrigated with wastewater. The values of SAR, CEC, organic matter and electric conductivity of WWS were higher as compared to CS as described in Table 2. The increase in EC, SAR at WWS could be attributed to the addition of considerable quantities of dissolved salts through effluent. The addition of organic matter from sewage waste water rich in nutrients having high BOD resulted in increase of organic matter. These findings are similar to those of Murtaza *et al.* (2003) who observed below 15 the SAR value of city effluents irrigated soils. The increase in CEC in wastewater irrigated soils may be due to the increase in clay contents due to wastewater irrigation.

Repeated application of effluents could accumulate metals into soil because soil is an important sink for heavy metals due to its high retention capacities (Nolan *et al.,* 2003). Transfer of heavy metals from water to soil and subsequently uptake and accumulation in edible part of vegetative tissue from soil represent a direct pathway for incorporation of heavy metals into human food chain (Liang *et al.,* 2011).

Cadmium. The concentration of total cadmium in WWS and CS studied soils ranged from 4.2 to 12.7 and 1.20-2.30 (Table 3) with an average value of 9.35 and 1.72 mg/kg, respectively, while the permissible limit is 0.5 mg/kg (Rowell, 1994). Generally, above 0.5 mg/kg for total cadmium in soil is considered evidence of soil contamination. As compared with the soils of CS the concentration of cadmium was very high in soils of WWC, which may be due to long irrigation practice with untreated wastewater that contain cadmium above the critical level (Table 3).

The concentration of cadmium in edible part of vegetables i.e., spinach (leaves), bitter gourd, chili, gourd (fruit) at WWS site ranged from 0.78 to 2.30 with an average value of 1.46 mg/kg (Fig. 5). While the concentration of Cd in maize (maize of the said area is

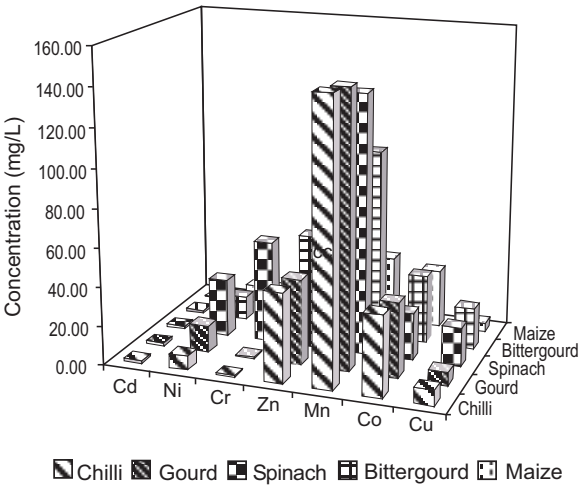

Fig. 5. Metal ions concentration (mg/L) in vegetables collected from wastewater irrigated fields.

Table 3. Metal concentration in wastewater irrigated (WWS) and in the control soil (CS)

Parameter (mg/kg)	WWS soil			CS soil			Permissible
	Max.	Min.	Average	Max.	Min.	Average	
Cadmium	12.7	4.2	9.3	2.30	1.20	1.72	0.5
Nickel	63.45	31.6	43.1	49.20	32.0	39.50	25.0
Chromium	76.0	43.2	61.7	48.80	28.50	37.62	200
Zinc	180	48.58	85.1	112.0	64.00	90.0	80
Managnese	476	230	347.7	319.0	150.0	243.3	900
Cobalt	117.5	59.2	88.6	45.20	34.0	38.93	20
Copper	48.5	12.7	32.4	21.60	15.20	18.20	20

used as fodder i.e., whole plant without roots) collected from CS site ranged between 0.03-0.24 with average value 0.11 mg/kg. The uptake of cadmium at contaminated site (WWS) was much greater than at CS. In fruit of all the vegetables and spinach leaves (i.e., edible parts), Cd was above the critical level of 0.01 mg/kg (WHO, 1996). Boon and Soltanpour (1992) observed maximum concentration of Cd in leaves of lettuce, cabbage and broccoli. Jaffer and Saleem (1987) also found higher Cd (>0.01) in radish, carrot, beans and spinach collected from Punjab, KPK and Azad Kashmir areas of Pakistan. Din *et al.* (2001) also found Cd concentration ranging from 0.10 to 1.58 ppm in various vegetable samples collected from some industrial area of Punjab.

Cadmium is one of the most toxic elements with reported carcinogenic effects in humans. It accumulates mainly in the kidney and liver. It induces cell injury and death by interfering with calcium (Ca) regulation in biological systems. It also causes bones to become brittle.

Nickel. Total nickel contents in soils ranged from 31.6 to 63.45 with average value of 43.1 mg/kg (Table 3). All studied soils of WWS contained total nickel above the permissible limit of 25 mg/kg (Rowell, 1994). Total concentration of nickel in soils that are partially irrigated with wastewater from few years ranged from 32.0-49.20 (Table 3) with an average value of 39.50 mg/kg.

The concentration of Ni ranged from 5.86 to 36.45 mg/kg in all vegetables collected from WWS. Maximum uptake (29.74 mg/kg) of Ni was by leaves (spinach), while uptake by fruits was lower i.e., 7.28, 13.85 and 11.9 for chili, gourd, and bitter gourd, respectively (Fig. 5). The average Ni concentration in maize from CS was 9.73 mg/kg and was within permissible limits of 10 mg/kg for food items by WHO (1996). The concentration of Ni in chilli at WWS was within limit, while for spinach, gourd and bitter gourd was above the limit. Jaffar and Saleem (1987) found Ni concentration < 1 mg/kg radish, onion, carrot, beans and spinach samples collected from the Punjab, KPK and Kashmir region of Pakistan. Sinha *et al.* (2005) also found higher concentrations of Ni in edible parts of vegetables that received river water for irrigation.

Chromium. In this study, total concentration of chromium ranged from 43.2 to 76.0 mg/kg with average value of 61.7 mg/kg (Table 3) in soils of WWS and ranged between 28.50-48.80 mg/kg with average value of 37.62 mg/kg in soils at CS. The chromium concen-tration was below the hazardous level of 200 mg/kg as reported by standard value by Huamain *et al.* (1999).

The uptake of Cr was maximum (52.65 mg/kg) by spinach leaves (Fig. 5) followed by bitter gourd with an average value of 18.98 mg/kg, while the uptake was very low by chilli and gourd at WWS. At CS the maize had chromium concentrations ranged from 0.00 to 0.16 mg/kg with average value of 0.10 mg/kg. The spinach and bitter gourd contained Cr above the permissible limit of 1.3 mg/kg recommended for food by WHO (1996). In general, leaves accumulated more Cr than the respective fruits. These results are in agreement with that of Din *et al.* (2001), who found 1.21-64.80 ppm of Cr in effluent irrigated vegetables.

Zinc. Zinc is a heavy metal of much interest since it is a plant micronutrient as well as potential contaminant in soils. Total zinc concentration (Table 3) in soils under different vegetables (WWS) ranged from 48.58 to 180 mg/kg the permissible limit in soil is 80 mg/kg (Rowell, 1994).

The concentration of Zn varied from 32.53 to 75.50 mg/kg in vegetables of WWS (Fig. 5). Maximum zinc was observed (58.52 mg/kg) in spinach leaves. The average uptake of zinc by maize collected from CS was 32.77. Zinc concentration in all samples studied from both sites was above the permissible limit of 5.0 mg/kg (WHO, 1996).

Manganese. Total manganese contents in soils under investigation ranged from 230 to 476 and 150 to 319 with average value of 347.7 mg/kg (Table 3). All the soils have Mn concentration within limits (400-900 mg/kg). The mean concentration (Fig. 5) of Mn in chilli, gourd, spinach and bitter gourd collected from farmer fields of WWS site was 144.22, 142.15, 133.98 and 98.62 mg/kg, respectively. The uptake of Mn in chili, gourd and spinach was greater as compared to bitter gourd. The mean concentration of Mn in maize from CS was 34.45 mg/kg and varied from 18-48 mg/kg. In all vegetables (edible portion) and fodder, Mn concentration was above the critical level of 6.61 mg/kg suggested by WHO (1996).

Cobalt. Total cobalt concentration (Table 3) in soils studied ranged from 59.2 to 117.5 with an average value of 88.63 mg/kg in soils of WWS and 34-45.20 with average value of 38.93 mg/kg in studied soils of CS. All the soils have cobalt concentration above the critical level of 20.0 mg/kg.

The Co concentration in vegetables (Fig. 5) and fodder ranged from 19.60 to 54.20 with mean value of 35.05 and 25.86 to 35.0 with mean value of 30.2 mg/kg, respectively. The uptake of cobalt by spinach was less as compared to bitter gourd, chilli, gourd and maize.

Copper. Total copper concentration in WWS and CS soils under investigation ranged from 12.7-48.5 mg/kg (Table 3) with an average value of 32.40, and 15.20-21.60 with average value of 18.20, respectively. All the studied soil samples of WWS total Cu concentration was found above 20.0 mg/kg, which is permissible limit as reported by Rowell (1994). While, the concentrations was within limit in partially irrigated soils of CS.

Copper concentrations (Fig.5) ranged from 5.87 to 29.10 mg/kg in vegetable samples. While, in maize Cu concentration varied from 3.98 to 5.54 mg/kg. In chilli and gourd the Cu concentration was within limit, while, the spinach and bitter gourd contained Cu above the permissible limit of the 10.0 mg/kg, recommended byWHO (1996) for food items.

Conclusion

The metals presence in wastewater is contributed from a number of sources, like electroplating, batteries, pigments, metal coatings, plastics etc. The presence of these industries at Rohi Nullah makes the possibility of accumulation of metals in effluent irrigated soils. Metals are non-degradable and when present in sufficient quantities, pose the most serious environmental threat. Many countries have legislation that prohibits the cultivation of vegetables, with untreated wastewater but allows other non edible crops like cotton and timber. An example is Mexico, a country that make extensive use of wastewater in agriculture.

In many countries including Pakistan, farmers consider wastewater a valuable resource because of its high productivity. The municipalities are aware of the value of wastewater and sell it to farmers. The practice could be good in areas where there is no industrialization but in the case of big cities like Lahore, the environmental risks of wastewater irrigation are prominent. These are the industries that make effluent worst, so the industries should treat their effluent before final disposal into drain.

References

Abdel-Saheb, I., Schwab, A.P., Banks, M.K., Hetrick, B.A. 1994. Chemical characterization of heavy metal contaminated soils in South-East Kensas. *Water, Air and Soil Pollution,* **78:** 73-82.

Antonious, F.G., San, O.D., Jason, M.U., John, C.S. 2011. Heavy metal uptake in plant parts of sweetpotato grown in soil fertilized with municipal sewage sludge. *International Journal of Geology,* **5:** 14-20.

AOAC, 2005. *Official Method of Analysis,* 18th edition, AOAC International, Gaithersburg, MD., USA.

APHA, 2005. *Standard Methods for the Examination of Water and Wastewater,* 21st edition, American Public Health Water Works Association/Water Environmental Federation, Washington, DC., USA.

Bashir, F., Shafiq, T., Kashmiri, M.A., Tariq, M. 2007. Contents and fractionation of heavy metals in soils irrigated with sewage effluents. *Journal of the Chemical Society of Pakistan,* **29:** 94-97.

Bigdeli, M., Seilsepour, M. 2008. Investigation of metals accumulation in some vegetables irrigated with wastewater in Shahre Rey- Iran and toxicological implications. *American-Eurasian Journal of Agricultural and Environmental Sciences,* **4:** 86-92.

Boon, D.Y., Soltanpur, P.N. 1992. Lead, cadmium and zinc contamination of Aspen Garden soils and vegetation. *Journal of Environmental Quality,* **21:** 82-86.

Day, A.D., Tucker, T.C. 1977. Effect of treated municipal wastewater on growth, fibre, protein and amino acid content of sorghum grain. *Journal of Environmental Quality,* **6:** 325-327.

Day, A.D., Taher, F.A., Katterman, F.R.H. 1975. Influence of treated municipal wastewater on growth, fibre, acid soluble nucleotides, protein and amino acid contents in wheat grain. *Journal of Environmental Quality,* **4:** 167-172.

Din, S., Salariya, A. M., Hafeez, J., Yasin, M., Ashraf, M. 2001. Heavy metal contents of some vegetables collected from fields irrigated with polluted water. *Pakistan Journal of Scientific Research,* **53:** 103-107.

Feigin, A., Ravina, I., Shalhevet, J. 1991. *Irrigation with Treated Sewage Effluent Management for Environmental Protection,* 244 pp., Heidelberg, Germany.

Gupta, A.P., Antil, R.S., Singh, A. 1986. Composition of some sewer water and their effect on soil properties. In: *Proceedings of National Seminar on Environmental Pollution Control and Monitoring,* pp. 419-425, Chundigarh Punjan, India.

Huamain, C. Chungrong, T., Cong, T., Yongguan, Z.

1999. Heavy metal pollution in soils in China, Status and Countermeasures. *Ambio,* **28:** 130-134.

Jaffar, M., Saleem, M. 1987. Concentration of selected toxic trace metals in some vegetable and fruits of local origin. *Pakistan Journal of Agricultural Sciences,* **24:** 140-145.

Kamel, Z.A., Nada, A.A. 2008. Performance of wastewater treatment plant in Jordan and sustainability for reuse. *African Journal of Biotechnology,* **7:** 2621-2629.

Kipnis, T., Feigin, A., Dovraf, A., Levanon, D. 1979. Ecological and agricultural aspects of nitrogen balance in perennial pasture irrigated with municipal effluents. *Progress in Water Technology,* **11:** 127-138.

Liang, J., Chen, C., Song, X., Han, Y., Liang, Z. 2011. Assessment of heavy metal pollution in soil and plant from dunhua sewage irrigation area. *International Journal of Electrochemical Sciences,* **6:** 5314-5324.

Magdaleno, H.F., Villa, O.R.M., Saenz, E.M., Carmen, M.D., Bolaos. O., Olivas, A.L.B. 2011. Heavy metal in agricultural soils and irrigation with wastewater of Mixquiahuala, Hidalgo, Maxico. *African Journal of Agricultural Research,* **6:** 5505-5511.

Misra, S.G., Srivastava, C.P. 1989. Environmental issues and programmes. In: *How Safe is Sewage Irrigation,* I. Mohan (ed.), 156 pp., New World Environment Series, ASHISH Publishing House, New Dehli, India.

Murtaza, M., Gafoor, A., Qadir, M., Rashid, M.K. 2003. Accumulation and Bioavallability of Cd, Co and Mn in soils and vegetables irrigated with city effluent, Faisalabad, Pakistan. *Pakistan Journal of Agricultural Sciences,* **40:** 18-24.

Nolan, A.L., Lombi, E., McLaughlin, M.J. 2003. Metal bioaccumulation and toxicity in soils-why bother with speciation. *Australian Journal of Chemistry,* **56:** 7791.

Overman, A.R., Evans, L.E. 1978. Effluent irrigation of sorghum sudan grass and kenaf. *Journal of the Environmental Engineering Division,* **104:** 1061-1066.

PEPA, 1997. *National Environmental Quality Standard for Municipal and Liquid Industrial Effluent, Pakistan Environmental Protection Act*, The Gazzette of Pakistan, 6 pp., Islamabad, Pakistan.

Pescod, M.B. 1992. *Wastewater Treatment and Use in Agriculture*, *FAO Irrigation and Drainage Paper no. 47*, Food and Agricultural Organization of the United Nations, Rome, Italy.

Quinn, B.F. 1979. Surface irrigation with sewage effluent in Newzeland, a case study. *Progress in Water Technology,* **11:** 103-126.

Rahmani, R.H. 2007. Use of Industrial and municipal effluent water in Esfahan Province - Iran. *Scientific Research and Essay,* **2:** 84-88.

Rai, P.K., Tripathi, B.D. 2008. Heavy metals in industrial wastewater, soil and vegetables in Lotha village, India. *Toxicological & Environmental Chemistry,* **90:** 247-257.

Richards, L.A. 1954. *Diagnostic and Improvement of Saline and Alkali Soils,* US Salinity Laboratory Staff, Handbook No. 60, USDA, Washington, DC., USA.

Rowell, D.L. 1994. *Soil Science: Method and Applications*, Longman Group Limited, Longman Scientific and Technical, Harlow, UK,

Sinha, S., Pandey, K., Gupta, A.K., Bhatt, K. 2005. Accumulation of metals in vegetables and crops grown in the area irrigated with river water. *Bulletin of Environmental Contamination and Toxicology,* **74:** 210-218.

Tessier, A., Campbell, P.G.C., Bisson, M. 1979. Sequential extraction procedure for the speciation of particulate trace metals. *Analytical Chemistry,* **51:** 844-851.

Van der Hoek, W., Hassan, M.U., Ensink, J.H.J., Feenstra, S., Richard-Sally, L., Munir, S., Aslam, R., Ali, N., Hussain, R., Matsuno, Y. 2002. *Urban Wastewater: A Valuable Resource for Agriculture Research Report no. 63*, *A Case Study from Haroonabad, Pakistan.* International Water Management Institute (IWMI), Colombo, Sri Lanka.

Wallace, G.A., Wallace, A. 1994. Lead and other potentially toxic heavy metals in soil. *Communications in Soil Science and Plant Analysis.,* **25:** 137-141.

WHO, 1996. *Guidelines for Drinking Water Quality, Health Criteria and Other Supporting Information,* vol. **2**, 973 pp., 2nd edition, World Health Organization, Geneva, Switzerland.

Pak. j. sci. ind. res. Ser. A: phys. sci. 2014 **57**(2) 95-102

Noise Pollution - A Case Study of Rawalpindi City, Pakistan

Younas Kalim*, Tahseen Aslam and Hajra Masood
Natinal Physical and Standards Laboratory, PCSIR, 16-H/9, Islamabad, Pakistan

(received February 1, 2013; revised May 2, 2013; accepted June 26, 2013)

Abstract. In this study, noise level was measured during day time in 88 different locations of the Rawalpindi city, Pakistan, which included roads, choaks, residential areas, educational institutions, hospitals, railway stations,airport, bus stands, shopping plazas and markets. The noise measurements were performed with a calibrated sound level meter. Study finds that overall minimum and maximum noise levels for the main roads and choaks were 55.4 and 101.9 dB(A), for residential areas 38.80 and 91.0 dB(A), for educational institutions 60.0 and 94.4 dB(A), for hospital 45.1 and 84.4 dB(A), for railway stations, airport, bus stands 59.2 and 102.5 dB(A) and for shopping plazas, markets 53.8 and 81.2 dB(A), respectively. The result of the study revealed that the noise level surpassed the prescribed NEQS limits as well as WHO guideline values for noise in specific environments in all areas under study, which can cause harmful effects on human health, animals and the environment.

Keywords: noise pollution, sound level, environment

Introduction

Noise pollution can be defined as intrusive noise that disrupts, distracts, or detracts from regular functioning. Noise pollution is not new, but it has become more problematic with the developments associated with industrialisation and urbanisation. Between 1987 and 1997, community noise levels in the United States were estimated to have increased by 11% and were predicted to continue increasing at that rate or more (Staples, 1997). The response of the human ear to sound depends both on the sound frequency (measured in Hertz, Hz) and the sound pressure, measured in decibels (dB). A normal ear in healthy young person can detect sounds with frequencies from 20 Hz to 20,000 Hz. Noise measurements are expressed by the term sound pressure level (SPL), which is logarithmic ratio of the sound pressure to a reference pressure and is expressed as a dimensionless unit of power, the decibel (dB). The reference level is 0.0002 microbars, the threshold of human hearing.

$$\text{Decibel } L_{eq} = 10 \log 10\ L/L^{\circ}$$

where:

L_{eq} = equivalent noise level; L = sound intensity; L° = reference level

Sound level becomes noise when it crosses the 70 dB mark. Noise levels above 80 decibels produce damaging effects to the ear. It can cause irreparable damage and lead to permanent hearing loss when noise level is above 100 decibels for a considerable period of time.

For measurement of noise emission a sound level meter is used. A measure of the level of sound is called the decibel. The zero of the decibel scale is the hearing threshold. Sounds at 0-10 decibel are so quiet that they are almost impossible to hear, while at the top end of the scale, at around 150 decibel, it can damage eardrums. (http://www.epa.vic.gov.au).

There are many sources of noise pollution such as different machines used in industries, horns and whistles of railway engines, switching and shunting operation in rail yards, airoplanes etc., that have significant negative impact on human health. Noise pollution is a significant environmental problem in many rapidly urbanising areas. This problem is not properly recognised despite the fact that it is steadily growing in developing countries (Murthy *et al*., 2007). Traffic noise is the biggest source of noise pollution, especially in urban areas. For example an average noise level produced by vehicular traffic on roads of Karachi city, Pakistan, is 90 dB (A) (Khan *et al*., 2010). Noise level of 112.3 dB(A) was observed in a study conducted in Tangail Municipal area, Bangladesh. Noise levels in this study area exceeded the recommended level by WHO at 34 out of 47 measuring points (Mia *et al*., 2012). Noise-induced hearing loss (NIHL) in humans is a major problem stemming from noise pollution as well as heart-related,

*Author for correspondence; E-mail: ykalim@yahoo.com

respiratory, neurological and other physiological problems. Stress, high blood pressure, anger and frustration, lower resistance to disease and infection, circulatory problems, ulcers, asthma, colitis, headaches, gastrointestinal disorders, and many other physiological and psychological problems have been linked directly to noise. In addition, children have been shown to suffer from slower language development and disruption of learning as a result of noise.

A study carried out at ENT Department, Sir Ganga Ram Hospital, Lahore, found that public transport drivers are exposed to excess noise on roads in Lahore and 65% of them had noise induced hearing loss (NIHL). 25% had normal hearing threshold and 10% had disabling hearing loss (Aslam *et al*., 2008). The hearing ability of the inhabitants of Dhaka city, Bangladesh, has reduced and they are suffering from permanent deafness due to noise pollution (Alam *et al*., 2001). In developed countries, as many as four to five million people, i.e., 12-15% of all employed people, are exposed to noise levels of 85 decibels or more (WHO, 2001). More than five million children in the United States, ages six to nineteen, suffer from noise-induced hearing impairment (Havas, 2006). In the exposure to noise impaired children's reading comprehension and caused a delay in reading skills development (Clark and Stansfeld, 2005). In children in noisier neighborhoods were shown to suffer from increased stress and diminished motivation (Evans *et al*., 2001).

In the present study, noise level was estimated in Rawalpindi city, Pakistan. Rawalpindi is situated at latitude 33.60 °N and longitude 73.04 °E, in the province of Punjab. It is the fourth largest city in Pakistan after Karachi, Lahore and Faisalabad. Rawalpindi city is divided into two tehsils:

Potohar (southern Rawalpindi)
Rawal (northern Rawalpindi)

The population of Rawalpindi city is approximately 19, 91,656 (World Gazetteer, 2010). The city is home to several industries and factories. The total area of the city is approximately 108.08 square km (Wiki/World Gazetteer). Murree road and Peshawar road are main roads of the city. Murree road has been a hot spot for various political and social events. Kashmir road, Haider road, Bank road, Hospital road, Jinnah road, Said pur road, IJP road, Rawal road, Tipu road, Tench road, Misrial road, Adiala road and Airport road are other important roads of the city. Main bazaars and markets of the city are Raja bazaar,Tench bazaar, Moti bazaar, Kashmiri bazaar, Sarrafa bazaar, Saddar area, Commercial market, Westridge market, Chah Sultan market and Kamran market. Number of shopping plazas and centers have been constructed on both sides of Murree road.

Being twin city of Islamabad, the capital of Pakistan, there is a rapid expansion in Rawalpindi city area. This expansion is mostly unplanned. Most of the areas particularly to the urban side are subjected to unacceptable noise conditions due to construction, manufacturing, traffic and recreational activities. A comprehensive national survey has not been conducted to assess the level of noise pollution in big cities of Pakistan. Present study was conducted to assess the noise level in the Rawalpindi city as well as its main causes. It will certainly help implementing agencies to understand the severity of the noise pollution problem of the city and take proper remedial measures.

Materials and Methods

In this study, sound level meter type 2240, Bruel & Kjaer, Denmark was used to measure the noise level. The microphone converts sound to an equivalent electric signal, which is processed by the instrument. Processing includes applying frequency and time weightings to the signal as specified by international standards, IEC 61672-1 to which this metre conforms.

Frequency weighting adjusts how the sound level meter responds to different sound frequencies. This is necessary because the human ear's sensitivity to sound varies according to the sound's frequency. The most common frequency weighting in use is A-weighting, which adjusts a signal in a way that best resembles the human ear's response at medium-range levels. It is the weighting required for nearly all environmental and workplace noise measurements and is specified in international and national standards and guidelines. All of Type 2240's measurement parameters apply A-weighting, except for measurement of peak levels, where the C frequency weighting is applied.

Time weighting specifies, how the sound level metre reacts to changes in sound pressure. It is an exponential

averaging of the fluctuating signal, providing an easy-to-read value. Type 2240 applies the Fast, or F time weighting, which is required weighting according to the vast majority of international and national standards and guidelines. Once the signal is processed through the weighting filters, the resulting sound pressure level is displayed in decibels (dB) on the instruments display.

All the measurements were taken at different times during day time (between 10 am to 3 pm) from August to October, 2012. Noise level was noted ten times at each point then averaged through summation of all values divided by the number of observation. At the time of collecting data of noise, values of frequent peaks were measured. The minimum and maximum levels of noise were recorded in each observation on the basis of maximum and minimum peaks noted during data recording. Standard deviation was calculated from ten observations obtained from each point.

Results and Discussion

In this study noise level was measured during day time in 85 points in different areas of the Rawalpindi city, Pakistan. The minimum, maximum and average noise levels were measured in dB(A) and standard deviation of all points is shown in Tables 1-6. Minimum and maximum noise levels at monitoring areas are shown in Fig. 1.

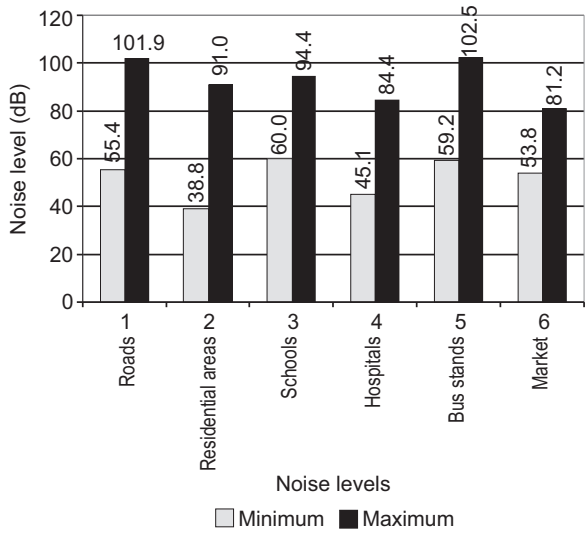

Fig. 1. Noise level (minimum and maximum).

The result of the study revealed that the noise level surpassed the prescribed NEQS (Table 7) as well as WHO guideline values (Table 8) in all areas under study, which can cause harmful effects on human health, animals and the environment. The study finds that overall minimum and maximum noise levels for main roads and choaks is 55.4 and 101.9 dB(A), with mean values 61.6±4.8-83.7±5.88 dB(A), higher than NEQS and WHO guideline value of 75(NEQS Table 7) and 70 dB (WHO guidelines,Table 8), respectively. Minimum and maximum noise level for residential areas is 38.8 and 91.0 dB(A), with mean values 47.7±5.2-78.2±4.9 dB(A). It is also on higher side as compared to NEQS and WHO limits of 55 dB (NEQS Table 7, WHO guidelines Table 8) set for outdoor living areas. At educational institutions minimum and maximum noise level is 60.0 and 94.4 dB(A), with mean values 65.7±3.7-85.0±4.3 dB(A), respectively. It is about 11-35 dB high than NEQS and WHO guideline value 50 dB(NEQS Table 7 and WHO guidelines, Table 8) set for school playground outdoor and silence zone. For hospitals minimum and maximum noise levels observed are 45.1 and 84.4 dB(A), with mean values 52.6±4.0-76.3±4.6 dB(A), which is on higher side as compared to WHO guideline values of 30 dB (WHO guidelines, Table 8) set for hospital, ward rooms, indoor as well as NEQS for silence zone, which is 50 dB(NEQS Table 7). It is an alarming sign for hospitals management. For railway stations, airport, and bus stands observed minimum and maximum noise level is 59.2 and 102.5 dB(A), with mean values 56.4±9.3-80.2±2.4 dB(A), higher than WHO as well as NEQS limits for traffic. For shopping plazas, markets minimum and maximum noise level observed is 53.8 and 81.2 dB(A), with mean values 58.8±5.2-78.7±1.5 dB(A), respectively. It is also higher than WHO guideline value of 70 dB (WHO guidelines, Table 8) set for industrial, commercial, shopping areas as well as NEQS limit of 65 dB (NEQS Table 7) set for commercial areas.

Conclusion

The results of the study revealed that the noise level surpassed the prescribed NEQS limits as well as WHO guideline values of noise level for specific environments, in all areas under study in Rawlpindi city which

Table 1. Results from noise measurements on roads and choaks

Roads and choaks	1	2	3	4	5	6	7	8	9	10	Max	Min	Mean	SD
IJP Peshawar road	69.0	76.8	75.8	70.3	71.6	68.2	88.2	74.8	75.1	80.1	88.2	68.2	75.0	6.0
IJP Toll plaza	80.5	92.3	73.7	82.1	94.2	81.9	75.8	70.0	82.5	77.9	94.2	70.0	81.1	7.6
IJP Carriage factory	81.3	80.9	72.9	86.5	89.7	78.0	82.2	83.2	80.8	70.2	89.7	70.2	80.6	5.8
IJP Pir wadhai more	80.0	89.4	76.0	84.1	101	71.2	77.1	76.0	80.0	89.0	101.0	71.2	82.4	8.8
IJP Pindora choak	84.8	75.5	78.1	89.7	98.1	82.0	69.9	74.4	81.1	90.1	98.1	69.9	82.4	8.5
Agha shahi avenue-9	72.4	70.6	75.1	72.0	76.6	78.2	69.2	66.6	78.1	71.0	78.2	66.6	73.0	3.9
Faizabad choak	70.1	69.1	66.2	69.0	71.3	68.2	82.6	70.9	75.2	68.5	82.6	66.2	71.1	4.7
6th road choak	67.7	69.0	68.1	69.1	66.0	65.1	86.9	68.9	75.6	71.6	86.9	65.1	70.8	6.4
Muslim town sadiqabad choak	70.2	66.8	68.2	75.2	65.9	78.8	80.1	70.0	65.7	80.0	80.1	65.7	72.1	5.9
Chandni choak flyover	77.7	66.4	64.0	63.3	62.8	69.4	61.9	68.9	101.9	98.2	101.9	61.9	73.5	14.8
Sirvice road dhoke kashmirian	69.3	67.8	72.2	67.4	68.4	69.9	67.0	71.9	61.9	66.8	72.2	61.9	68.3	2.9
Banni choak	72.3	71.9	68.6	68.9	69.8	76.1	73.8	74.0	72.6	70.2	76.1	68.6	71.8	2.4
Asghar maal choak	80.0	77.7	75.5	80.6	76.7	78.2	73.1	79.7	74.7	77.2	80.6	73.1	77.3	2.4
Pindora chungi choak	72.5	71.4	75.4	78.4	68.2	70.6	73.1	60.7	58.9	61.3	78.4	58.9	69.1	6.7
Siddiqui choak	77.1	74.0	68.1	69.5	69.0	71.0	72.7	70.6	69.7	68.3	77.1	68.1	71.0	2.9
Committee choak	77.5	76.5	80.0	92.5	79.5	81.1	78.3	84.1	78.8	76.1	92.5	76.1	80.4	4.8
PAF Auditorium choak chaklala base	72.1	72	66.8	65.4	72.8	76.8	69.1	63.2	59.8	78.2	78.2	59.8	69.6	5.9
RDA/WASA Liaqat bagh murree road	67.2	68.8	69.5	66.5	90.5	71.5	76.3	78.9	81.5	85.5	90.5	66.5	75.6	8.3
Moti mahal murree road	73.7	75.6	75.0	94.8	87.6	90.1	82.6	80.5	83.5	89.4	94.8	73.7	83.3	7.2
Mareer hasan choak	68.9	85.5	72.5	83.5	77.4	70.8	69.5	68.0	70.0	92.2	92.2	68.0	75.8	8.5
Kachahri choak	72.9	68.9	70.5	71.9	68.6	71.5	90.2	89.0	80.0	73.5	90.2	68.6	75.7	8.0
Ammar choak	68.3	71.5	72.2	69.8	75.5	81.6	61.8	60.7	79.9	62.4	81.6	60.7	70.4	7.3
Ayub park Main gate GT road	66.4	69.1	70.2	65.4	67.3	64.8	68.8	69.8	74.1	77.5	77.5	64.8	69.3	3.9
Chungi no.22 choak	86.4	81.6	80.9	75.6	81.4	77.5	86.9	82.6	79.4	79.0	86.9	75.6	81.1	3.6
Tench bhata dispensary road	77.6	83.5	83.9	91.8	81.1	84.1	82.2	80.5	76.8	95.6	95.6	76.8	83.7	5.9
Kalma choak Dhoke syyedan	75.0	69.7	64.4	70.4	68.7	70.3	74.4	80.1	67.3	72.2	80.1	64.4	71.3	4.4
Fawara choak raja bazaar	82.9	77.4	75.4	71.7	84.6	79.3	80.0	87.9	90.1	70.9	90.1	70.9	80.0	6.5
Dinghi khui raja bazaar	71.5	70.7	79.1	66.5	66.9	78.4	68.9	70.0	69.2	81.5	81.5	66.5	72.3	5.4
Bohar bazaar choak	83.2	80.5	74.1	79.3	74.8	75.6	81.9	80.2	78.6	88.6	88.6	74.1	79.7	4.4
F.G Boys school Peshawar road	85.2	84.4	73.6	69.1	74.4	70.4	76.0	69.7	78.4	78.8	85.2	69.1	76.0	5.7
Chuhar choak Peshawar road	66.8	67.4	59.4	68.1	55.4	58.2	60.1	60.0	64.2	55.9	68.1	55.4	61.6	4.7
Dhoke ratta bazaar	80.8	80.2	70.8	67.3	71.1	69.8	72.6	73.4	71.3	73.7	80.8	67.3	73.1	4.3

Table 2. Results from noise measurements on residential areas

Area	1	2	3	4	5	6	7	8	9	10	Max	Min	Mean	SD
A-Block satellite town	77.9	64.4	67.5	66.4	72.2	68.0	65.7	71.5	67.4	74.3	77.9	64.4	69.5	4.3
B-Block satellite town	58.6	59	62.1	61.4	54.6	55.8	62.5	50.8	56.3	64.2	64.2	50.8	58.5	4.2
D-Block satellite town	78.1	74.4	73.6	75.3	76.6	69.0	70.0	68.2	69.1	67.3	78.1	67.3	72.2	3.9
Dhoke khabba	56.4	58.2	60.1	52.8	56	62.2	65.1	67.8	58.7	64.6	67.8	52.8	60.2	4.7
Chaklala village nazir abad	48.5	57.9	60.1	66.7	71.6	72.9	54.0	63.2	55.0	52.3	72.9	48.5	60.2	8.3
Residential area DHA-1	50.1	58.4	54.2	56.5	49.3	61.2	55.6	52.9	60.2	54.6	61.2	49.3	55.3	4.0
Hazarat abbas colony morghah	61.5	51.2	52.4	50.2	60.9	66.3	68.8	56.7	54.4	57.3	68.8	50.2	58.0	6.3
Lal kurti residential area	59.6	58.4	64.2	59.2	66.5	67.4	55.8	52.6	60.1	68.3	68.3	52.6	61.2	5.2
Markazi jamia mosque	77.9	78.2	75.2	80.2	73.4	75.2	76.0	91.0	78.3	76.5	91.0	73.4	78.2	4.9
Askari-11 residential area	53.1	52.2	49.5	55.9	57	59.2	68.1	71.8	61.3	65.4	71.8	49.5	59.4	7.3
PIA colony	55.6	56.2	50.8	48.4	45.4	53.6	58.8	52.1	51.5	50.6	58.8	45.4	52.3	3.9
Cantt view colony	54.3	50.7	50.9	43.1	42.9	53.1	59.2	53.2	54.1	51.2	59.2	42.9	51.3	5.0
Ilyaas colony misrial road	50.0	56.5	53.7	48.2	49.6	54.2	58.6	53.5	51.8	52.4	58.6	48.2	52.9	3.2
Officers colony main entrance	55.4	54.2	57.1	52.6	48.7	47.9	56.4	57.2	58.6	49.5	58.6	47.9	53.8	3.9
Railway scheme-7	66.9	65.5	70.4	66.4	67.3	80.7	71.9	64.5	63.1	63.8	80.7	63.1	68.1	5.2
Khayabane sir syyed area	56.4	54.3	55.6	64.2	66.1	53.6	67.4	58.3	60.0	55.1	67.4	53.6	59.1	5.1
Bangash colony residential area	64.5	70.1	68.1	65.8	64.1	63.9	66.2	68.3	64.3	63.7	70.1	63.7	65.9	2.2
Workshopi mohallah area	58.2	56.7	62.2	55.2	49.8	50.3	56.9	60.1	61.4	61.0	62.2	49.8	57.2	4.4
Eid gah sihaam residential area	43.5	45.6	53.2	52.1	48.2	38.8	55.2	50.1	42.4	47.5	55.2	38.8	47.7	5.2

Table 3. Results from noise measurements on schools and colleges

School/college	1	2	3	4	5	6	7	8	9	10	Max	Min	Mean	SD
Govt.College for womens/town	65.3	64.8	63.1	77.8	67.8	70.8	68.8	68.7	70.7	72.2	77.8	63.1	69.0	4.2
Divisional public school	71.3	73.6	69.6	68.9	70.6	72.3	68.8	69.2	70.2	72.1	73.6	68.8	70.7	1.6
Asghar maal degree college	70.9	68.2	64.6	66.3	70.0	68.5	65.1	62.3	61.5	60.0	70.9	60.0	65.7	3.7
Army public school adiala road	82.1	80.6	81.5	79.9	84.6	82.3	80.0	85.6	89.8	90.1	90.1	79.9	83.7	3.8
Gordon college main gate	80.8	81.0	82.4	79.8	84.6	90.1	90.2	88.9	90.1	82.2	90.2	79.8	85.0	4.3
Gordon college inside	79.5	80.1	77.8	79.8	79.6	78.6	77.5	76.8	78.3	80.2	80.2	76.8	78.8	1.2
Army public school westridge-iii	80.8	81.0	82.4	79.8	84.6	90.1	90.2	88.9	90.1	82.2	90.2	79.8	85.0	4.3
F.G Boys school Peshawar road	82.9	77.4	75.4	71.7	84.6	79.3	80.0	87.9	90.1	70.9	90.1	70.9	80.0	6.5
Women college dhoke hassu	81.9	76.1	94.4	81.7	78.8	77.8	81.0	92.2	73.3	88.1	94.4	73.3	82.5	6.9

Table 4. Results from noise measurements in hospitals

Hospital	1	2	3	4	5	6	7	8	9	10	Max	Min	Mean	SD
Central hospital main gate	82.0	73.3	79.1	68.5	77.6	68.4	70.4	72.5	84.2	73.2	84.2	68.4	74.9	5.5
Central hospital inside	65.2	64.5	66.3	58.4	60.0	58.1	67.6	69.2	55.4	54.2	69.2	54.2	61.9	5.3
Holy family hospital inside	63.2	63.4	62.1	61.6	64.9	76.8	71.4	67.5	63.8	65.0	76.8	61.6	66.0	4.8
Holy family hospital main gate	72.2	78.3	80.3	77.1	74.9	73.6	71.9	70.0	84.4	80.3	84.4	70.0	6.3	4.6
Fauji foundation hospital	54.3	50.7	50.9	45.1	48.9	53.1	59.2	55.2	52.1	56.2	59.2	45.1	52.6	4.0
AFIC,CMH	55.3	54.9	52.8	56.3	50.6	53.7	59.5	57.6	55.7	59.2	59.5	50.6	55.6	2.8
Military hospital	60.4	63.4	63.1	59.8	64.9	70.2	68.7	67.5	63.8	62.6	70.2	59.8	64.4	3.4

Table 5. Results from noise measurements at bus stands, airport and railway stations

Site	1	2	3	4	5	6	7	8	9	10	Max	Min	Mean	SD
Pir Wadhai bus stand	82.6	80.4	82.2	85.3	68.4	80.3	72.8	74.1	75.9	68.1	85.3	68.1	77.0	6.1
Pir Wadhai bus stand main entrance	80.2	78.7	78.6	79.9	78.3	80.2	81.2	78.2	80.6	86.4	86.4	78.2	80.2	2.4
Islamabad International airport	59.2	67.4	72.6	70.7	71.9	74.0	69.1	77.2	101.2	102.5	102.5	59.2	76.6	14.1
Chaklala railway station	50.0	43.8	56.2	53.2	71.0	72.4	62.2	53.7	51.1	50.8	72.4	43.8	56.4	9.3
Sowan wagon stand	65.5	60.6	70.4	62.3	61.9	67.5	83.4	70.4	66.8	72.8	83.4	60.6	68.2	6.7
Rawalpindi Railway station outside	78.3	79.0	78.6	78.8	79.3	76.8	75.4	79.6	80.1	81.0	81.0	75.4	78.69	1.61
Rawalpindi Railway station inside	77.6	76.4	73.8	72.3	75.9	76.3	77.7	77.4	76.5	75.7	77.7	72.3	75.96	1.72
Pir Wadhai bus stand	82.6	80.4	82.2	85.3	68.4	80.3	72.8	74.1	75.9	68.1	85.3	68.1	77.01	6.06

Table 6. Results from noise measurements in markets and shopping plazas

Market/plazas	1	2	3	4	5	6	7	8	9	10	Max	Min	Mean	SD
Food street cricket stadium	67.7	59.4	71.5	67.1	68.9	72.9	70.0	66.0	69.8	68.5	72.9	59.4	68.2	3.7
Shamas abad furniture market	64.5	69.5	68.5	63.8	62.4	71.4	64.7	64.0	63.2	66.4	71.4	62.4	65.8	3.0
Commercial market sat/town	68.9	65.4	67.3	64.3	69.1	72.5	73.4	74.3	75.1	75.9	75.9	64.3	70.6	4.2
Rahman abad choak market	75.2	76.4	68.8	63.6	72.6	73.1	74.7	76.6	65.9	70.0	76.6	63.6	71.7	4.5
National market satellite town	66.5	67.3	70.1	72.5	60	62.6	71.7	70.3	66.8	78.3	78.3	60.0	68.6	5.2
Chaklala market	54.6	53.8	59.1	69.0	55.1	59.4	55.2	66.7	58.5	56.4	69.0	53.8	58.8	5.2
Sadar kamran market	75.4	76.2	75.8	79.6	77.9	80.2	81.0	79.8	80.3	78.5	81.0	75.4	78.5	2.1
Bohar bazaar	75.0	69.7	64.4	70.4	68.7	70.3	74.4	80.1	67.3	72.2	80.1	64.4	71.3	4.4
Wesrtidge market	78.2	78.4	77.6	80.1	79.6	78.8	76.9	76.5	81.2	80.1	81.2	76.5	78.7	1.5
Westridge market post office	76.4	76.8	81.0	79.2	78.6	78.4	79.3	74.8	76.7	77.9	81.0	74.8	77.9	1.8
Khayabane sir syyed market	80.8	80.2	70.8	67.3	71.1	69.8	72.6	73.4	71.3	73.7	80.8	67.3	73.1	4.3

Table 7. National environmental quality standards (NEQS) for noise effective from 1st July, 2012

Category of area/zone	dB(A) L_{eq}	
	Day time	Night time
Residential area	55	45
Commercial area	65	55
Industrial area	75	65
Silence zone	50	45

The Gazette of Pakistan, extra, November 26, 2010 (Part-II), SRO 1064(1)/2010.

can cause harmful effects on human health, animals and the environment. Motor vehicular traffic using pressure horns, musical systems and ill tuned engins are the main source of noise pollution at main roads as well as residential areas, main entrances of hospitals and educational institutions situated near roads. The problem of traffic noise created by these vehicles is a significant source of noise pollution in areas near roads and bus stands. Air conditioners, fans and generators cause noise pollution to some extent in markets and shopping plazas.

Table 8. WHO guideline values for community noise in specific environments, April 1999

Specific environment	L_{eq} [dBA]	L_{max}, fast [dBA]
Outdoor living area	55	-
Dwelling, indoors	35	45
Inside bedrooms	30	45
Outside bedrooms	45	60
School class rooms and Pre-schools, indoors	35	-
Pre-school bedrooms, indoors	30	45
School, playground outdoor	55	-
Hospital, ward rooms, indoors	30	40
Industrial, commercial shopping and traffic areas, indoors & outdoors	70	110
Ceremonies, festivals and entertainment events	100	110
Public addresses, indoors and outdoors	85	110
Music through headphones/ earphones	85	110

During load shedding of electricity, mostly generators are used to generate electricity. These are creating too much noise in commercial areas. Excessive use of loudspeakers and musical equipments in musical centers is causing noise pollution in markets and shopping plazas. Overcrowding of people is creating noise in markets, schools, colleges, hospitals, bus stands airports and railway stations. Unplanned urbanisation has severly damaged the natural green areas of the city. These all are contributing to noise pollution, which can cause health problems to the exposed population of the city. Present study will certainly divert attention of the concerned implementing authorities to understand the severity of the noise pollution problem of the city and take proper remedial measures.

Recommendations

- To wear ear protection, while working in noisy conditions is an effective way to manage noise. Vehicles and factory machines need to be maintained properly and checked from time to time.
- Sound insulation at the top of the roof and addition of a layer of plasterboard or wood to the dividing wall can provide a protection from the noise.
- A comprehensive campaign should be launched to create public awareness about noise pollution.
- Effective solution for noise pollution is to plant bushes and trees around the sound generating sources. Planned housing schemes should be allowed which must have green areas.
- Use of loudspeakers at public places, use of pressure horns and sound systems in buses and other transport vehicles should be banned and strict laws should be imposed against them.
- For overcoming the effects of noise pollution latest active noise control (ANC) technologies should be used such as white noise machine. This device converts the unbearable noise into pleasant sound.

References

Alam, M.J.B., Rauf, A.F.M.A., Ahmed, M.F. 2001. Traffic induced noise pollution in Dhaka City. *Journal of Civil Engineering*, **CE29:** 55-63.

Aslam, M.J., Aslam, M.A., Batool, A. 2008. Effect of noise pollution on hearing of public transport drivers in Lahore city. *Pakistan Journal of Medical Sciences*, **24:** 142-146.

Clark, C., Stephen, A.S. 2005. The effect of aircraft and road traffic noise on children's reading. *Literacy Today*, **44:** 24-25.

Evans, G.W. *et al*. 2001. Community noise exposure and stress in children. *Journal of the Acoustical Society of America*, **109:** 1023-1027.

Havas, V. 2006. Noise, the invisible pollution. *Current Health*, **32:** 10-11.

Khan, M.W., Memon, M.A., Khan, M.N., Khan, M.M. 2010. Traffic noise pollution in Karachi, Pakistan. *Journal of Liaquat University of Medical and Health Sciences*, **9:** 114-120.

Mia, M.Y., Hossain, Md.U., Farzana, S. 2012. Measurement of noise intensity in Tangail municipal area, Bangladesh. *Pakistan Journal of Scientific and Industrial Research, Ser. A: phys. sci*., **55:** 92-97.

Murthy, V.K., Majumder, A.K., Khanal, S.N., Subedi, D.P. 2007. Assessment of traffic noise pollution at

banepa, a semi urban town of Nepal. *Kathmandu University Journal of Science, Engineering and Technology*, **1:** 1-9.

NEQS, 2010. National environmental quality standards for noise, *The Gazette of Pakistan, Extra.*, (SRO 1064(I) / 2010), for noise, (Part-II) 26th November, 2010.

Staples, S.L. 1997. Public policy and environmental noise, Modeling exposure or understanding effects. *American Journal of Public Health*, **87:** 2063-2067.

WHO, 2001. Fact Sheet No. 258. Geneva, WHO Press. http://www.who.int/mediacentre/factsheets/fs258/en/.

WHO, 1999. *Organization Guidelines for Community Noise*, April 1999, London, UK.

WWW.World Gazetteer.com, Top 100 most populous cities in Asia 2010.

Pak. j. sci. ind. res. Ser. A: phys. sci. 2014 **57** (2) 103-108

A Study on Noise in Indian Banks: An Impugnation in the Developing Countries

Bijay Kumar Swain[a] and Shreerup Goswami[b]*

[a]Department of Environmental Science, Utkal University, Vani Vihar, Bhubaneswar-751004, Odisha, India
[b]Department of Geology, Ravenshaw University, Cuttack-753003, Odisha, India

(received April 9, 2012; revised March 27, 2013; accepted April 3, 2013)

Abstract. In the present study, noise levels were monitored in twenty one different banks of the Cuttack, the largest commercial city of the State Odisha, India, in the months of January to April, 2011 during two specified times (10 a.m.-1 p.m. and 1-4 p.m.). Different noise descriptors such as L_{10}, L_{50}, L_{90}, L_{eq}, NPL (noise pollution level), NC (noise climate) etc., were analysed to infer the extent of noise pollution in the investigated commercial banks of Cuttack. The noise levels in different banks ranged from 51.1 to 90.5 dB and from 51.4 to 91.1 dB during 10 a.m.-1 p.m. and 1 -4 p.m., respectively. Similarly, L_{eq} ranged from 71.5 to 82.1 and 67.4 to 72.2 dB and NPL ranged from 90.6 to 105.5 dB and 81.6 to 100.8 dB during 10 a.m.-1 p.m. and 1-4 p.m., respectively, which is more than permissible limit i.e., 50 dB (as prescribed in USA). T-test was also computed for all the 21 banks to infer the existence and statistical significance of the variations in noise levels.

Keywords: office noise, bank, noise distraction, noise descriptors, Cuttack

Introduction

Now-a-days, there were records of high level of dis satisfaction due to noise incidence in different offices, especially in commercial banks of India. Due to increase in population, economic development and industrial growth around Cuttack, there are many nationalised and private banks in different parts of the city. Total population of Cuttack is 2,618,708. Thus, the increase in number of customers, increased transactions of different industrial and business establishments of Cuttack make the environment of bank noisy. It is interesting to note that salary solely is disbursed in different banks to the employees and pensioners of government offices, universities, colleges, schools, industries located at Cuttack. So, especially on last working day of the month or during first week of the month, huge crowd rush into the banks to collect their salary. Unlike environmental noise in banks of foreign countries, Indian banks having thousands of customers are always noisy. The Indian banks are usually much noisier than their counterparts in developed countries, where less number of customers, central air-conditioning and carpeted floors and their location away from main roads reduce the noise to fairly low levels. The study on environmental noise of different banks in major cities of India in terms of standard noise indices were not empirically assessed so far except preliminary assessment of Goswami and Swain (2012a) in Balasore and that of Kudesia and Tiwari (2007) in Rourkela. The objective of the study was to assess the level of noise exposure of 21 different banks (both private and nationalised) of Cuttack, Odisha, India. As no agency in India has so far recommended the acceptable limits of noise levels in the offices especially that of banks, therefore, noise levels of the banks in India were studied and compared with the recommended noise levels of bank in USA (50 dB) (Kudesia and Tiwari, 2007; Rettinger, 1977).

*Author for correspondence;
E-mail: goswamishreerup@gmail.com

Materials and Methods

Study site. Cuttack city, the commercial and judicial caipital of Odisha, is located at 20 °16' North latitude and 85°31' East Longitude (Fig. 1). Noise levels were monitored in 21 commercial banks of Cuttack city (Table 1).

Acoustic study. The present noise monitoring was conducted with the help of sound level meter (Model LUTREN, SL-4010). This light weight calibrated instrument (wt = 460 g with batteries) is primarily designed for community noise survey. Sound level meter works on the principle of evaluation of sound pressure on a linear or weighted scale. Thus, the noise

Fig. 1. Map of India showing location of Cuttack city (study area).

levels were measured following standard procedure during January to April, 2011, at selected banks around Cuttack (Goswami and Swain, 2013; 2012b; 2011; Swain and Goswami, 2013; Mohapatra and Goswami, 2012a; 2012b; Pradhan *et al.*, 2012; Swain *et al*., 2012a; 2012b; Goswami, 2011; 2009; Goswami *et al*., 2011; Krishna Murthy *et al*., 2007). 180 measurements were made within three hour duration (i.e., at 1 min., interval) during two specified times from 10 a.m. -1 p.m. and 1-4 p.m. in the common corridors of all twenty one investigated banks. Sound level meter was kept in hand at arm's length at the chest level to minimise any error. The noise levels of different banks in different time intervals were predicted along with their equivalent noise levels (L_{eq}). The value of L_{eq} in dB (A) unit was calculated by using the formula given by Robinson, (1971) i.e.:

$$L_{eq} = L_{50} + (L_{10}-L_{90})^2 / 56$$

For the present study, the different percentile noise levels used were:

L_{10} : the level that were exceeded during 10% of the measuring time in dB(A).

L_{50} : the level that were exceeded during 50% of the measuring time in dB(A).

L_{90} : the level that were exceeded during 90% of the measuring time in dB(A).

L_{eq} represents the equivalent energy sound level of a steady state and invariable sound.

It includes both intensity and length of all sounds occurring during a given period (Piccolo *et al*., 2005).

Table 1. Noise level (dB) variations of different banks of Cuttack city at different time intervals

Location	10 a.m.-1 p.m.							1 p.m.-4 p.m.						
	Mean ± SD	L_{10}	L_{50}	L_{90}	L_{eq}	NC	NPL	Mean ± SD	L_{10}	L_{50}	L90	L_{eq}	NC	NPL
UCO Bank, College Square	70.0± 9.0	80.1	72.4	56.7	82.1	23.4	105.5	67.1±7.2	78.5	66.8	58.5	73.9	20	93.9
Central Bank of India, Mahatab Road	68.1±7.4	79.1	69.2	58.5	76.7	20.6	97.3	67.8±7.1	78.6	67.4	59.4	73.9	19.2	93.1
State Bank of India, Link Road	70.8±6.6	79.4	72.2	59.8	79.0	19.6	98.6	68.2± 6.9	77.6	65.6	60.7	70.7	16.9	87.6
ING Vyasa Bank, Arunodaya Nagar	66.2±7.1	76.5	64.7	56.9	71.5	19.6	91.1	65.0±5.5	73.4	63.8	59.2	67.4	14.2	81.6
Union Bank of India, Choudhury Bazar	70.6±6.4	78.6	71.4	61.6	76.5	17	93.5	69.0±6.8	78.4	70.4	58.8	77.2	19.6	96.8
IDBI Bank, College Square	68.5±7.7	79.6	70.1	58.6	77.9	21	98.9	66.8±6.5	75.8	65.4	58.2	70.9	17.6	88.5
Syndicate Bank, Bajrakabati Road	67.1±6.8	78.2	65.5	59.4	71.8	18.8	90.6	66.2±5.8	76.6	64.1	61.4	68.2	15.2	83.4
Bank of Baroda, Buxi Bazar	70.2±7.0	76.3	71.4	58.6	76.9	17.7	94.6	69.9±5.8	77.2	70.1	61.6	74.4	15.6	90
Bank of India, Ranihat	69.1±8.5	79.5	69.3	60.1	76.0	19.4	95.4	67.7± 6.3	73.7	68.8	60.1	72.1	13.6	85.7
Canara Bank, Badambadi	69.8±8.4	81.4	68.5	60.4	76.3	21	97.3	66.0±7.6	74.5	67.2	57.3	72.4	17.2	89.6
Andhra Bank, Malgodown	70.2±8.3	81.2	69.9	60.6	77.4	20.6	98	68.1±6.8	78.2	68.5	60.7	73.9	17.5	91.4
Punjab National Bank, Buxi Bazar	68.2±6.7	79.2	67.4	60.8	73.4	18.4	91.8	66.8±7.2	78.3	64.7	57.2	72.6	21.1	93.7
Dena Bank, Naya Sarak	66.8±8.1	78.4	65.2	57.1	73.3	21.3	94.6	65.8±7.5	78.6	63.2	57.2	71.3	21.4	92.7
~~Oriental Bank of Commerce, Link Road~~	~~68.4±8.5~~	~~81.1~~	~~67.4~~	~~57.4~~	~~77.4~~	~~23.7~~	~~101.1~~	~~65.2±7.2~~	~~76.8~~	~~64.5~~	~~56.9~~	~~71.5~~	~~19.9~~	~~91.4~~
Allahabad Bank, Cantonment Road	69.8±7.8	80.6	69.4	61.3	76	19.3	95.3	66.6±8.3	78.5	65.4	56.5	74.0	22	96
HDFC Bank, Bajrakabati Road	69.0±8.3	81.4	67.3	59.6	75.7	21.8	97.5	66.7±8.4	78.4	65.4	57.3	73.3	21.1	94.4
Axis Bank, Badambadi	66.4±8.4	78.9	63.4	55.8	72.9	23.1	96	64.5±7.5	78.4	62.1	57.2	70.1	21.2	91.3
Vijaya Bank, Buxi Bazar	68.7±7.5	80.7	67.4	60.5	74.6	20.2	94.8	65.6±8.1	78.2	64.3	57.3	72.1	20.9	93
Urban Co-operative Bank, College Square	68.9±9.9	82.1	64.5	58.4	74.5	23.7	98.2	67.5±9.0	82.1	65.1	57.3	76.0	24.8	100.8
ICICI Bank, Bajrakabati Road	67.2±9.4	80.3	63.4	55.8	74.1	24.5	98.6	65.6±9.0	81.1	62.5	56.6	73.2	24.5	97.7
Corporation Bank, Bajrakabati Road	69.3±7.6	81.2	68.5	60.5	76.1	20.7	96.8	65.4±7.5	79	64.1	56.8	72.9	22.2	95.1

As L_{eq} is an insufficient descriptor of the annoyance caused by fluctuating noise (Robinson, 1971), noise pollution level (NPL) in dB (A) was calculated by using the following formula:

$$NPL = L_{eq} + a\ (L_{10}\text{-}L_{90})$$

where:

a = 1.0 (constant in the equation)

NPL takes into account the variations in the sound signal and hence serves as better indicator of the pollution in the environment for physiological and psychological disturbance of the human system (Robinson, 1971).

Noise climate (NC) is the range over which the sound levels were fluctuating in an interval of time and was assessed using the following formula (Robinson, 1971):

$$NC = (L_{10}\text{-}L_{90})$$

where:

L_{10} = the level exceeded for 10% of the time of record (peak noise level); L_{90} = the level exceeded for 90 % of the time of record, is very near to the background noise level in the absence of any motor vehicle traffic.

Statistical analysis. The analysis of the measured noise levels generally depicted that there were existence of variations of noise with variables as the time of day. In order to determine the existence and statistical significance of the variations and trends, t-test was assessed on the observed data of the two different time intervals (Gupta, 2010).

Results and Discussion

Acoustic analysis. The noise data collected from different banks displayed wide ranges of noise level varying in two different specified times (10 a.m. -1 p.m. and 1-4 p.m.). The noise levels ranged from 51.1 to 91.1 dB at the common corridor of 21 investigated banks (Fig. 2). The minimum noise level was recorded at Punjab National Bank, Buxi Bazar (51.1 dB), while maximum noise was observed at Allahabad Bank, Cantonment Road (91.1 dB). Similarly, the maximum mean noise level was assessed at State Bank of India, Link Road Branch (70.8 dB), while minimum was assessed at Axis Bank, Badambadi Branch (64.5 dB).

Average peak noise level (L_{10}) values of all 21 monitored banks ranged from 76.3 to 82.1 dB and 73.4 to 82.1 dB during 10 a.m.-1 p.m. and 1-4 p.m., respectively. Similarly, L_{50} (median value of sound level) and L_{90}

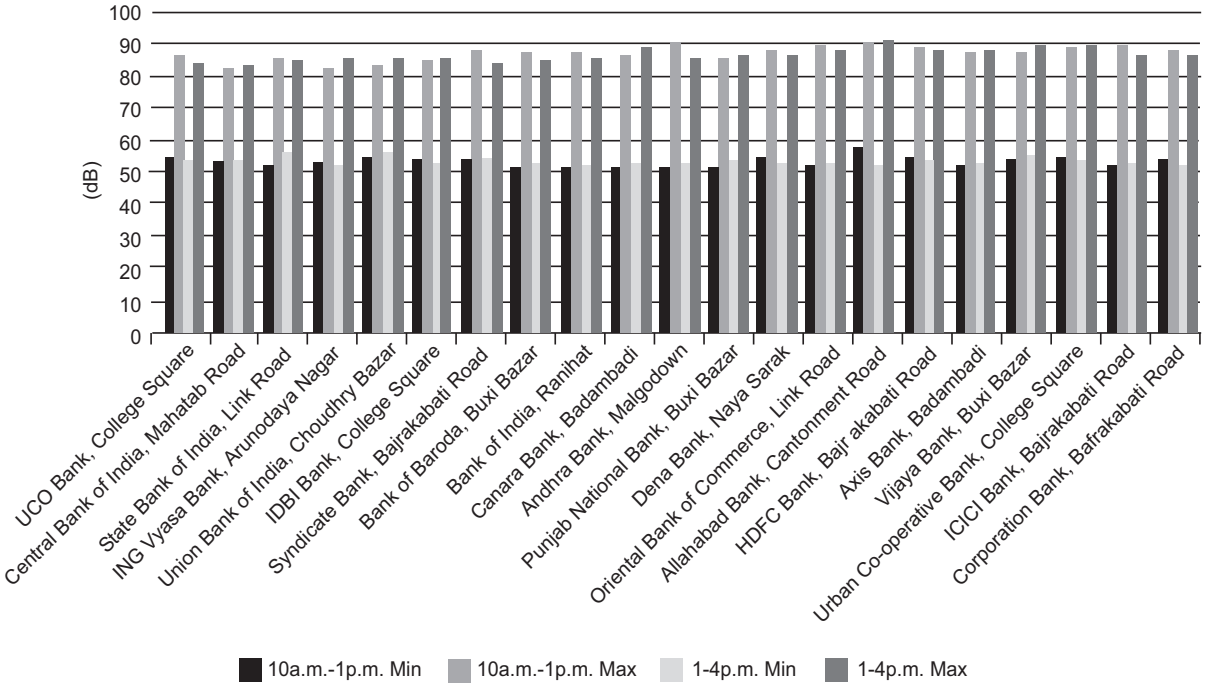

Fig. 2. Maximum and minimum noise level (dB) variations of different banks of cuttack city at two different specified time intervals.

(average background level) values of all 21 banks varied from 63.4 to 72.4 dB and 55.8 to 61.6 dB; 62.1 to 70.4 dB and 56.5 to 61.6 dB during 10 a.m.-1 p.m. and 1-4 p.m., respectively. Accordingly, the calculated L_{eq} (equivalent noise levels) values ranged from 71.5 to 82.1 dB and 67.4 to 77.2 dB during 10 a.m.-1 p.m. and 1 -4 p.m., respectively. All these values clearly showed higher noise levels in banks of Cuttack city mostly during 10 a.m.-1 p.m. NPL (noise pollution level) values of all 21 monitored banks ranged from 90.6 to 105.5 dB and 81.6 to 100.8 dB during 10 a.m.-1 p.m. and 1-4 p.m., respectively (Table 1). Minimum NPL values were more than 80 dB, which clearly revealed extent of noise pollution in the banks. NC (Noise climate) values ranged from 17 to 24.5 dB and 13.6 to 24.8 dB during 10 a.m.-1 p.m., and 1 -4 p.m., respectively (Table 1). NC is otherwise known as the difference between peak (L_{10}) and background (L_{90}) noise. The values of NC simply demonstrated that although the noise levels during any period of the day were generally constant but the presence of single – event noise was sufficient to affect the values of different noise percentile levels and consequently NC. t-test was computed between two different time intervals (10 a.m.-1 p.m. and 1- 4 p.m.). The observed value of t-test was 5.1. The tabulated value of 't' for 40 degree of freedom at 5% level of significance for two tailed test was 2.021. Since, the calculated value is more than the tabulated't', so it is significant. Thus, it was concluded with 95% confidence that the noise levels at 10 a.m.-1 p.m. was more than the noise levels at 1-4 p.m. The present study demonstrated that peak levels of activity occur in the banks in the forenoon i.e., during 10 a.m.-1 p.m. There are fairly less noise during 1-4 p.m. Lastly, it is inferred that even the minimum noise levels are beyond the permissible limit (50 dB as prescribed in USA) in all the cases (Table 2).

It was observed that main sources of noise in the investigated commercial banks were generators, air conditioners, fans, printers, computers, ventilation systems, notes-counting machines, telephone ringing, and chattering among the (bank) employees or the customers. These sounds are classified into steady (continuous hum from a ventilation system, fans, air conditioner or a computer, server); intermittent (sound that comes and goes such as a telephone ringing; printer, notes counting machine, fax, copier); impact (sounds of short duration such as the snap of a stapler or a punching machine; impact on door push bar during opening/closing, walking on hard surfaces) and human generated noise (human conversation and conversation on the phone). Moreover, all the investigated commercial banks are located in the heart of this city and along the main road. Thus, the noise from road traffic was also major contributor to the noisy bank. It was also noticed that the problem of office noise is aggravated due to multiple reflections of sound from concrete walls and bare floors. It was also observed that one of the imperative sources of noise pollution in the banks was the portable electric generator and it is becoming more and more common now-a-days due to frequent power failures. Most of the employees experience annoyance, and in turn disturbance in their work when the noise level crosses 65 dB. It was evident that all the employees of the banks might be experiencing some degree of noise related annoyance.

Table 2. Recommended acceptable noise levels in unoccupied offices in USA (Kudesia and Tiwari, 2007)

Type of office	Recommended noise level
General office	50
Private office	45
Small conference room	45
High standard office	35
High standard conference room	35
Bank	50
Accounting office	50

Noise source generated from chattering among the (bank) employees or the customers, indeed brought much distraction as compared to all other generated noise within the office environment since noise generated are audible and can be understood (Passhier, 1993). Machine generated intermittent noise, and impact noise in contrast is less distractive as there is no content with it. Background noise, would cause even less distraction, perhaps no distraction as it assists in masking the noise around since it has no uniformity. Although noise generated in the office in general and in bank in particular bring no conclusive evidence to physical health impact to the employees after long hour exposure, but studies demonstrated that it brings psychological distraction and annoyance to the employee, which may reduces their productivity (NyunLing and Cheung Chan, 2007; EPA, 1981).

It was also evident that bank employees were highly annoyed by the noise and their work efficiency had

been somehow affected. Moreover, they might be suffered from headache, bad temper, hearing problem and loss of concentration during their working hours manifested by noise pollution (Goswami and Swain, 2012a; Jakovljevic *et al*., 2009; Bluhm *et al*., 2004). One of the most annoying aspects of noise is that it interferes with speech. In the presence of background noise (L_{90}) i.e., 55.8-61.6 dB as measured in the banks of Cuttack, one has to raise the voice to carry out conversation and this contributes to further noise pollution. Maximum speech interference levels are quoted in Table 3 (Kudesia and Tiwari, 2007). This table demonstrates that if the noise level is 67dB (A) – a rather conservative value for Indian offices as evident in the present study- one has to speak in a very loud voice to talk to a person at one meter and has to shout at two meters. For example, if the noise level is 73 dB (L_{eq} during 10 a.m.-1 p.m. of all the investigated banks crosses this limit); one has to shout to talk to a person at one meter. According to (Kudesia and Tiwari, 2007) maximum speech inference levels for normal voice is 55 dB from 1m; 49 dB from 2 m and 43 dB from 3 m; while that of raised, very loud and shouting voices are 61, 67, and 73 dB from 1 m; 55, 61, 67 dB from 2 m and 49, 55, 61 dB from 3 m, respectively (Table 3). Thus, bank employees and customers have to speak in a louder voice due to speech interference, which possibly irritates them and reduces their working efficiency (Kudesia and Tiwari, 2007).

Table 3. Maximum speech interference levels in dB (A), which permit satisfactory hearing (after Kudesia and Tiwari, 2007)

Types of voice	Maximum speech interference levels in dB (A) distance from speaker		
	1 m	2 m	3 m
Normal voice	55	49	43
Raised voice	61	55	49
Very loud voice	67	61	55
Shouting	73	67	61

Conclusion

The present study demonstrates that the noise levels of all the investigated banks are more than the permissible limit (50 dB). Even minimum noise levels and the background noise level (L_{90}) are more than this recommended acceptable noise level of banks (50 dB). So it is apparent that the employees of these banks are experiencing noise related infuriation. Such noise pollution is steadily growing in the public offices of developing countries like India. It is also observed that investigated banks are commonly noisier during forenoon (10 a.m.-1 p.m.) than during afternoon (1-4 p.m.). Moreover, it is pertinent to mention here that the background noise and minimum noise levels are less in private banks such as Axis Bank, Badambadi and ICICI Bank, Bajrakabati road and the noise environment is better in these banks than the investigated nationalised banks of the city.

Since noise is a subjective feeling, the amount of noise caused distraction produced depends up on psychological sensitivity of that individual and loudness of that particular noise. Severe distraction may classify as annoyance (NyunLing and Cheung Chan, 2007; Evans and Johnson, 2000). Recent research suggests acoustics can have a large impact on work efficiency, performance and productivity. Even moderately noisy offices might contribute significantly, to health problems such as heart disease due to increased level of a stress hormone (epinephrine) and musculoskeletal problems (NyunLing and Cheung, 2007; Evans and Johnson, 2000). Noise level of offices such as banks has modest but adverse effects on physiological stress and motivation. Thus, noise is probably the most prevalent annoyance source in offices, and can lead to increased stress for occupants (NyunLing and Cheung, 2007; Evans and Johnson, 2000). Yet, acoustics in most cases do not received the same level of design consideration as thermal, ventilation and lighting as well as other architectural and engineering considerations (NyunLing and Cheung, 2007; Evans and Johnson, 2000; Sundstrom *et al.,* 1994). Therefore, bank administrations should take some imperative steps and regulatory measures to abate noise pollution in the respective banks so that work efficiency can be doubled with every perfection. The opening of new markets, deregulations and developments in information technology over the past few decades have led to heightened competition and greater struggle for survival among banking organiza-tions, encouraging them to take a fresh look at the conventional ways of making business. In order to remain competitive in this turbulent scenario, they have to make bank-environment conducive for customers.

References

Bluhm, G., Nordling, E., Berglind, N. 2004. Road traffic noise and annoyance- an increasing environmental

health problem. *Noise and Health,* **6:** 43-49.

EPA, 1981. *Noise Effects Handbook, A Desk Reference to Health and Welfare Effects of Noise,* EPA 500/9-82-106, Environmental Protection Agency Office of Noise Abatement and Control, Published by the National Association of Noise Control Officials, Fort Walton Beach, Florida, USA.

Evans, G., Johnson, D. 2000. Stress and open-office noise. *The Journal of Applied Psychology*, **85:** 779-783.

Goswami, S., Swain, B.K. 2013. Soundscape of Baripada, India; An appraisal and evaluation from urban noise perspective. *The Ecoscan:* Special Issue, **3:** 29-34.

Goswami, S., Swain, B.K. 2012a. Preliminary information on noise pollution in commercial banks of Balasore, India. *Journal of Environmental Biology,* **33:** 999-1002.

Goswami, S., Swain, B.K. 2012b. Occupational exposure in stone crusher industry with special reference to noise: A pragmatic appraisal. *Journal of Acoustical Society of India,* **39:** 70-78.

Goswami, S., Nayak, S., Pradhan, A., Dey, S.K. 2011. A study of traffic noise of two campuses of University, Balasore, India. *Journal of Environmental Biology*, **32:** 105-109.

Goswami, S., Swain, B.K. 2011. Soundscape of Balasore City, India: A study on urban noise and community response. *Journal of Acoustical Society of India,* **38:** 59-71.

Goswami, S. 2011. Soundscape of Bhadrak Town, India: An analysis from road traffic noise perspective. *Asian Journal of Water, Environment and Pollution*, **8:** 85-91.

Goswami, S. 2009. Road traffic noise: A case study of Balasore town, Orissa, India. *International Journal of Environmental Research*, **3:** 309-316.

Gupta, S.C. 2010. *Fundamentals of Statistics*, pp. 19.1-19.37, 6th edition, Himalaya Publishing House Pvt., Ltd., Mumbai, India.

Jakovljevic, B., Paunovic, K., Belojevic, G. 2009. Road traffic noise and factors influencing noise annoyanance in an urban population. *Environment International,* **35:** 552-556.

Krishna Murthy, V., Majumdar, A.K., Khanal, S.N., Subedi, D.P. 2007. Assessment of traffic noise pollution in BANEPA, a semi urban town of Nepal, Kathamandu. *University Journal of Science, Engineering and Technology*, **1:** 1-9.

Kudesia, V.P., Tiwari, T.N. 2007. *Noise Pollution & Its Control,* 3rd edition, Pragati Prakashan, Meerut, India.

Mohapatra, H., Goswami, S. 2012a. Assessment and analysis of noise levels in and around Ib River coalfield, Orissa, India. *Journal of Environmental Biology,* **33:** 649-655.

Mohapatra, H., Goswami, S. 2012b. Assessment of noise levels in various residential, commercial and industrial places in and around Belpahar and Brajrajnagar, Orissa, India. *Asian Journal of Water Environment and Pollution*, **9:** 73-78.

NyunLing, P., Cheung, C.M. 2007. Study on noise perception and distraction in office. In: *Proceedings of IASDR07* (International Association of Societies of Design Research Hongkong, November, 2007). http: //www.sd. polyu. edu.hk/ iasdr/proceeding.

Passhier, V. W. 1993. *Noise and Health*, Netherlands. The Hague, Health Council of the Netherlands (Publication No. a93/02E)

Piccolo, A., Plutino, D., Cannistraro, G. 2005. Evaluation and analysis of the environmental noise of Messina, Italy. *Applied Acoustics,* **66:** 447-465.

Pradhan, A., Swain, B.K., Goswami, S. 2012. Measurements and model calibration of traffic noise pollution of an industrial and intermediate city of India. *The Ecoscan,* Special Issue, **1:** 377-386.

Robinson, D.W. 1971. Towards a unified system of noise assessment. *Journal of Sound and Vibration,* **14:** 279-288.

Rettinger, M. 1977. *Acoustic Design and Noise Control: Acoustic Design,* vol. **1&2**, Chemical Publishing Company, New York, USA.

Sundstrom, E., Town, J.P., Rice, R.W., Osborn, D.P., Brill, M. 1994. Office noise, satisfaction and performance. *Environment and Behavior*, **26 :** 195-222.

Swain, B.K., Goswami, S. 2013. Integration and comparison of assessment and modeling of road traffic noise in Baripada town, India. *International Journal of Energy and Environment,* **4:** 303-310.

Swain, B.K., Panda, S., Goswami, S. 2012a**.** Dynamics of road traffic noise in Bhadrak city, India. *Journal of Environmental Biology,* **32:** 1087-1092.

Swain, B.K., Goswami, S., Panda, S. 2012b**.** Road traffic noise assessment and modeling in Bhubaneswar, Capital of Odisha State, India: A comparative and comprehensive monitoring study. *International Journal of Earth Sciences and Engineering,* **5:** 1358-1370.

Pak. j. sci. ind. res. Ser. A: phys. sci. 2014 **57**(2) 109-124

Review

Advances in Nanotechnology: Influence on Biomolecular Detection Sensors

Khalid Mahmood Arif[ab]*, Kutay Icoz[b] and Ijaz Ahmad Chaudhry[a]
[a]Mechatronics and Control Engineering, University of Engineering and Technology Lahore-54890, Pakistan
[b]Birck Nanotechnology Center, Purdue University, West Lafayette, Indiana-47907, USA

(received April 6, 2012; revised February 8, 2013; accepted February 26, 2013)

Abstract. Nanodevices and biomolecules have incredibly strong correspondence in terms of size and physical properties. In this review, three major types of nanodevices, namely cantilevers, nanowires and carbon nanotubes, have been discussed and how they have resulted in new sensor designs or helped push the limits of detection in existing schemes. After brief overview of each type and the ways it could be used in biosensing, recent research efforts are presented to emphasise the challenges and achievements in that particular category.

Keywords: nanobiosensors, biosensors, nanodevices, cantilevers, nanowires, carbon nanotubes

Introduction

Detection and analysis of low concentrations of biomolecules for medical diagnostics, environmental monitoring, and quality control of products have always been of great interest and active topic of research due to associated benefits. For instance, precise detection of cancer biomarkers in blood allows timely diagnosis and treatment of the disease or detection of airborne pathogens can lead to early counter measures. However, the isolation and detection of these biomolecules present many challenges due to the fact that biomolecules are part of complex environments, such as blood, urine, air or water, and numerous other chemical and biochemical agents. Another challenge is the nanometer size scale of the biomolecules and need for same size devices to interact with them. To meet these challenges the collaboration of various engineering and science disciplines under the umbrella of nanotechnology and nanoscience has brought together innovative methods and techniques to design smaller and better devices known as nanobiosensors or simply biosensors-devices that can identify and recognise biological molecules and their activities. Blood, gas, glucose monitoring devices and pregnancy test strips are a few examples of commercially available biosensors, which not only benefit the patients but also underscore the need and the potential for more sophisticated systems even for DNA and protein detection (Gruhl *et al*., 2013; Carrascosa *et al*., 2006; Murphy, 2006; Wang, 2006; Collings and Caruso, 1997).

*Author for correspondence; E-mail: kmarif@uet.edu.pk

Generally, a biosensor has three major units, detector, transducer and signal processor. The detector accomplishes target specific recognition to detect the biochemical phenomenon (e.g., antibody-antigen binding), the transducer (e.g., cantilever, nanowire) generates measurable signals, and finally the processor unit (e.g., microcontroller or computer) filters, amplifies, and displays the output signal. Nanotechnology has been playing a vital role to better all these units (biosensors, detectors and transducers) therefore, getting benefits of devices based on these technologies. Utilising the concepts from already advanced field of semiconductor manufacturing, researchers have started producing micro-electro-mechanical systems (MEMS) and nano-electro-mechanical systems (NEMS) out of silicon well as polymers, metals, carbon, and etc., (Staples *et al*., 2006; Grayson *et al*., 2004; Moore and Syms, 1999). These days, some MEMS and NEMS devices are commercially available in the market (e.g., drug delivery systems, micro-needles, stents), (Murphy, 2006; Staples *et al*., 2006; Grayson *et al*., 2004) and some of them readily outperform widely used conventional systems. Their success attributes to short response time, mass fabrication, and capacity to integrate with other lab-on-chip devices and undoubtedly opens up possibilities of cost effective and portable devices for detecting biomolecules (Dhayal *et al*., 2006; Ziegler, 2004; Arntz *et al*., 2003).

A variety of biomolecular detection sensors based on nanodevices have been reported in the last many years

in the published literature. Similarly, numerous comprehensive review articles on various perspectives of nanobiosensing have also been published (Gao *et al*., 2012; Yeom *et al*., 2011; Curreli *et al*., 2008; Erickson *et al*., 2008; Nicu and Leichle, 2008; Cheng *et al*., 2006; Patolsky *et al*., 2006; Wanekaya *et al*., 2006). Contrary to usual reviews, main emphasis in this review was on the detectors and transducers that are direct result of nanotechnology, e.g., cantilevers, nanowires (NWs) and carbon nanotubes (CNTs). Properties and usage of these nanodevices have been discussed for particular biomolecules, however, signal transduction, processing and other aspects have been only mentioned if needed to elaborate a certain technique. A brief description of each device is followed by common sub-types of device variants and methods to incorporate in a biosensor design as detector and/or transducer. Then research examples from literature have been discussed to highlight the challenges and achievements in that particular category.

Micro cantilevers. Micro cantilevers are diving-board like structures that fall in the category of mechanical detection of biomolecules. A typical schematic diagram of the optical measurement setup, scanning electron micrograph (SEM) of micro-fabricated cantilevers and an illustration of molecular hybridisation and bending of cantilevers are shown in Fig. 1. Generally, the cantilevers are fabricated from silicon (Si), silicon oxide (SiO_2) and silicon nitride (Si_3N_4) through state of the art and standard semiconductor fabrication methods. However, specific applications and signal transduction methods may require coating of cantilevers with different materials to increase affinity for certain probe molecules or to provide shiny surface for laser reflection. Usually, gold (Au) coatings are used because alkane chain with thiol groups binds to gold and proteins adsorb on gold surface (Raiteri *et al*., 2001; Storri *et al*., 1998).

Gold coated Si cantilevers arrays were used by Fritz *et al*. (2000), as pioneering work in the field, to detect mismatch of oligonucleotides. Later on, arrays of individually functionalised cantilevers were employed for label-free multiple DNA detection by McKendry *et al*. (2002) as well. These works were reported more than a decade ago and since then gold coating has widely been adopted as preferred method of immobilisation. Polymer based cantilevers for biosensing applications have also been reported. Fluorocarbon coated polymeric cantilevers have been shown to have

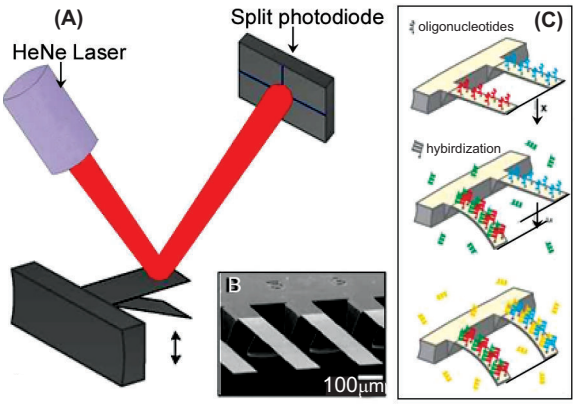

Fig. 1. (A) Schematic diagram of laser deflection setup used to measure transverse vibrations of the mechanical oscillators. (B) SEM micrograph of a section of a microfabricated Si cantilever array. (C) Scheme showing an example of hybridisation experiments with cantilever functionalisation on one side (Fritz *et al*., 2000).

some advantages over gold-coated silicon nitride cantilevers such as stability for temperature and pH changes (Calleja *et al*., 2006). However, the fabrication and immobilisation techniques for developing higher sensitivity polymer cantilevers require further improvements.

Cantilevers are mainly used to respond to stress or mass changes on the surface of the free end. Stress change results in deflection of the free end of the cantilever (static mode), while mass change influences both vibration frequency (resonant mode) and deflection. In static mode, the adsorption of molecules onto the surface causes the cantilever to bend. The well-known Stoney's equation (Stoney, 1909) explains the relation between the surface stress change and cantilever's tip deflection:

$$\Delta z = 3 \frac{(1 - v)}{E} \frac{L^2}{t^2} \Delta\sigma \quad \text{..... (1)}$$

where:

Δz = the cantilever's tip deflection; v = Poisson's ratio; E = Young's modulus; L = the length of the cantilever; t = is the thickness of the cantilever; and $\Delta\sigma$ = change in the surface stress (N/m). The Stoney's equation could be employed to estimate the tip deflection of simple rectangular (Fig. 1) or complex (Fig. 3) cantilever geometries.

When the cantilever is loaded with additional mass, resonant frequency decreases and the additional mass can be calculated by:

$$\Delta m = \frac{k}{4\pi^2}\left[\frac{1}{f_1^2} - \frac{1}{f_0^2}\right] \quad \text{..... (2)}$$

where:

k = the spring constant; f_0 = the initial frequency; f_1 = the resonant frequency after the mass loading. In order to increase the sensitivity, external actuation through piezoelectric devices may be used to create vibrations at specific frequencies (Johnson *et al*., 2006; Gupta *et al*., 2004).

Through optical and/or electrical methods, changes in tip deflection and resonant frequency may be readily detected and amplified for correlation (Johnson *et al*., 2006; Sone *et al*., 2006; Wu *et al*., 2001; Fritz *et al*., 2000; Ilic *et al*., 2000). However, laser based measurements are considered superior to other methods due to their higher sensitivity. Figure 1 shows a laser based measurement setup (also called optical lever method) wherein a laser beam, reflected from the surface of the cantilever, is detected by split photo-detectors that can measure the deflections with high accuracy (0.1 nm) as reported by Fritz *et al*. (2000).

Gupta *et al*. (2004) demonstrated detection of *Listeria innocua* cells using micro-fabricated cantilevers in resonant mode (Fig. 2). In this work, the cantilevers were loaded with cells and frequency shifts were observed on an optical measurement setup. It was observed that 180 bacterial cells caused nearly 2 kHz frequency shift. This work not only highlighted the modes of operation of cantilevers for biosensing but also served as seminal preliminary work for further development. In the recent years, numerous biosensing systems based on surface functionalised cantilevers-through immobilising biomolecular probes-have been reported for detection of various biological targets such as glucose (Pei *et al*., 2004), bacterial cells *Escherichia coli* (Gfeller *et al*., 2005), *Bacillus subtilis* spores (Dhayal *et al*., 2006), *Vaccinia* virus particles (Johnson *et al*., 2006), RNA (Zhang *et al*., 2006), and liposome-protein interaction (Hyun *et al*., 2006).

Cantilevers with shape novelties. Even though standard mechanical shape of a cantilever has one fixed and the other free end (Fig. 1), various geometrical changes are possible to meet the particular requirements of signal transduction and surface biochemical reactions. In this

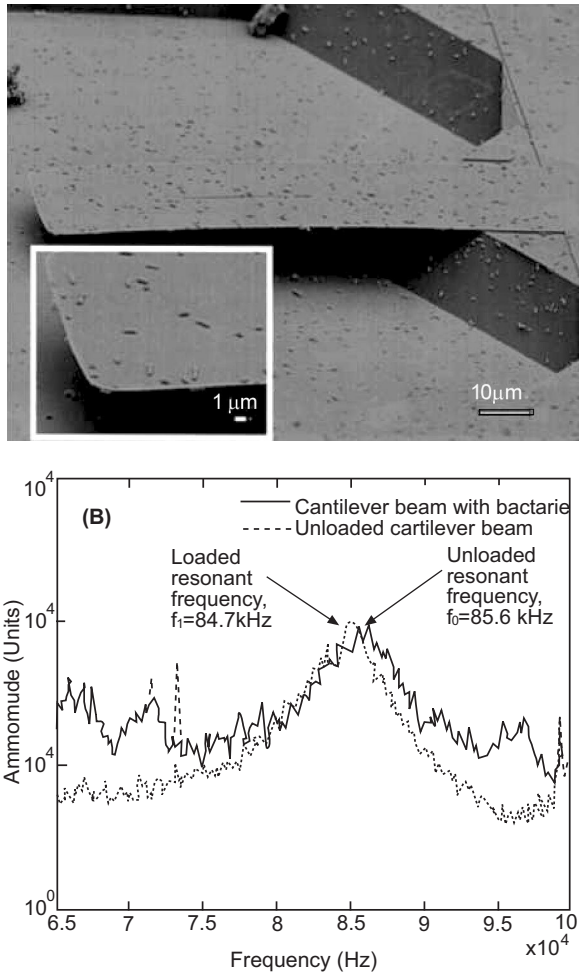

Fig. 2. (A) SEM micrograph of *Listeria innocua* cells on the cantilever surface. (B) Unloaded and loaded resonant frequencies of the cantilever (Gupta *et al*., 2004).

regard, fabrication of cantilevers for biosensor design with integrated optical interferometric features has been a hot topic of research for many years. Originally, these cantilevers were developed for atomic force microscopy (AFM), where cantilevers were used as scanning probes (Onaran *et al*., 2006; Yaralioglu *et al*., 1998; Manalis *et al*., 1996).

The first ever cantilever biosensor incorporating interferometry features was reported by Sulchek *et al*. (2001). In this work, the transducer, with interdigital fingers at the end of the cantilever to form a diffraction grating, was fabricated from Si_3N_4 and coated with 20 nm Au by evaporation. During experiments, hydrophobic

perfluorocarbon was applied to one arm (reference) to prevent covalent binding between the cantilever surface and thiol groups. Later, the thiol self-assembled monolayers (SAMs) on the other cantilever (sensor) were observed with optical lever and interferometry methods. It was found that interferometry method produced signal-to-noise ratio (SNR) of 18, while optical lever method resulted in SNR of 3.

The sensor shown in Fig. 3 (Savran *et al*., 2004) was designed to sense surface stress changes caused by the adsorption of biomolecules onto the cantilever. In this example, the molecules of interest were aptamers [single-stranded DNA or RNA (ssDNA or ssRNA) molecules that bind with high affinity and specificity to proteins and peptides etc.] and ligands. Aptamer molecules were immobilised on the gold-coated sensor surface with a thiol linker. ssDNA was immobilised to the reference cantilever in order to prevent nonspecific binding of target molecules to the reference cantilever. The L-shaped geometry of the sensor (Fig. 3A) allowed each cantilever to be functionalised individually by dipping one side (either sensor part or reference part) into a micropipette. In the experiment, ligand-aptamer binding created a surface stress change, which bent the sensor cantilever, while the reference cantilever was unaffected. The tip deflection of the cantilever was measured by a laser beam based on interferometry. Injection of 500 ρM Taq DNA polymerase solution into the chamber, including the cantilever, caused a differential deflection of 32 nm, while injection of 75 nM thrombin solution did not induce a measurable differential deflection. These results proved that differential deflection occurred as a result of specific binding.

Differential measurements with interferometry have considerable advantages over single measurements in terms of background noise. However, researchers who do not use differential cantilevers employ other methods to reduce noise. For instance, Fritz *et al*. (2000) employed one cantilever as a control and used optical lever measurements twice to subtract background noise from the biological signal. In another case, Alvarez and Tamayo (2005) employed a scanning laser source for recording measurements from cantilever arrays. Both of these techniques required additional signal processing and more complex measurement systems, when compared with the interdigitated cantilevers.

Cantilever geometries are not necessarily modified for sensitive measurements or noise reduction as mentioned

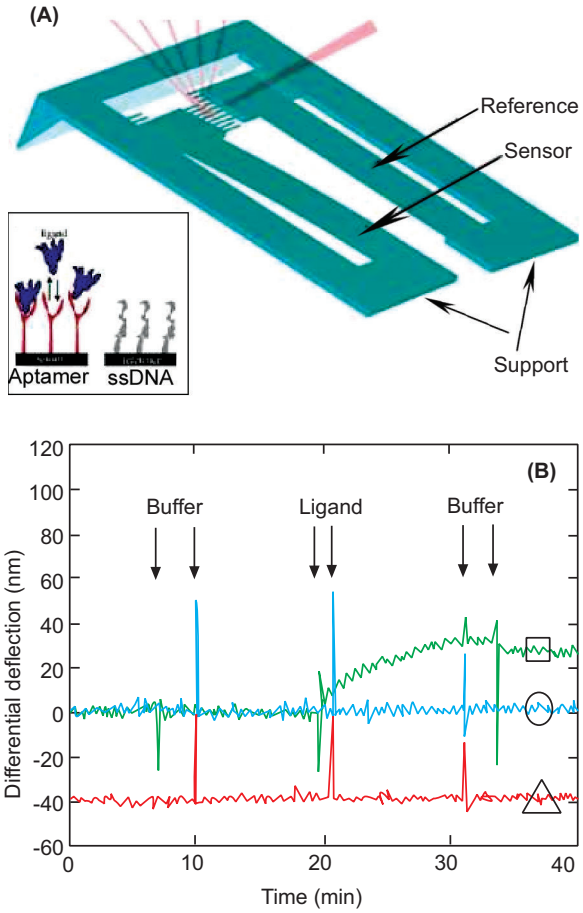

Fig. 3. (A) Schematic layout of an interferometric cantilever sensor. Both cantilevers (sensor and reference) are supported by L-shaped thick structures. Inset shows configuration of the front view of Au coated and functionalised sensor and reference cantilevers. (B) The result of DNA polymerase (□) and trombin (○) injection (Δ) is the response to Taq DNA polymerase when both the sensor and the reference are functionalized with ssDNA (Savran *et al*., 2004).

above. Fabrication of microfluidic channels on the top surface of cantilevers (Fig. 4A) was introduced by Burg *et al*. (2007) and Godin *et al*. (2007) and since then numerous devices with embedded microfluidic channels have been reported (Grover *et al*., 2011; Park *et al*., 2010). Burg *et al*. (2007) produced a microfluidic channel on the top surface of Si cantilever to weigh cells, biomolecules or particles by delivering them to the tip of cantilever through a continuous flow of fluid. The device was reported to have lower resolution (0.01 ng/cm^2) compared to quartz crystal microbalance

(QCM) and surface plasmon resonance (SPR). The device was used for both bound and unbound masses (Fig. 4B), however, the bound species paved way for specific detection by way of immobilisation. Experiments with particle position dependent signal measurements were also conducted. In these cases, the peak frequency shifts induced at the apex quantified the exact mass excess of a particle (Fig. 4C).

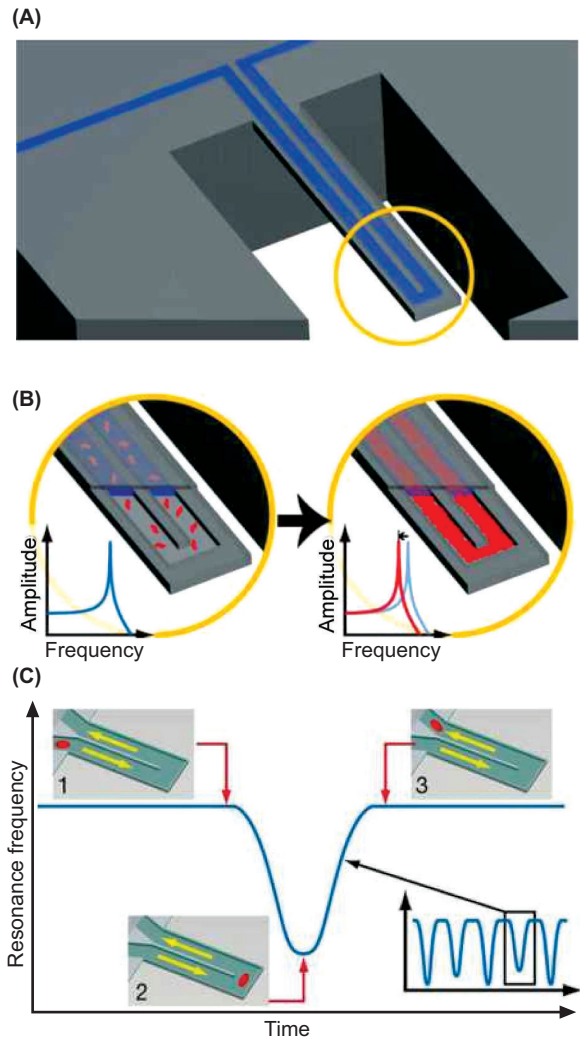

Fig. 4. (A) Schematic illustration of a cantilever with buried microfluidic channel to allow two mass measurement modes. (B) Frequency shift for accumulated (due to binding to the channel wall) particles shows possibility of specific detection by way of immobilised receptors. (C) Signal dependence on the position of flowing particle (inset 1-3) with the peak frequency shift induced at the apex (Burg *et al*., 2007).

Cantilevers with magnetic nanoparticles. According to equation 2, the sensitivity of measurements with cantilevers depends upon frequency of vibration, which in turn depends on the mass of particle. However, the loaded particles (biomolecules, cells, viruses, etc.) do not generally produce large frequency shifts e.g., a frequency shift of only 2 kHz was observed by Gupta *et al*. (2004). One of the methods to increase mass is by using magnetic nanoparticles (or beads) with cantilevers. For interaction with biomolecules, the surface of these nanoparticles can be modified by attaching the appropriate ligands such as antibodies, proteins or oligonucleotides (Bryant *et al*., 2007).

Moreover, these particles are magnetic only under the magnetic field, they could be easily separated from complex environments by applying external magnetic fields (Neuberger *et al*., 2005). A demonstration of the employment of magnetic beads with cantilevers for biosensor application is illustrated in Fig. 5 (Weizmann *et al*., 2004).

The setup shown in Fig. 5 was used for ultra-sensitive detection of viral (M13φ) DNA, single-base mismatch in a nucleic acid, and telomerase (Weizmann *et al*., 2004). Si cantilevers were coated with Au and functionalised with avidin and the deflection of cantilevers was measured by laser beam reflection on a photodiode, using an optical setup similar to Fig. 1A. Functionalised magnetic beads were injected onto the cantilevers to bind with avidin already present on the cantilever surface. When a magnetic field was introduced by an external magnet, the deflection of the cantilever was observed and 7.1×10^{-20} M of M13φ DNA was reported as the minimum detectable concentration with this method.

For the single-base mismatch (mutant gene) experiment the same procedures were employed. Functionalised magnetic beads (appropriately probed) hybridised with normal genes resulted in cantilever deflection, whereas, no signal change was observed in the presence of the mutant gene. Similarly, for the telomerase experiment, functionalised magnetic beads were introduced to HeLa cancer cell extract in the presence of telomerase, nucleotides, and biotinylated dUTPs (deoxyuridine triphosphate). When the magnetic beads coupled with biotin label and telomere bound to the avidin-coated cantilevers, the applied magnetic field caused deflection. A detection limit of 100 cancer cells was reported.

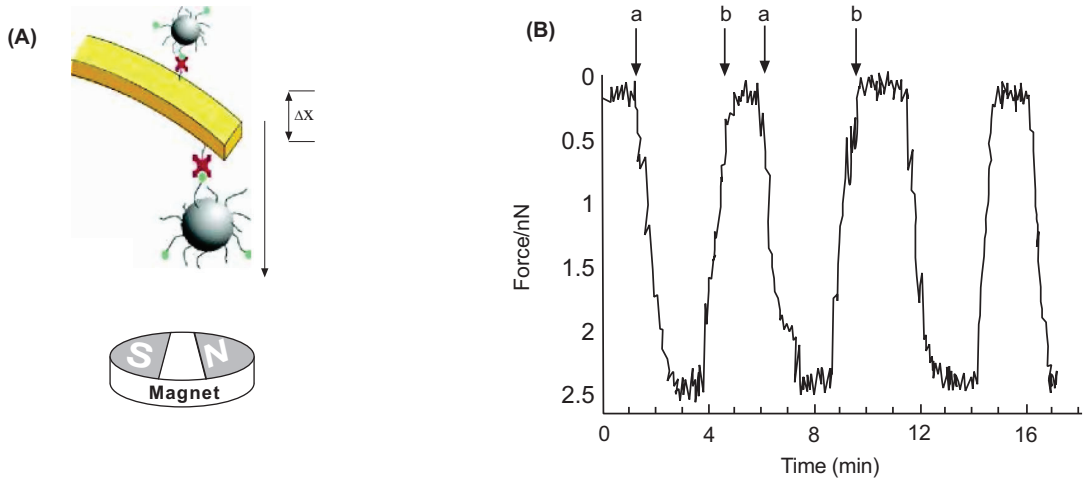

Fig. 5. (A) Schematic layout of magneto-mechanical analysis of biorecognition process on functionalised cantilevers. (B) Magneto-mechanical deflection of the cantilever. At points marked as 'a' cantilever is subjected to the external magnet, while at points marked as 'b' the external magnet is removed. Adapted from Weizmann *et al*. (2004).

Another biosensor application of magnetic beads and cantilevers for detection of endonuclease activity has been presented by Weizmann *et al*. (2005). Gold-coated cantilevers were functionalised with nucleic acids and the magnetic beads were functionalised with complementary nucleic acids. The endonuclease activity was tested by DNA cleavage and detected by cantilever deflection when magnetic field was applied.

Furthermore, analysis of actuation setup for the two systems in Weizmann *et al*. (2005) and Weizmann *et al*. (2004), tells that sensitivity of cantilevers with standard rectangular geometries could be increased by magnetic beads, when a permanent magnet is placed underneath to apply force to cantilevers. Weak magnetic field intensity causes no deflection, whereas when the magnet is moved towards the cantilever, stronger magnetic field intensity causes bigger deflections. However, the noise in the output signal remained as a limiting factor and these sensors only served as early stage development in the area of force applied biological sensor.

Building upon findings of interferometric (Savran *et al*., 2004) and magneto-mechanical (Weizmann *et al*., 2005; Weizmann *et al*., 2004) cantilever devices, recently Icoz *et al*. (2008) presented actuation of interferometric cantilevers at low noise region using magnetic beads as shown in Fig. 6. The control arm of the differential cantilever was passivated with bovine serum albumin (BSA) and sensing arm was probed with biotin-BSA. The probe molecules were placed on the cantilevers using nanojet dispensing system as an alternative method to micro-pipetting (Bietsch *et al*., 2004). Nanoject dispensing was reported to have allowed only one side of the cantilever to interact with the biomolecules and only small amount of drops were needed to functionalise the surface. The electromagnet was controlled by a function generator so that the frequency of excitation signal could be adjusted. In this way, cantilevers were excited at low noise region allowing a resolution of 0.065 Å. Later, using this setup, 0.28 nM concentration of streptavidin was detected (Icoz and Savran, 2010). In this study, streptavidin from serum was captured and separated by biotin-coated magnetic beads.

Nanowires. Nanowires (NWs) are nanometer sized structures with large aspect ratios. This small size and large aspect ratio renders them very different physical and electrical properties compared to bulk material from which they are made e.g., very small conductivity due to scattering from boundaries. NWs fabricated out of Si and indium oxide (Ahn *et al*., 2012; Li *et al*., 2005; Tang *et al*., 2005) are commonly used in biosensor applications. Both, top-down (Ahn *et al*., 2010) and bottom-up (Zheng *et al*., 2005) methods are employed

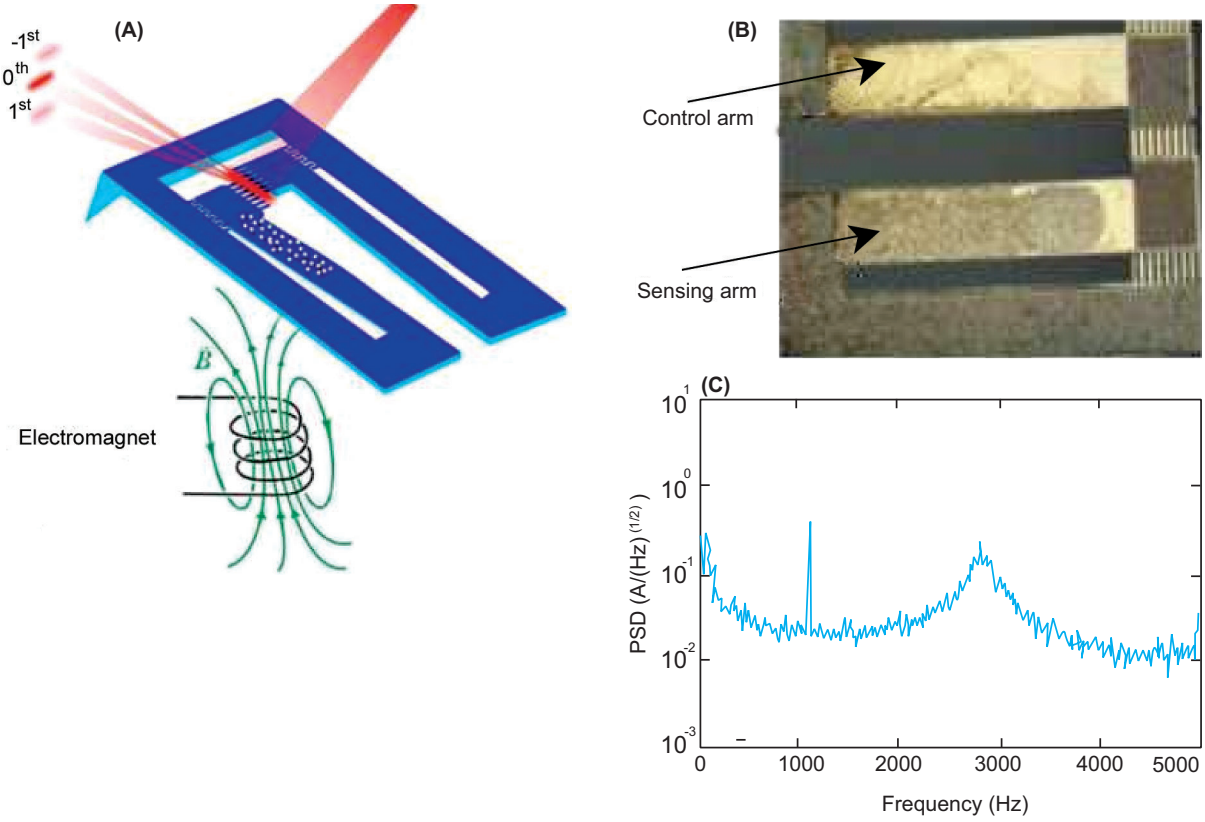

Fig. 6. (A) Magnetic actuation and interferometric detection scheme. (B) Magnified image of the functionalised cantilever device showing insignificant number of magnetic beads on the control arm and huge numbers of the same bound to the sensing arm. (C) Cantilever actuation at 1103 Hz and resonant frequency around 3000 Hz (Icoz *et al*., 2008).

for NW fabrications. Top- down methods, which utilise lithography, deposition, and etching, randomly orient the NWs and they need to be positioned and aligned on the electrodes through different alignment techniques (He *et al*., 2008). Bottom-up methods, which utilise chemical vapour deposition (CVD), are better for functionalisation before the alignment on the chip and hence easier than functionalising multiplexed NWs already placed on a chip. NWs which are lightly doped, have short length and smaller diameter, show increased sensitivity. However, in order to have smaller diameters new fabrication techniques have to be developed (Stern *et al*., 2008).

Mostly, NWs are used in biosensors as NW field effect transistor (NW-FET) and their structure is similar to conventional FETs, which includes drain, source, semiconductor channel, and gate electrodes. NW forms the semiconductor channel with a high surface area-to-volume ratio. The binding of biomolecules to the NW causes accumulation or depletion of charge carriers both on the wire surface and inside the wire resulting in detectable conductivity changes. Detection of antibodies (Stern *et al*., 2007), ssDNA (Kim *et al*., 2007), virus (Patolsky *et al*., 2004), proteins (Cui *et al*., 2001), and electrical activities of neuron cells (Patolsky *et al*., 2006) have been reported. A typical representation of these FETs is given in Fig. 7.

Use of NWs is not limited to FET-based sensors, instead they have been used in many other ways such as amperometric (Lu *et al*., 2007), impedimetric, and potentiometric (Zhang *et al*., 2009). However, for the sake of brevity, NW-FET-based sensors have been discussed here. An elaborative investigation of such electrochemical biosensors has been done by Grieshaber *et al*. (2008).

In case of NW-FETs, the effective magnitude of surface charge highly depends on the ionic concentration and ionic strength of the buffer solution. Ionic strength (I)

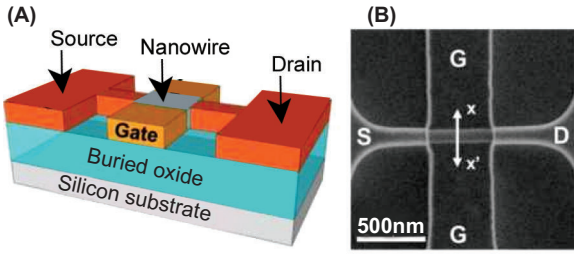

Fig. 7. (A) Illustration of a nanowire FET biosensors fabricated on Si substrate. NW surface is functionalised with receptor molecules to capture target molecule. (B) SEM micrograph of the top view of the fabricated biosensor showing Source, Drain and Gate of FET (Ahn *et al*., 2012).

of the buffer solution determines an important parameter, the Debye length the length in which mobile charge carriers screen out the external electric field, causing small charge movement (Fig. 8), given by Maehashi *et al*. (2007).

$$\text{Debye length} \sim 0.32(I)^{-12} \quad \text{..... (3)}$$

In order to improve device performance against Debye length limitation (equation 3), various probe molecules have been investigated. Advancement in probe molecules is linked with the advancement in the NW based biosensors.

Nanowires and probe molecules. Functionalisation of Si NW-FETs with aptamers (1-2 nm), oligonucleic acid or peptide molecules that bind to a specific target molecule, helps reduce the Debye length as compared to antibodies (~10 nm) (Fig. 8). This strategy has been used to detect thrombin (Kim *et al*., with ~330 ρmol/L sensitivity and to detect vascular endothelial growth

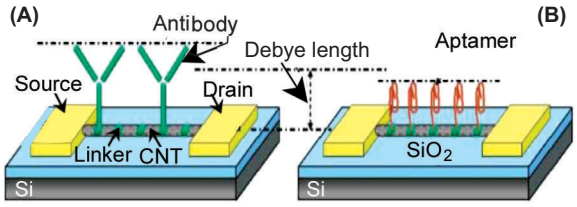

Fig. 8. Illustration of Debye length in NW/CNT-FET biosensor. (A) Functionalisation with antibody results in size larger than Debye length, while (B) aptamer functionalisation produces size smaller than Debye length and thus causes higher charge interaction (Maehashi *et al*., 2007).

factor (VEGF) with 100 ρM sensitivity (Lee *et al*., 2009). Sophisticated probe molecules can be designed through protein engineering, leading to detection of uncharged hormones (steroid, 19- noradrostendione) with Si-FETs (Chang *et al*., 2009). The reported sensitivity in this case is in fM range. Engineered antibody mimic proteins (AMPs) have improved binding affinity and recognition with sizes (typically 2-5 nm) smaller than antibodies (Ishikawa *et al*., 2009). The application of AMPs on indium oxide FETs was demonstrated to detect SARS biomarker N-protein. When compared to enzyme-linked immunosorbent assay (ELISA) which takes hours, this method only takes 10 min to detect SARS biomarker.

Immobilising peptide nucleic acid (PNA) on the nanowires does not cause significant charge formation on the surface thus, yielding higher sensitivity. The hybridisation efficiency of PNA and micro RNA (miRNA) have been shown to be higher than DNA and miRNA (Zhang *et al*., 2009). In this study, PNA functionalised Si FET sensor was able to detect 1 fM of miRNA. PNA functionalised Au NWs were used to detect 100 fM of mRNA (Fang and Kelley, 2009), while a previous study reported PNA functionalised Si FET sensor to detect 10 fM of DNA (Gao *et al*., 2007). One method of covalent binding of PNA molecules to SiO_2 NW has been described by Cattani-Scholz *et al*. (2008), which is an alternative way to physisorption. Zhang *et al*. (2010) recently reported a highly sensitive and rapid sensor based on PNA-DNA hybridisation to detect reverse-transcription-polymerase chain reaction (RT-PCR) product of Dengue serotype 2 (DEN-2). As shown in (Fig. 9), Si NW was functionalised with PNA and resistance change of the sensor before and after hybridisation was measured. Compared to previously reported long hybridisation time (about 16 h), this scheme worked for as little as 30 min of hybridisation and showed 6% response change, which corresponds to detection of 10 fM concentration of the RT-PCR product of DEN-2. The assay is also reported as highly reproducible, with less than 15% relative standard deviation on different chips.

NWs may also be functionalised with lipid bilayers (Martinez *et al*., 2009). The lipid bilayers include various types of ion channels, so these channels can act as barrier and transport the specific ions through NW. In this proof-of-concept work, lipid membrane with 1.4 nm pores formed by α-hemolysin polypeptide promoted the ion transport. This kind of selectivity can

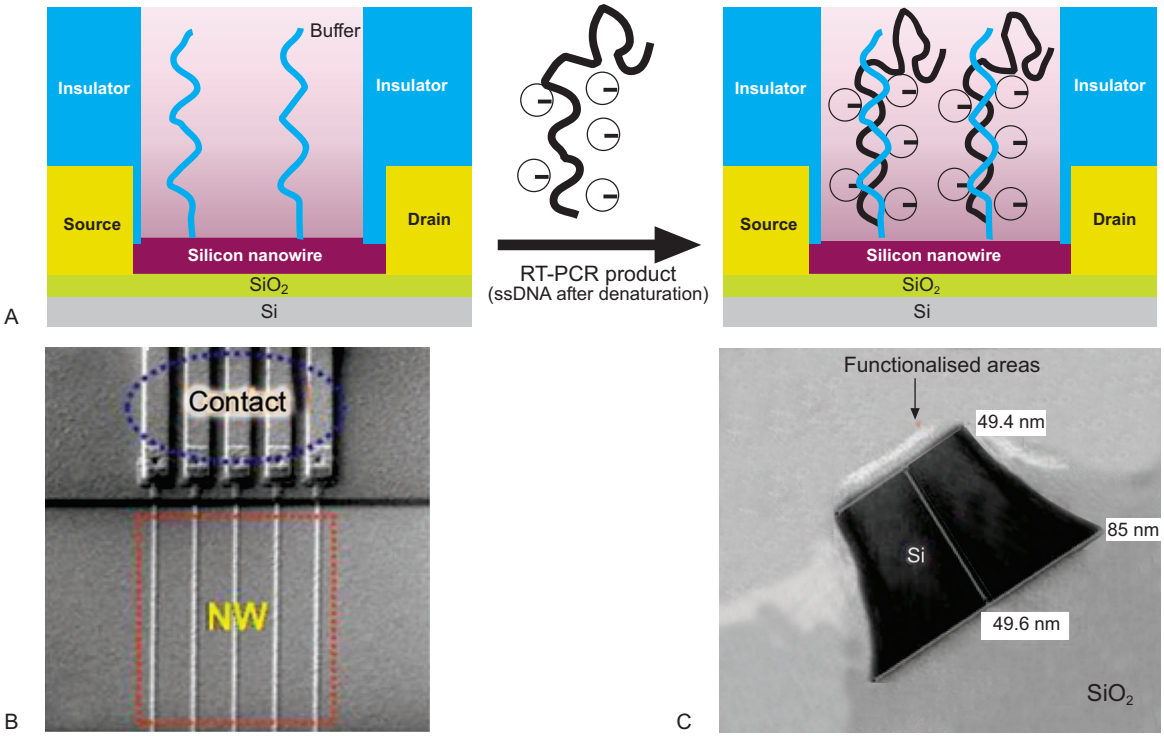

Fig. 9. Schematic diagram of the RT-PCR product of DEN-2 hybridised to the PNA-functionalised Si NW sensor. (B) SEM image of NW arrays and the corresponding contact lines. (C) TEM image of a single NW embedded in SiO_2 after surface functionalization (Zhang *et al*., 2010).

shield the NW surface from the other ions present in the surrounding liquid.

Novel materials for nanowires. In order to reduce the fabrication costs and overcome the limitations of NW reproducibility, and non-specific binding of biomolecules, other materials such as polymers and hybrid materials are also being investigated. Polymers draw attention because of their electrical, magnetic and optical properties. Electrochemically synthesised polypyrrole (Ppy) - a conducting polymer-NW has been used to make a chemiresistive biosensor to detect cancer marker, CA 125, where 1 U/mL was reached as the limit of detection (Bangar *et al*., 2009). Another work on conducting polymer (pyrrolepropylic acid) FET resulted in 50 nM detection limit for human serum albumin (Tolani *et al*., 2009). Electrochemical detection of oligonucleotides has been demonstrated by using polyaniline nanotubes with low nanomolar detection limit (Zhang *et al*., 2007). In an electrochemical impedance spectroscopy experiment, GaN NWs with diameter of 25-100 nm were fabricated with CVD process for the detection of DNA (Chen *et al*., 2009). For a FET sensor, poly-Si NWs with diameters of 80 nm were fabricated applying a low-cost sidewall spacer technique, where fM DNA detection limit was reported (Lin *et al*., 2009). Another material investigated for NW biosensor is iridium oxide (IrO_2) (Zhang *et al*., 2008). IrO_2 has been reported to have advantages when used as a stimulating and recording electrode and characterised NW has been proposed for biosensing or neuron electrode.

A multi-segment NW-FET biosensor was introduced for ssDNA detection (Wang and Ozkan, 2008). In this study, NWs had a heterostructure of CdTe-Au-CdTe with 230 nm diameters. Electrochemically deposited CdTe and Au NWs had a *p*-type semiconductor behaviour. Au part of the NW was functionalised with thiol-ssDNA and 1 μM of ssDNA detection was reported. Even though the sensitivity is not at the desired level, multisegment NWs have the advantage of selective functionalisation. Thus, the non-specific binding of probe molecules to electrode contacts and bulk material can be avoided.

Instead of using single wire, using multiple wires can be advantageous in some applications. For example, detection of bacteria based on impedance measurements

are reported by Wang *et al*. (2008), where TiO_2 NW bundle (~1 mm length) was easily placed on electrodes under optical microscopy. In another example, Si NWs with 30 nm diameters and 100 μm length were fabricated using a top-down approach. As it was mentioned earlier, top-down approach leads to highly controlled orientation of NWs. The orientation and size of the NWs allowed detection of electrical activity of cardiac cells (Pui *et al*., 2009).

Carbon nanotubes. Carbon nanotubes (CNTs) are very thin (with diameter in nm), hollow cylindrical structures made of carbon atoms. CNTs can be mainly classified into single-wall carbon nanotubes (SWCNTs) or multi-walled carbon nanotubes (MWCNTs) depending upon the location of carbon atoms on the surface of nanotubes. Figure 10 depicts three different types of SWCNTs resulting from roll-up of graphene sheet and a MWCNT made up of three shells of differing chirality (a property of asymmetry). When CNTs are fabricated by CVD the semiconducting properties are controlled during the growth process. Generally, CNT biosensors consist of either SWCNTs or a network of nanotubes (Claussen *et al*., 2009). SWCNTs demonstrate ultra-high sensitivity because of their size (~1 nm diameter). When using CNTs in FETs they form the semiconductor channel and interact with the analyte in a similar fashion as nanowires (Fig. 7-8).

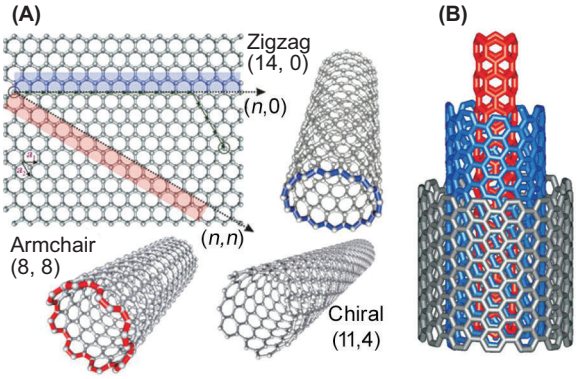

Fig. 10. (A) Three different types of SWCNTs result from roll-up of graphene sheet. Numbers in parentheses, m and n, are positive integers called chiral indices. These two numbers govern all physical properties of SWNTs. (B) Structure of a MWCNT made up of 3 shells of differing chirality (Balasubramanian and Burghard, 2005).

Proteins (Strehlitz *et al*., 2008; Kojima *et al*., 2005), glucose (Besteman *et al*., 2003), DNA (Li *et al*., 2003) and swine influenza virus H1N1 (Lee *et al*., 2011) are among a few demonstrations of CNT-FETs in biosensing applications. CNTs could also be designed as part of capacitive biosensors e.g., SWCNT network formed the one plate of the capacitor in a sensor designed for the detection of prostate specific antigen (PSA) (Briman *et al*., 2007). The CNT network was functionalised with specific antibody against PSA. The charge alteration was detected by measuring the capacitance change of the circuit and a detection limit of 100 ng/mL was reached in untreated calf blood serum, although in previous works with NWs (Li *et al*., 2005; Zheng *et al*., 2005) lower detection limits of PSA were reported.

Numerous valuable review articles have been written on CNT-based sensors (Musameh *et al*., 2012; Kerman, 2008; Allen *et al*., 2007; Gruner, 2006), therefore, in this part, present discussion is confined to most recent research and progress directed towards improvement in sensing capabilities of CNT-FET biosensor only.

Though single molecule level detection schemes using CNT-FETs have been demonstrated (Choi *et al*., 2012; Sorgenfrei *et al*., 2011), problems such as sensor-to-sensor variation, non-specific binding and charge noise are among major issues associated with CNT-FET biosensors. Recently, determination of extent and cause of these problems has gotten attention of many researchers. A dual-mode biosensor was reported by Oh *et al*. (2010), wherein CNT-based metal semiconductor FET (CNT-MESFET) structure was fabricated on a quartz substrate (Fig. 11). The Au strip (middle of the CNT channel) acted as the top gate of FET because of the Schottky contact between the CNT and the Au strip. DNA hybridisation occurring on the Au top gate can be detected by simultaneously measuring the change in the electrical conductance and the SPR. These two techniques were chosen, in an expectation, for this dual-mode biosensor to provide high sensitivity and reliability in electrical and SPR measurements, respectively. The authors report a shift in SPR reflectance minimum and decrease in the I_{SD} (current between source and drain), upon hybridisation of DNA with the Au top gate. It was further noticed that SPR measurements could be reproduced independent of the sensor and thus could be used to measure sensor-to-sensor variation of conductance.

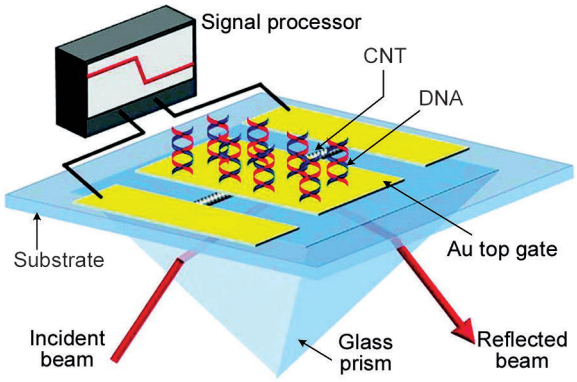

Fig. 11. Layout of a dual-mode CNT-MESFET biosensor. Adapted from Oh *et al*. (2010).

To better understand the mechanism and origins of charge noise in CNT-based FETs, a noise measurement setup have been reported by Sharf *et al*. (2012) to bring to light new design considerations for nano-FETs that are used to interface biological systems with electronics (Fig. 12). The environment in contact with ultraclean CNT was systematically controlled to quantify the contribution of noise from substrate interactions and surface adsorbates. Prior to experiments, Raman spectroscopy and transistor curves were used to quantify any lattice defects in the CNTs or measurement hysteresis in ambient conditions (Fig. 12C-12D). Identification of single CNTs was done using scanning photocurrent microscopy (inset of Fig. 12D). Initial experiment on device-to-device variability revealed that suspended CNT devices were considerably quieter than standard CNT-FET sensors. Therefore, the suspended CNT biosensor platform could be used to search for the noise sources in traditional CNT-FET sensors. It was found that the contact with substrates and adsorbates significantly, increased the charge noise in CNT-FET biosensors. For a 1 μm channel length, and a measurement bandwidth of 0.1-100 Hz, the effective gate voltage fluctuations were approximately 0.5 mV (pristine suspended), 1.1 mV [with poly(L-lysine) or horse heart cytochrome c], 1.8 mV (with substrate interactions), and 2.3 mV (with substrate interactions and PR residue). The authors speculated that the fluctuating protonation state of chemical moieties near the CNT can account for this noise.

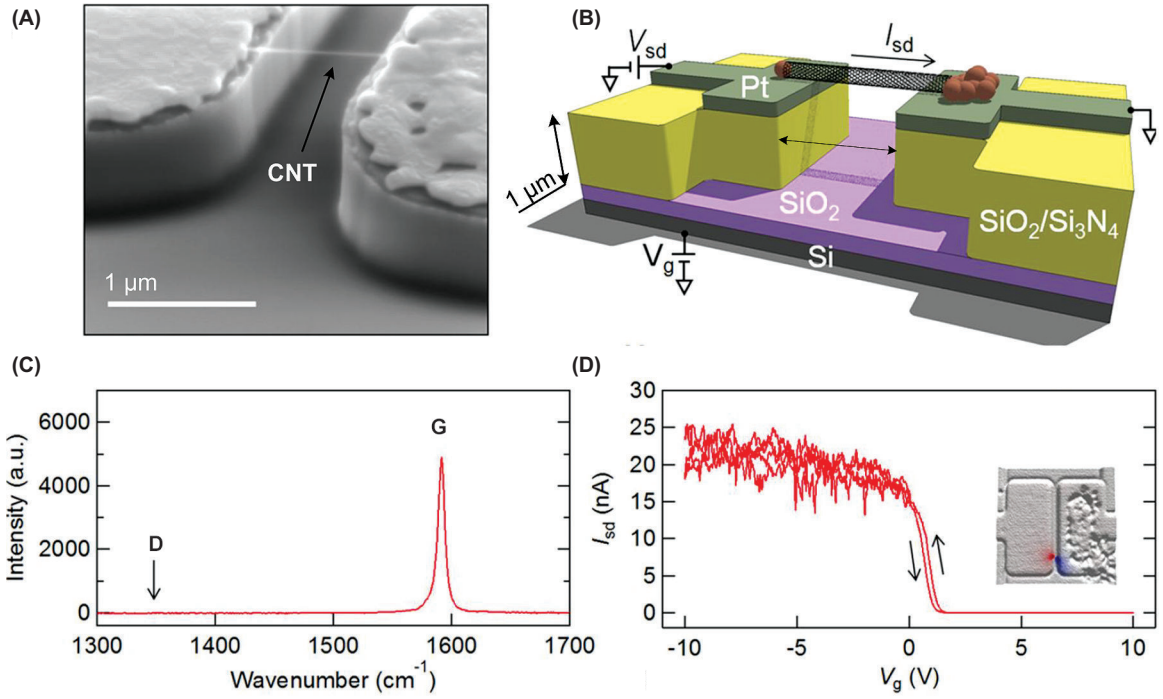

Fig. 12. (A) SEM image of a CNT bridging the gap between two platinum electrodes. (B) Schematic of hanging CNT device. (C) Raman spectra from a hanging CNT grown by fast-heat CVD. (D) Transistor curve of a hanging device in air under ambient conditions and no hysteresis. Photocurrent response (coloured dots in the inset) is superposed on top of reflectance image (Sharf *et al*., 2012).

Optimisation of the sensitivity of CNT-based biosensor with biasing and surface charge is another very recent research effort (Shoorideh and Chi On, 2012) that focused on Debye screening. This work concluded that sensitivity may also be affected by other charges present in the vicinity of the analyte.

Conclusion

In this paper some emerging nanobiosensors namely cantilevers, NWs and CNTs have been reviewed. In general, advantages of these NEMS and MEMS biosensors over today's widely used procedures like ELISA, QCM, electron microscopy, and fluorescence staining assays, are short response time, mass fabrication, multiplexing and capacity to integrate with other lab-on-a-chip devices. They also offer the possibility of cost-effective and portable devices for detecting biomolecules. These systems have promising features, however, there are some limitations which require more research efforts.

Cantilevers have ultra-high sensitivity, however, they have not been fully developed for clinical applications. Noise and sample preparation issues need new approaches. The highest sensitivities are achieved when optical methods are used and optical methods need precise alignment with extra components. Incorporating cantilevers with magnetic nanoparticles and fabrication of microfluidic channels inside the cantilever are two different approaches to improve the cantilever operation.

NW biosensors have important features like label-free detection, ultra-high sensitivity and possibility of integration with electronic devices. Additionally, NW sensors do not need any optical components for the detection of output signals leading to more compact biosensor designs. New fabrication strategies and appropriate functionalisation methods could result in promising detection limits. As explained in the section 3, Debye length is an important limiting factor, however, alternative and novel probing agents have been developed to deal with this limitation.

CNTs are among highly investigated nanodevices researched for biosensing applications. Quite a number of recent research efforts have been directed towards understanding of noise, sensor-to-sensor variation and other problems. However, more research efforts and development are needed to optimise and understand the exact mechanism of CNT-based FET biosensors.

Overall, the influence of nanotechnology based devices on biosensors has been tremendous in the past decade or so. Many new and incremental solutions, based upon the work of other researchers, have been reported. However, there is still a long way to go for wide-spread availability and usage of these biosensors. Particularly, this is because of the fact that most of the work is still targeted towards new assays and improvements in the existing solutions. Point-of-care or clinical setting solutions are yet to come out of laboratory controlled environments.

References

Ahn, J.H., Kim, J.Y., Choi, K., Moon, D.I., Kim, C.H., Seol, M.L., Park, T.J., Lee, S.Y., Choi, Y.K. 2012. Nanowire FET biosensors on a bulk silicon substrate. *IEEE Transactions on Electron Devices*, **59:** 2243-2249.

Ahn, J.H., Choi, S.J., Han, J.W., Park, T.J., Lee, S.Y., Choi, Y.K. 2010. Double-gate nanowire field effect transistor for a biosensor. *Nano Letters*, **10:** 2934-2938.

Allen, B.L., Kichambare, P.D., Star, A. 2007. Carbon nanotube field-effect-transistor-based biosensors. *Advanced Materials*, **19:** 1439-1451.

Alvarez, M., Tamayo, J. 2005. Optical sequential readout of microcantilever arrays for biological detection. *Sensors and Actuators B:Chemical*, **106:** 687-690.

Arntz, Y., Seelig, J.D., Lang, H.P., Zhang, J., Hunziker, P., Ramseyer, J.P., Meyer, E., Hegner, M., Gerber, C. 2003. Label-free protein assay based on a nanomechanical cantilever array. *Nanotechnology*, **14:** 86-90.

Balasubramanian, K., Burghard, M. 2005. Chemically functionalized carbon nanotubes. *Small*, **1:** 180-192.

Bangar, M.A., Shirale, D.J., Chen, W., Myung, N.V., Mulchandani, A. 2009. Single conducting polymer nanowire chemiresistive label-free immunosensor for cancer biomarker. *Analytical Chemistry*, **81:** 2168-2175.

Besteman, K., Lee, J.O., Wiertz, F.G.M., Heering, H.A., Dekker, C. 2003. Enzyme-coated carbon nanotubes as single-molecule biosensors. *Nano Letters*, **3:** 727-730.

Bietsch, A., Zhang, J.Y., Hegner, M., Lang, H.P., Gerber, C. 2004. Rapid functionalization of cantilever array sensors by inkjet printing. *Nanotechnology*, **15:** 873-880.

Briman, M., Artukovic, E., Zhang, L., Chia, D.,

Goodglick, L., Gruner, G. 2007. Direct electronic detection of prostate-specific antigen in serum. *Small*, **3:** 758-762.

Bryant, H.C., Sergatskov, D.A., Lovato, D., Adolphi, N.L., Larson, R.S., Flynn, E.R. 2007. Magnetic needles and superparamagnetic cells. *Physics in Medicine and Biology*, **52:** 4009-4025.

Burg, T.P., Godin, M., Knudsen, S.M., Shen, W., Carlson, G., Foster, J.S., Babcock, K., Manalis, S.R. 2007. Weighing of biomolecules, single cells and single nanoparticles in fluid. *Nature*, **446:** 1066-1069.

Calleja, M., Tamayo, J., Nordstrom, M., Boisen, A. 2006. Low-noise polymeric nanomechanical biosensors. *Applied Physics Letters*, **88:** 113901-113903.

Carrascosa, L.G., Moreno, M., Alvarez, M., Lechuga, L.M. 2006. Nanomechanical biosensors: a new sensing tool. *TrAC-Trends in Analytical Chemistry*, **25:** 196-206.

Cattani-Scholz, A., Pedone, D., Dubey, M., Neppl, S., Nickel, B., Feulner, P., Schwartz, J., Abstreiter, G., Tornow, M. 2008. Organophosphonate-based PNA-functionalization of silicon nanowires for label-free DNA detection. *ACS Nano*, **2:** 1653-1660.

Chang, K.S., Chen, C.C., Sheu, J.T., Li, Y.K. 2009. Detection of an uncharged steroid with a silicon nanowire field-effect transistor. *Sensors and Actuators B:Chemical*, **138:** 148-153.

Chen, C.P., Ganguly, A., Wang, C.H., Hsu, C.W., Chattopadhyay, S., Hsu, Y.K., Chang, Y.C., Chen, K.H., Chen, L.C. 2009. Label-free dual sensing of DNA molecules using GaN nanowires. *Analytical Chemistry*, **81:** 36-42.

Cheng, M.M.C., Cuda, G., Bunimovich, Y.L., Gaspari, M., Heath, J.R., Hill, H.D., Mirkin, C.A., Nijdam, A.J., Terracciano, R., Thundat, T., Ferrari, M. 2006. Nanotechnologies for biomolecular detection and medical diagnostics. *Current Opinion in Chemical Biology*, **10:** 11-19.

Choi, Y., Moody, I.S., Sims, P.C., Hunt, S.R., Corso, B.L., Perez, I., Weiss, G.A., Collins, P.G. 2012. Single-molecule lysozyme dynamics monitored by an electronic circuit. *Science*, **335:** 319-324.

Claussen, J.C., Franklin, A.D., ul Haque, A., Porterfield, D.M., Fisher, T.S. 2009. Electrochemical biosensor of nanocube-augmented carbon nanotube networks. *ACS Nano*, **3:** 37-44.

Collings, A.F., Caruso, F. 1997. Biosensors: recent advances. *Reports on Progress in Physics*, **60:** 1397-1445.

Cui, Y., Wei, Q.Q., Park, H.K., Lieber, C.M. 2001. Nanowire nanosensors for highly sensitive and selective detection of biological and chemical species. *Science*, **293:** 1289-1292.

Curreli, M., Zhang, R., Ishikawa, F.N., Chang, H.K., Cote, R.J., Zhou, C., Thompson, M.E. 2008. Real-time, label-free detection of biological entities using nanowire-based FETs. *IEEE Transactions on Nanotechnology*, **7:** 651-667.

Dhayal, B., Henne, W.A., Doorneweerd, D.D., Reifenberger, R.G., Low, P.S. 2006. Detection of *Bacillus subtilis* spores using peptide-functionalized cantilever arrays. *Journal of the American Chemical Society*, **128:** 3716-3721.

Erickson, D., Mandal, S., Yang, A.H.J., Cordovez, B. 2008. Nanobiosensors optofluidic, electrical and mechanical approaches to biomolecular detection at the nanoscale. *Microfluidics and Nanofluidics*, **4:** 33-52.

Fang, Z.C., Kelley, S.O. 2009. Direct electrocatalytic mRNA detection using PNA-nanowire sensors. *Analytical Chemistry*, **81:** 612-617.

Fritz, J., Baller, M.K., Lang, H.P., Rothuizen, H., Vettiger, P., Meyer, E., Guntherodt, H.J., Gerber, C., Gimzewski, J.K. 2000. Translating biomolecular recognition into nanomechanics. *Science*, **288:** 316-318.

Gao, C., Guo, Z., Liu, J.H., Huang, X.J. 2012. The new age of carbon nanotubes: An updated review of functionalized carbon nanotubes in electrochemical sensors. *Nanoscale*, **4:** 1948-1963.

Gao, Z.Q., Agarwal, A., Trigg, A.D., Singh, N., Fang, C., Tung, C.H., Fan, Y., Buddharaju, K.D., Kong, J.M. 2007. Silicon nanowire arrays for label-free detection of DNA. *Analytical Chemistry*, **79:** 3291-3297.

Gfeller, K.Y., Nugaeva, N., Hegner, M. 2005. Rapid biosensor for detection of antibiotic-selective growth of *Escherichia coli*. *Applied and Environmental Microbiology*, **71:** 2626-2631.

Godin, M., Bryan, A.K., Burg, T.P., Babcock, K., Manalis, S.R. 2007. Measuring the mass, density, and size of particles and cells using a suspended microchannel resonator. *Applied Physics Letters*, **91:** 123121-123123.

Grayson, A.C.R., Shawgo, R.S., Johnson, A.M., Flynn, N.T., Li, Y.W., Cima, M.J., Langer, R. 2004. A BioMEMS review: MEMS technology for physiologically integrated devices. *Proceedings of the IEEE*, **92:** 6-21.

Grieshaber, D., MacKenzie, R., Voros, J., Reimhult, E. 2008. Electrochemical biosensors-sensor principles and architectures. *Sensors*, **8:** 1400-1458.

Grover, W.H., Bryan, A.K., Diez-Silva, M., Suresh, S., Higgins, J.M., Manalis, S.R. 2011. Measuring single-cell density. *Proceedings of the National Academy of Sciences of the United States of America*, **108:** 10992-10996.

Gruhl, F.J., Rapp, B.E., Länge, K. 2013. Biosensors for diagnostic applications, *Advances in Biochemical Engineering/Biotechnology*, **133:** 115-148.

Gruner, G. 2006. Carbon nanotube transistors for biosensing applications. *Analytical and Bioanalytical Chemistry*, **384:** 322-335.

Gupta, A., Akin, D., Bashir, R. 2004. Detection of bacterial cells and antibodies using surface micromachined thin silicon cantilever resonators. *Journal of Vacuum Science & Technology B*, **22:** 2785-2791.

He, B., Morrow, T.J., Keating, C.D. 2008. Nanowire sensors for multiplexed detection of biomolecules. *Current Opinion in Chemical Biology*, **12:** 522-528.

Hyun, S.-J., Kim, H.-S., Kim, Y.-J., Jung, H.-I. 2006. Mechanical detection of liposomes using piezoresistive cantilever. *Sensors and Actuators B: Chemical*, **117:** 415-419.

Icoz, K., Savran, C. 2010. Nanomechanical biosensing with immunomagnetic separation. *Applied Physics Letters*, **97:** 123701-123703.

Icoz, K., Iverson, B.D., Savran, C. 2008. Noise analysis and sensitivity enhancement in immunomagnetic nanomechanical biosensors. *Applied Physics Letters*, **93:** 103902-103904.

Ilic, B., Czaplewski, D., Craighead, H.G., Neuzil, P., Campagnolo, C., Batt, C. 2000. Mechanical resonant immunospecific biological detector. *Applied Physics Letters*, **77:** 450-452.

Ishikawa, F.N., Chang, H.K., Curreli, M., Liao, H.I., Olson, C.A., Chen, P.C., Zhang, R., Roberts, R.W., Sun, R., Cote, R.J., Thompson, M.E., Zhou, C.W. 2009. Label-free, electrical detection of the SARS virus N-protein with nanowire biosensors utilizing antibody mimics as capture probes. *ACS Nano*, **3:** 1219-1224.

Johnson, L., Gupta, A.T.K., Ghafoor, A., Akin, D., Bashir, R. 2006. Characterization of *Vaccinia* virus particles using microscale silicon cantilever resonators and atomic force microscopy. *Sensors and Actuators B*: *Chemical*, **115:** 189-197.

Kerman, K. 2008. Nanomaterial-based electrochemical biosensors for medical applications. *TrAC-Trends in Analytical Chemistry*, **27:** 585-592.

Kim, K.S., Lee, H.S., Yang, J.A., Jo, M.H., Hahn, S.K. 2009. The fabrication, characterization and application of aptamer-functionalized Si-nanowire FET biosensors. *Nanotechnology*, **20:** 235501.

Kim, A., Ah, C.S., Yu, H.Y., Yang, J.H., Baek, I.B., Ahn, C.G., Park, C.W., Jun, M.S., Lee, S. 2007. Ultrasensitive, label-free, and real-time immunodetection using silicon field-effect transistors. *Applied Physics Letters*, **91:** 103901-103903.

Kojima, A., Hyon, C.K., Kamimura, T., Maeda, M., Matsumoto, K. 2005. Protein sensor using carbon nanotube field effect transistor. *Japanese Journal of Applied Physics*, **44:** 1596.

Lee, D., Chander, Y., Goyal, S.M., Cui, T. 2011. Carbon nanotube electric immunoassay for the detection of swine influenza virus H1N1. *Biosensors & Bioelectronics*, **26:** 3482-3487.

Lee, H.S., Kim, K.S., Kim, C.J., Hahn, S.K., Jo, M.H. 2009. Electrical detection of VEGFs for cancer diagnoses using anti-vascular endotherial growth factor aptamer-modified Si nanowire FETs. *Biosensors & Bioelectronics*, **24:** 1801-1805.

Li, C., Curreli, M., Lin, H., Lei, B., Ishikawa, F.N., Datar, R., Cote, R.J., Thompson, M.E., Zhou, C.W. 2005. Complementary detection of prostate-specific antigen using ln(2)O(3) nanowires and carbon nanotubes. *Journal of the American Chemical Society*, **127:** 12484-12485.

Li, J., Ng, H.T., Cassell, A., Fan, W., Chen, H., Ye, Q., Koehne, J., Han, J., Meyyappan, M. 2003. Carbon nanotube nanoelectrode array for ultrasensitive DNA detection. *Nano Letters*, **3:** 597-602.

Lin, C H., Hung, C.H., Hsiao, C.Y., Lin, H.C., Ko, F.H., Yang, Y.S. 2009. Poly-silicon nanowire field-effect transistor for ultrasensitive and label-free detection of pathogenic avian influenza DNA. *Biosensors & Bioelectronics*, **24:** 3019-3024.

Lu, Y.S., Yang, M.H., Qu, F.L., Shen, G.L., Yu, R.Q. 2007. Amperometric biosensors based on platinum nanowires. *Analytical Letters*, **40:** 875-886.

Maehashi, K., Katsura, T., Kerman, K., Takamura, Y., Matsumoto, K., Tamiya, E. 2007. Label-free protein biosensor based on aptamer-modified carbon nanotube field-effect transistors. *Analytical Chemistry*, **79:** 782-787.

Manalis, S.R., Minne, S.C., Atalar, A., Quate, C.F. 1996. Interdigital cantilevers for atomic force microscopy. *Applied Physics Letters*, **69:** 3944-3946.

Martinez, J.A., Misra, N., Wang, Y.M., Stroeve, P., Grigoropoulos, C.P., Noy, A. 2009. Highly efficient biocompatible single silicon nanowire electrodes with functional biological pore channels. *Nano Letters*, **9:** 1121-1126.

McKendry, R., Zhang, J.Y., Arntz, Y., Strunz, T., Hegner, M., Lang, H.P., Baller, M.K., Certa, U., Meyer, E., Guntherodt, H.J., Gerber, C. 2002. Multiple label-free biodetection and quantitative DNA-binding assays on a nanomechanical cantilever array. *Proceedings of the National Academy of Sciences of the United States of America*, **99:** 9783-9788.

Moore, D.F., Syms, R.R.A. 1999. Recent developments in micromachined silicon. *Electronics & Communication Engineering Journal*, **11:** 261-270.

Murphy, L. 2006. Biosensors and bioelectrochemistry. *Current Opinion in Chemical Biology*, **10:** 177-184.

Musameh, M.M., Gao, Y., Hickey, M., Kyratzis, I.L. 2012. Application of carbon nanotubes in the extraction and electrochemical detection of organophosphate pesticides: A review. *Analytical Letters*, **45:** 783-803.

Neuberger, T., Schopf, B., Hofmann, H., Hofmann, M., von Rechenberg, B. 2005. Superparamagnetic nanoparticles for biomedical applications. Possibilities and limitations of a new drug delivery system. *Journal of Magnetism and Magnetic Materials*, **293:** 483-496.

Nicu, L., Leichle, T. 2008. Biosensors and tools for surface functionalization from the macro-to the nanoscale. The way forward. *Journal of Applied Physics*, **104:** 101-111.

Oh, J., Chang, Y.W., Kim, H.J., Yoo, S., Kim, D.J., Im, S., Park, Y.J., Kim, D., Yoo, K.-H. 2010. Carbon nanotube-based dual-mode biosensor for electrical and surface plasmon resonance measurements. *Nano Letters*, **10:** 2755-2760.

Onaran, A.G., Balantekin, M., Lee, W., Hughes, W.L., Buchine, B.A., Guldiken, R.O., Parlak, Z., Quate, C.F., Degertekin, F.L. 2006. A new atomic force microscope probe with force sensing integrated readout and active tip. *Review of Scientific Instruments*, **77:** 023501-7.

Park, K., Millet, L.J., Kim, N., Li, H., Jin, X., Popescu, G., Aluru, N.R., Hsia, K.J., Bashir, R. 2010. Measurement of adherent cell mass and growth. *Proceedings of the National Academy of Sciences of the United States of America*, **107:** 20691-20696.

Patolsky, F., Timko, B.P., Yu, G.H., Fang, Y., Greytak, A.B., Zheng, G.F., Lieber, C.M. 2006. Detection, stimulation, and inhibition of neuronal signals with high-density nanowire transistor arrays. *Science*, **313:** 1100-1104.

Patolsky, F., Zheng, G., Lieber, C.M. 2006. Nanowire sensors for medicine and the life sciences. *Nanomedicine*, **1:** 51-65.

Patolsky, F., Zheng, G.F., Hayden, O., Lakadamyali, M., Zhuang, X.W., Lieber, C.M. 2004. Electrical detection of single viruses. *Proceedings of the National Academy of Sciences of the United States of America*, **101:** 14017-14022.

Pei, J.H., Tian, F., Thundat, T. 2004. Glucose biosensor based on the microcantilever. *Analytical Chemistry*, **76:** 292-297.

Pui, T.S., Agarwal, A., Ye, F., Balasubramanian, N., Chen, P. 2009. CMOS-compatible nanowire sensor arrays for detection of cellular bioelectricity. *Small*, **5:** 208-212.

Raiteri, R., Grattarola, M., Butt, H.J., Skladal, P. 2001. Micromechanical cantilever-based biosensors. *Sensors and Actuators B*: *Chemical*, **79:** 115-126.

Savran, C.A., Knudsen, S.M., Ellington, A.D., Manalis, S.R. 2004. Micromechanical detection of proteins using aptamer-based receptor molecules. *Analytical Chemistry*, **76:** 3194-3198.

Sharf, T., Kevek, J.W., DeBorde, T., Wardini, J.L., Minot, E.D. 2012. Origins of charge noise in carbon nanotube field-effect transistor biosensors. *Nano Letters*, **12:** 6380-6384.

Shoorideh, K., Chi On, C. 2012. Optimization of the sensitivity of FET-based biosensors via biasing and surface charge engineering. *IEEE Transactions on Electron Devices*, **59:** 3104-3110.

Sone, H., Ikeuchi, A., Izumi, T., Okano, H., Hosaka, S. 2006. Femtogram mass biosensor using self-sensing cantilever for allergy check. *Japanese Journal of Applied Physics*, **45:** 2301-2304.

Sorgenfrei, S., Chiu, C.-y., Gonzalez, R.L., Yu, Y.-J., Kim, P., Nuckolls, C., Shepard, K.L. 2011. Label-free single-molecule detection of DNA-hybridization kinetics with a carbon nanotube field-effect transistor. *Nature Nanotechnology*, **6:** 126-132.

Staples, M., Daniel, K., Cima, M.J., Langer, R. 2006. Application of micro- and nanoelectromechanical devices to drug delivery. *Pharmaceutical Research*, **23:** 847-863.

Stern, E., Vacic, A., Reed, M.A. 2008. Semiconducting nanowire field-effect transistor biomolecular sensors. *IEEE Transactions on Electron Devices*, **55:** 3119-3130.

Stern, E., Klemic, J.F., Routenberg, D.A., Wyrembak, P.N., Turner-Evans, D.B., Hamilton, A.D., LaVan, D.A., Fahmy, T.M., Reed, M.A. 2007. Label-free immunodetection with CMOS-compatible semiconducting nanowires. *Nature*, **445:** 519-522.

Stoney, G.G. 1909. The tension of metallic films deposited by electrolysis. *Proceedings of the Royal Society of London Series A, Mathematical, Physical Engineering Sciences*, **82:** 172-175.

Storri, S., Santoni, T., Minunni, M., Mascini, M. 1998. Surface modifications for the development of piezoimmunosensors. *Biosensors & Bioelectronics*, **13:** 347-357.

Strehlitz, B., Nikolaus, N., Stoltenburg, R. 2008. Protein detection with aptamer biosensors. *Sensors*, **8:** 4296-4307.

Sulchek, T., Hsieh, R., Minne, S.C., Quate, C.F., Manalis, S.R. 2001. Interdigital cantilever as a biological sensor. In: *Proceedings of the 1st IEEE Conference on Nanotechnology*, pp. 562-566.

Tang, T., Liu, X.L., Li, C., Lei, B., Zhang, D.H., Rouhanizadeh, M., Hsiai, T., Zhou, C.W. 2005. Complementary response of In_2O_3 nanowires and carbon nanotubes to low- density lipoprotein chemical gating. *Applied Physics Letters*, **86:** 103903.

Tolani, S.B., Craig, M., DeLong, R.K., Ghosh, K., Wanekaya, A.K. 2009. Towards biosensors based on conducting polymer nanowires. *Analytical and Bioanalytical Chemistry*, **393:** 1225-1231.

Wanekaya, A.K., Chen, W., Myung, N.V., Mulchandani, A. 2006. Nanowire-based electrochemical biosensors. *Electroanalysis*, **18:** 533-550.

Wang, J. 2006. Electrochemical biosensors. Towards point-of-care cancer diagnostics. *Biosensors & Bioelectronics*, **21:** 1887-1892.

Wang, R.H., Ruan, C.M., Kanayeva, D., Lassiter, K., Li, Y.B. 2008. TiO_2 nanowire bundle microelectrode based impedance immunosensor for rapid and sensitive detection of Listeria monocytogenes. *Nano Letters*, **8:** 2625-2631.

Wang, X., Ozkan, C.S. 2008. Multisegment nanowire sensors for the detection of DNA molecules. *Nano Letters*, **8:** 398-404.

Weizmann, Y., Elnathan, R., Lioubashevski, O., Willner, I. 2005. Magnetomechanical detection of the specific activities of endonucleases by cantilevers. *Nano Letters*, **5:** 741-744.

Weizmann, Y., Patolsky, F., Lioubashevski, O., Willner, I. 2004. Magneto-mechanical detection of nucleic acids and telomerase activity in cancer cells. *Journal of the American Chemical Society*, **126:** 1073-1080.

Wu, G.H., Ji, H.F., Hansen, K., Thundat, T., Datar, R., Cote, R., Hagan, M.F., Chakraborty, A.K., Majumdar, A. 2001. Origin of nanomechanical cantilever motion generated from biomolecular interactions. *Proceedings of the National Academy of Sciences of the United States of America*, **98:** 1560-1564.

Yaralioglu, G.G., Atalar, A., Manalis, S.R., Quate, C.F. 1998. Analysis and design of an interdigital cantilever as a displacement sensor. *Journal of Applied Physics*, **83:** 7405-7415.

Yeom, S.-H., Kang, B.-H., Kim, K.-J., Kang, S.-W. 2011. Nanostructures in biosensor, a review. *Frontiers in Bioscience*, **16:** 997-1023.

Zhang, F.Y., Ulrich, B., Reddy, R.K., Venkatraman, V.L., Prasad, S., Vu, T.Q., Hsu, S.T. 2008. Fabrication of submicron IrO_2 nanowire array biosensor platform by conventional complementary metal-oxide-semiconductor process. *Japanese Journal of Applied Physics*, **47:** 1147-1151.

Zhang, G.-J., Zhang, L., Huang, M.J., Luo, Z.H.H., Tay, G.K.I., Lim, E.-J.A., Kang, T.G., Chen, Y. 2010. Silicon nanowire biosensor for highly sensitive and rapid detection of Dengue virus. *Sensors and Actuators B: Chemical*, **146:** 138-144.

Zhang, G.J., Chua, J.H., Chee, R.E., Agarwal, A., Wong, S.M. 2009. Label-free direct detection of MiRNAs with silicon nanowire biosensors. *Biosensors & Bioelectronics*, **24:** 2504-2508.

Zhang, J., Lang, H.P., Huber, F., Bietsch, A., Grange, W., Certa, U., McKendry, R., Guntgerodt, H.J., Hegner, M., Gerber, C. 2006. Rapid and label-free nanomechanical detection of biomarker transcripts in human RNA. *Nature Nanotechnology*, **1:** 214-220.

Zhang, L.J., Peng, H., Kilmartin, P.A., Soeller, C., Travas-Sejdic, J. 2007. Polymeric acid doped polyaniline nanotubes for oligonucleotide sensors. *Electroanalysis*, **19:** 870-875.

Zhang, X.Y., Li, D., Bourgeois, L., Wang, H.T., Webley, P.A. 2009. Direct electrodeposition of porous gold nanowire arrays for biosensing applications. *Chemphyschem*, **10:** 436-441.

Zheng, G.F., Patolsky, F., Cui, Y., Wang, W.U., Lieber, C.M. 2005. Multiplexed electrical detection of cancer markers with nanowire sensor arrays. *Nature Biotechnology*, **23:** 1294-1301.

Ziegler, C. 2004. Cantilever-based biosensors. *Analytical and Bioanalytical Chemistry*, **379:** 946-959.